THIS REPORT IS COMPLETED BY MIE491-CAPSTONE DESIGN, TEAM ARL-MLS2-2. UNAUTHORIZED USE IS NOT PERMITTED.

Executive Summary

The Chamber Temperature Control System is a **compact and high-precision** device that can maintain a **uniform and stable temperature distribution** within a 3D printer **at a user-defined target temperature**. It is projected to significantly reduce defects induced by uneven chamber temperature distribution in the printed parts without interfering with the printer's normal operation, thereby significantly alleviating the client's problem of common defects in printed parts due to uneven chamber temperature distribution.

Relying on forced convection, the system uses a fan to draw chamber air, heats it with a PTC element, and discharges it back into the chamber. To validate that the design meets the criteria of **temperature stability**, **control accuracy**, and **spatial temperature uniformity**, this report outlines the key design features and the Design of Experiments (DOE) optimization process that ensured all three core criteria were achieved within the system's functional decomposition.

To accurately maintain the chamber at the target temperature, the system adopted a custom-designed, novel, and original "**PD-like"** control algorithm that employs a control mechanism dynamically adjustable to the target setpoint. Its specific parameters were optimized through a combination of polynomial **regression modeling of system response** and **discrete trials**.

To achieve spatial temperature uniformity, the device takes in chamber air at an experimentally optimized height and circulates the chamber air vertically. Meanwhile, the experimentally optimized air deflector diverts the heated air horizontally. Such **bidirectional convection** enables the device to maintain optimal spatial uniformity in the chamber air. In optimizing the geometric dimensions that affect temperature uniformity, **full-factorial DOE** was conducted, **Response Surface Methodology** was applied to capture the interdependence of the control factors, and the **Generalized Reduced Gradient** technique was used to determine the optimal geometry.

With these optimized design features, the current prototype can achieve a (spatial temperature) **standard deviation < 2°C** at steady state and **control accuracy of ±0.5°C** and **high stability with oscillation amplitude** $<$ **0.5°C** for all tested target temperatures 40°C , 50°C , 60°C , and 65°C. However, much space for future improvements can still be identified due to the tight time and budget constraints of this project. Examples are the exclusion of the original printer's cooling fans, the heat emission from the print bed and the hot end, and the lack of > 10-hour extended endurance testing.

Last but not least, a series of industry standards and regulations were researched and referenced to validate design choices made. Following that, key conclusions from the life cycle analysis were presented to validate the downstream environmental impacts of the design.

1. Introduction

Composite Fiber Co-extrusion (CFC) is an innovative filament extrusion process where continuous composite fiber is embedded into molten thermoplastic filament through a specialized print head. The Anisoprint A3 printed currently in service with the Advanced Research Laboratory for Multifunctional Lightweight Structures (ARL-MLS) employs this technique. However, it is not equipped with an active chamber temperature control system, which could potentially result in a non-uniform temperature gradient within the printer chamber. Such non-uniformity could introduce residual stresses that weaken inter-layer adhesion, resulting in voids, warpage, distortion, and delamination during the printing process (Figure 1). These defects undermine the structural integrity of the printed product, diminishing its tensile strength and other mechanical properties.

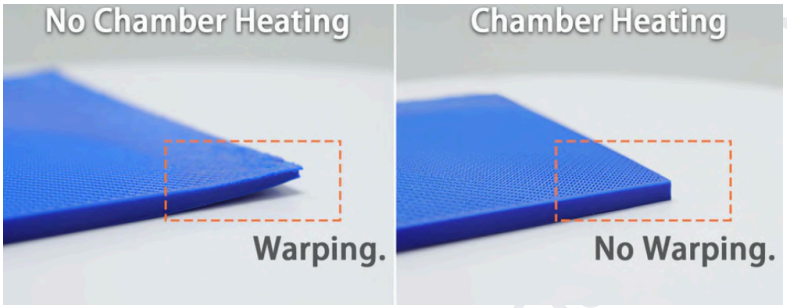

Figure 1. Warping caused by no chamber heating [1]

The team was tasked with developing a chamber temperature control unit capable of maintaining a uniform and stable temperature distribution within a 3D printer at a user-specified target temperature. With the integration of this design into the original printer, **the structural integrity of printed parts is expected to improve significantly**, thereby supporting the client's prototyping needs for ongoing research endeavors.

2. Project Requirements

2.1 Functions

The temperature control system **maintains the chamber temperature at a set point and ensures even temperature distribution throughout the chamber**. The functions are divided into Primary Function and Secondary Functions as listed below:

Table 1. Functions Table

Functions	Description
Primary Function	1. maintain stable, accurate chamber temperature at a setpoint 2. maintain uniform temperature distribution
Secondary Function	1. Monitor chamber temperature. 2. Allow the user to select target temperature.

2.2 Objectives

Table 2. Objectives Table

Objectives	Metrics
The design must maintain a **stable and uniform** chamber temperature distribution.	The chamber spatial average temperature should be maintained within ± **1°C** about the target temperature. The maximum standard deviation across the entire chamber should be < **2.5 °C**.
The design should monitor and track chamber temperature fluctuation.	The continuous temperature fluctuation throughout a printing session accessible to the user.
The design should incorporate a catalog of optimal printing temperatures for common polymers.	A catalog of optimal target temperature presets for all supported polymers should be included .

2.3 Constraints

Table 3. Constraints Table

Constraints	Metrics
The design must ensure stable and accurate chamber temperature in steady-state operation.	At steady state, the chamber spatial average temperature must not exceed ± **1°C** of the target temperature.
The design must not intrude on the normal operation of the 3D printer.	The design must not disrupt the normal operation of the 3D printer.
The design must allow the users to input the target chamber temperature.	Users must be able to adjust the target temperature.
The design must not exceed the power limit.	The maximum power consumption of the entire design must not exceed the power limit of 900W.
The design must not exceed the overall project budget.	The overall project budget is limited to under 1000 $CAD.

2.4 Project Requirements Revision

The final project requirements have been refined from the previous version. Although most numerical objectives remain unchanged, the team made two key modifications:

1. The wattage limit was increased from 160W to 900W because real-world experiments showed that 160W was insufficient to heat the entire chamber (reaching a steady state around 35°C, see Section 6.2.1);

2. The 3-minute heat-up time objective was also removed because real-world experiments showed that even using a 800W high-power heater, the time for achieving a maximum setpoint (65°C) is far longer than 3-minute. Although increasing power can accelerate the

heat-up process, using a higher-power PTC heater alongside the printer may raise safety concerns by potentially triggering circuit protection mechanisms, and the combined energy consumption could become excessive, thereby reducing overall user practicality.

3. Final Design Specifications

3.1 Product Summary

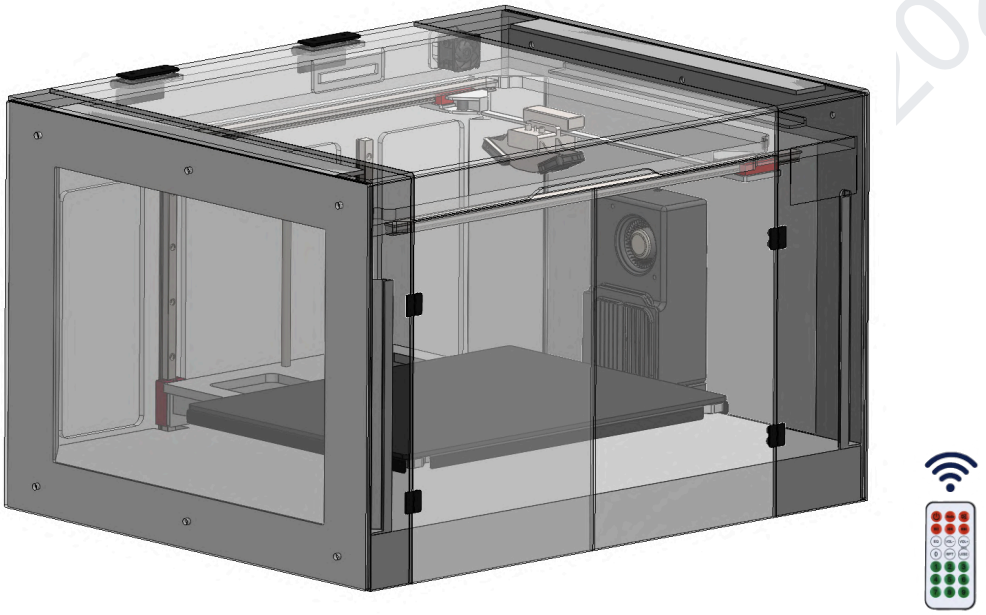

Figure 2. Final Design (in the printer)

The design is a **remote-controlled, portable, modular, and compactly packaged** temperature controller unit able to **maintain a stable and uniform** temperature distribution at a preset target temperature within the printer chamber. The design maintains high performance in **three key aspects**:

1. it holds the chamber's spatial average temperature within ±0.5°C of the setpoint (accuracy);
2. it achieves a (spatial) standard deviation of less than 2°C during steady-state operation (uniformity);
3. It limits fluctuations in the spatial average temperature to under 0.5°C at steady state (stability).

With its excellent thermal performance, the design is projected to **significantly reduce interlayer delamination and warpage**, addressing common defects previously observed in printed parts of conventional printers. In terms of its operation, the device is highly **user-friendly**: all action required for the user is to input the target temperature using a remote controller to achieve such excellent temperature control. Moreover, the design's fully enclosed layout and compact footprint offer **high compatibility** with a wide array of printers of similar dimensions; **non-intrusion** installation can be

achieved due to the design's non-permanent mounting method and due to the compact footprint, therefore no interference to the normal operation of the printer.

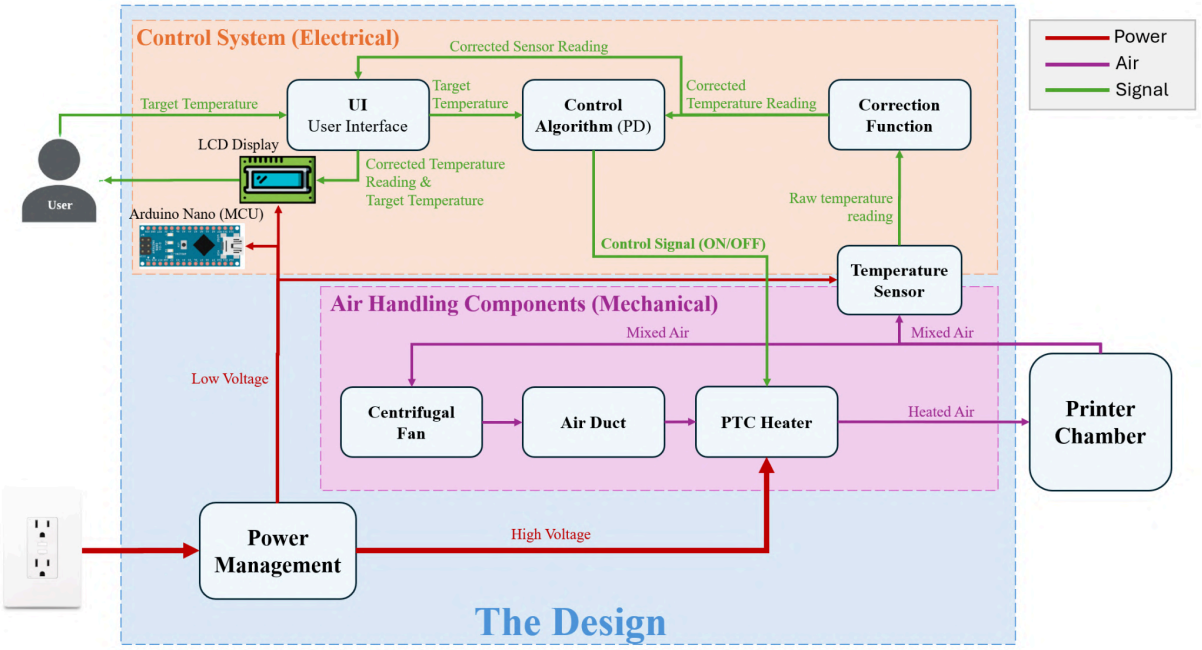

Figure 3. High-level systems diagram

The overall working principle of the device is outlined in the systems map and overall layout diagram (Figure 3). In the following subsections, each subsystem is introduced **in the sequence that a user follows as they interact with the device during typical operation**. For each subsystem, its location within the enclosed system, function, interfacing method with other components, and design decisions shaped by performance objectives and constraints are presented in detail. The reader is encouraged to refer to the system map and layout diagram for visual reference as each subsystem is described.

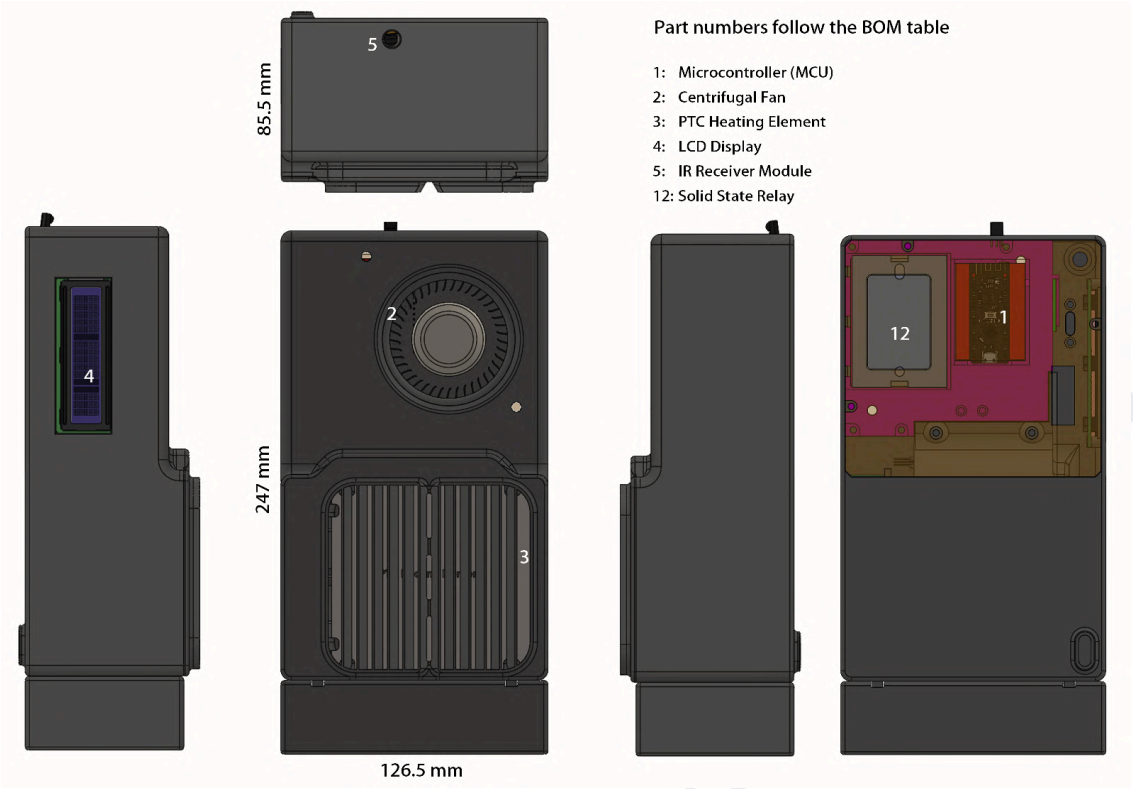

Figure 4. Product isometric diagram

Figure 5. Product isometric diagram (transparent)

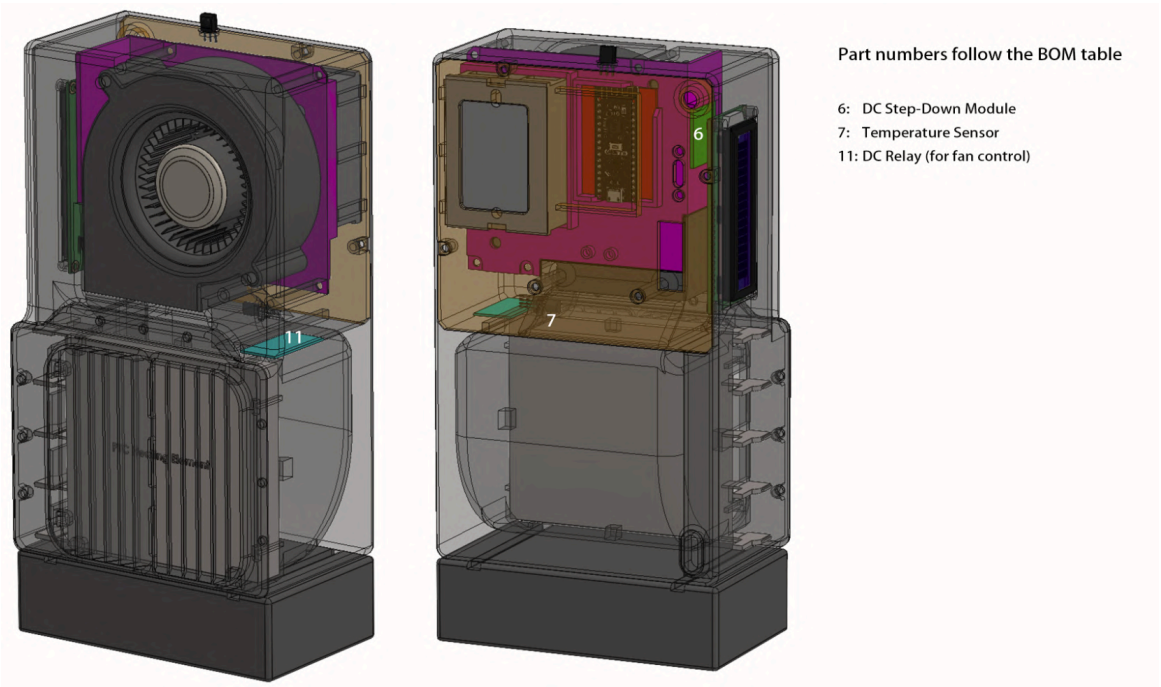

Figure 6. Product 3D diagram (transparent)

3.2 Electrical Wiring

Before the start of a printing session, the user powers on the temperature controller unit to preheat the chamber to a preset target temperature ideal for the specific printing material. As the user switches on the device, all components are connected through the **electrical wiring subsystem**. This connection activates power supply and control signals feeding into the PTC heater, the centrifugal fan, and all electronics.

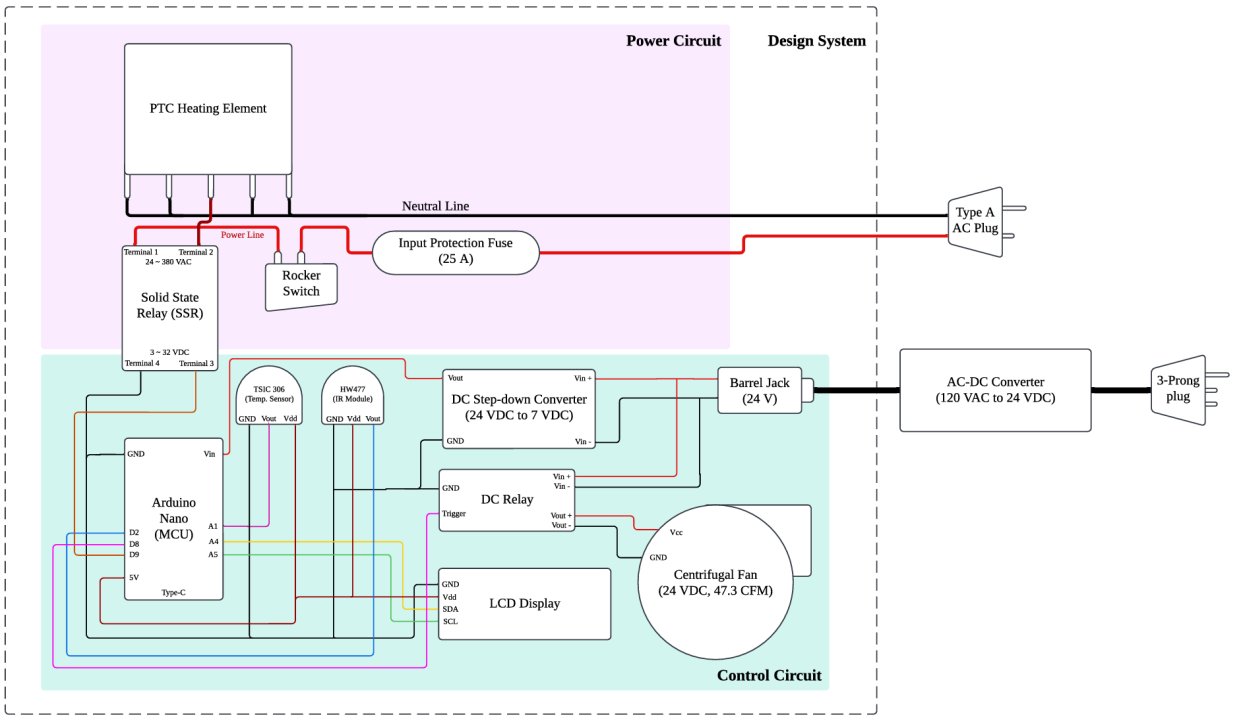

Figure 7. Circuit Diagram

This subsystem employs a **dual** power management strategy, dividing the system into two independent circuits: a high-voltage power circuit and a low-voltage control circuit. The power circuit runs on 120 VAC and solely powers the PTC heater (800W, 6.7A), while the control circuit operates on ≤ 24 VDC and manages signal transmission. Separating power and control circuits meets the heater's energy demand and minimizes electromagnetic interference, ensuring MCU reliability [2].

The complete combined circuit is shown in Figure 7. The 120 VAC, 60 Hz supply passes through a 125 VAC, 15 A switch and a 25 A fuse, which protects downstream components by interrupting overcurrent. Power then reaches SSR Terminal 1, with Terminal 2 connected to the PTC heater's center pin. The outer pins connect to neutral (Appendix B), and SSR terminals 3 and 4 connect to the MCU's control pin (D8) and GND.

When the MCU outputs 5 V, the SSR closes the high-voltage circuit, powering the heater; at 0 V, the circuit opens. This enables safe digital control and underpins the control algorithm (Section 3.8).

The control circuit distributes 24 VDC (converted from 120 VAC via a 40W AC-DC converter; Appendix C) through a DC barrel jack. One path powers the 24V, 20W centrifugal fan; the other feeds a 24V-to-7V converter supplying the Arduino Nano via its Vin pin. The Nano's regulator provides 5 V to the LCD, temperature sensor, and IR module. A shared ground ensures reliable voltage references and data transmission.

Cable routing space in the enclosure (Figures 8, 9) keeps wiring organized, simplifies maintenance, and prevents overheating hazards.

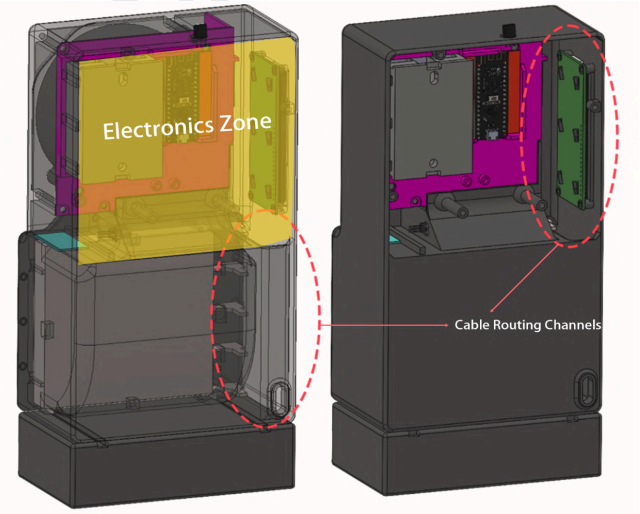

Figure 8. Internal cable routing channels

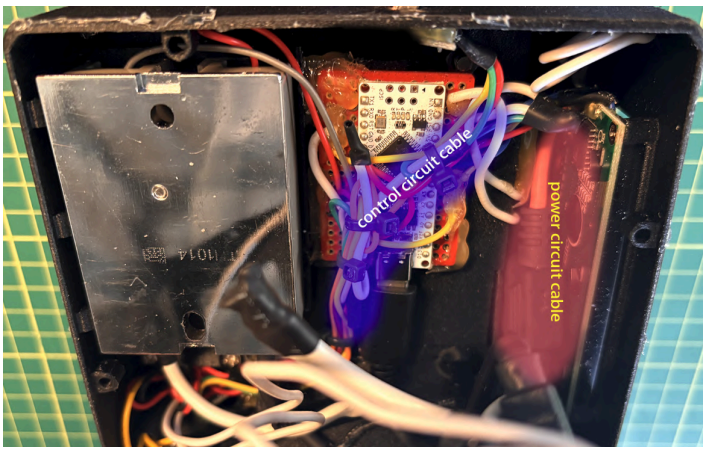

Figure 9. Separate wiring for dual power system

3.3 User Interface (UI) and Data Acquisition - Electrical

With the power turned on and all electrical connections functioning, the user now needs to **select and communicate their desired target temperature to the device** via the user interface (UI). To simplify operator interaction, the team decided that the **target temperature should be set remotely**. An Infrared radiation (IR) remote module receives inputs from the user's hand-held remote keypad and transmits them to the MCU. The MCU reads the resulting digital output, and a control algorithm uses this data to set the target temperature.

Once the target temperature has been set, heating begins according to the control algorithm. During this process, the user can **monitor the current chamber temperature** as it is being heated. An I2C protocol supported 16×2 character LCD is mounted on the side of the device (see Figure 10).

Figure 10. LCD Display (Unit: °C)

Additionally, if the users wish to acquire feedback for further data processing or documentation, they can access **real-time device status** on their computers via the MCU's data acquisition port, which extends to the device's back panel via a USB 3.0 Type-C cable (see Figure 11). Users can simply plug the cable into this port to read detailed device status information.

Figure 11. Data Acquisition / Device Reprogramming Port

In certain cases, the user may want to modify or reprogram the default Arduino control code provided by the team for algorithm upgrade. To this end, they can upload new code using the same Type-C port on the back panel.

3.4 Air-handling Components - Mechanical

With all electrical wirings connected properly and the target temperature set, the heating process finally begins. The unheated air is first taken in by the centrifugal fan into the design's built-in air duct (Figure 12). A centrifugal fan is selected to orient the suction and discharge channels perpendicular to each other, consistent with the overall geometry of the device. The air duct forces the airflow to pass through the PTC heater fins in a perpendicular direction, thereby maximizing the contact area between the air and the fin to ensure heat exchange efficiency. The length of the air duct is 10 cm, and it has been optimized through a full-factorial Design of Experiment (DOE) process described in Section 6.2.3.

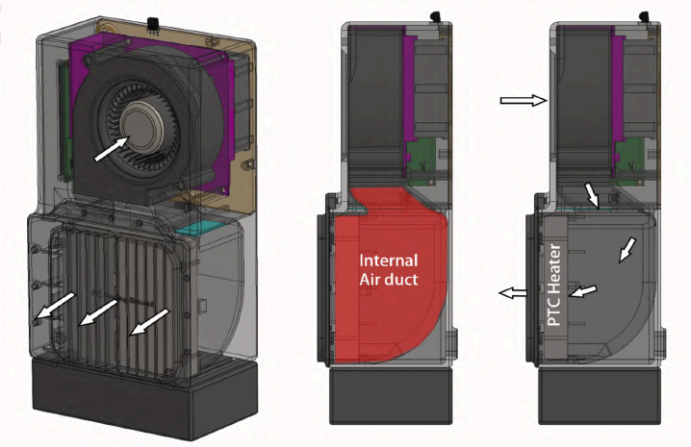

Figure 12. Built-in air duct

After being heated by the PTC heater, the airflow is directed by a louver-like wind deflector at the outlet before entering the printer chamber (Figure 13). The vertically aligned deflector deflects the heated air horizontally to the left and right. The heated air then rises vertically from the bottom of the chamber towards the top (Figure 14). **Such bidirectional convection (force + natural convection) is vital for achieving a spatially uniform chamber temperature distribution.**

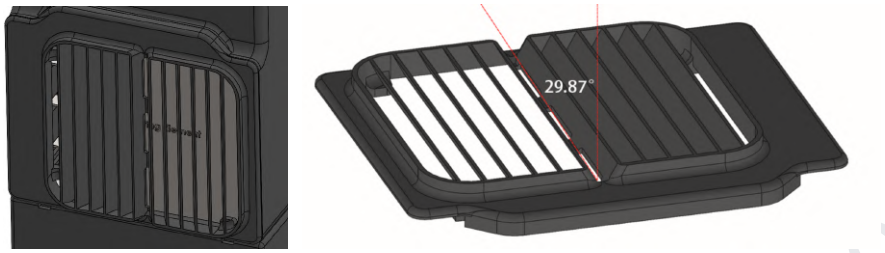

Figure 13. Wind Deflector Geometry

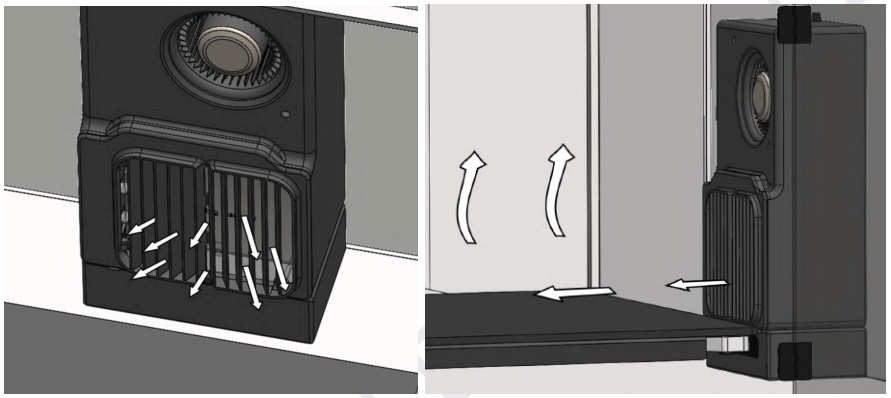

Figure 14. Air spreading direction (force + natural convection)

The grilles are arranged in parallel at an angle of approximately 30° (29.87°) and evenly spaced to guide the airflow. The deflector attaches to the product's outlet with nine magnets (Figure 15), creating a modular design that allows users to easily swap out or customize it to suit different printers or heating requirements.

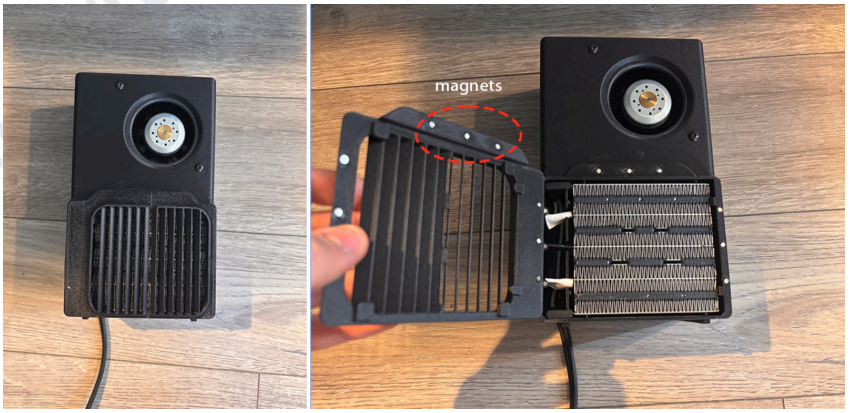

Figure 15. Deflector Installation Mechanism

For the Anisoprint A3 model, the presented deflector design has already been optimized for the best performance, as determined by the DOE process described in Section 6.2.3.

3.5 Internal Layout Configuration and Enclosure Design - Mechanical

All hardware components described above are housed in an enclosure. The overall dimension of the product's enclosure is 247 mm × 126.5 mm × 85.5 mm, facilitating an easy one-hand lift and installation inside a 3D printer.

The enclosure features a multi-layer internal layout that consists of an upper and lower section. The top section mainly houses the high flow rate (47.3 CFM) centrifugal fan and the bottom section is equipped with a high-power PTC heater.

With the above partitioning, the internal structure of the design is divided into four major regions based on the different functionalities (Figure 16):

1. **PTC Mounting Slot:** Reserved space for the heater's placement.
2. **Intake Fan Mounting Slot:** Reserved space for the intake fan's placement.
3. **Air Duct:** The internal channel connects the output of the intake fan and PTC element.
4. **Electronic Compartment:** Stored all the electronics (MCU, SSR, etc.).

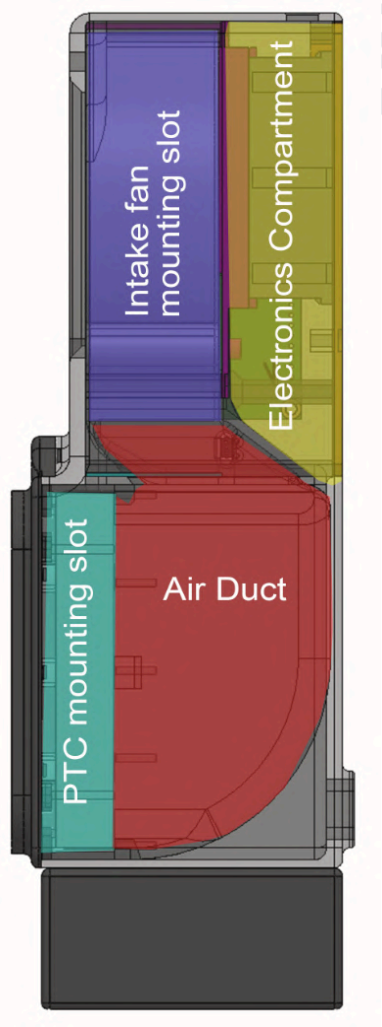

Figure 16. Design side view

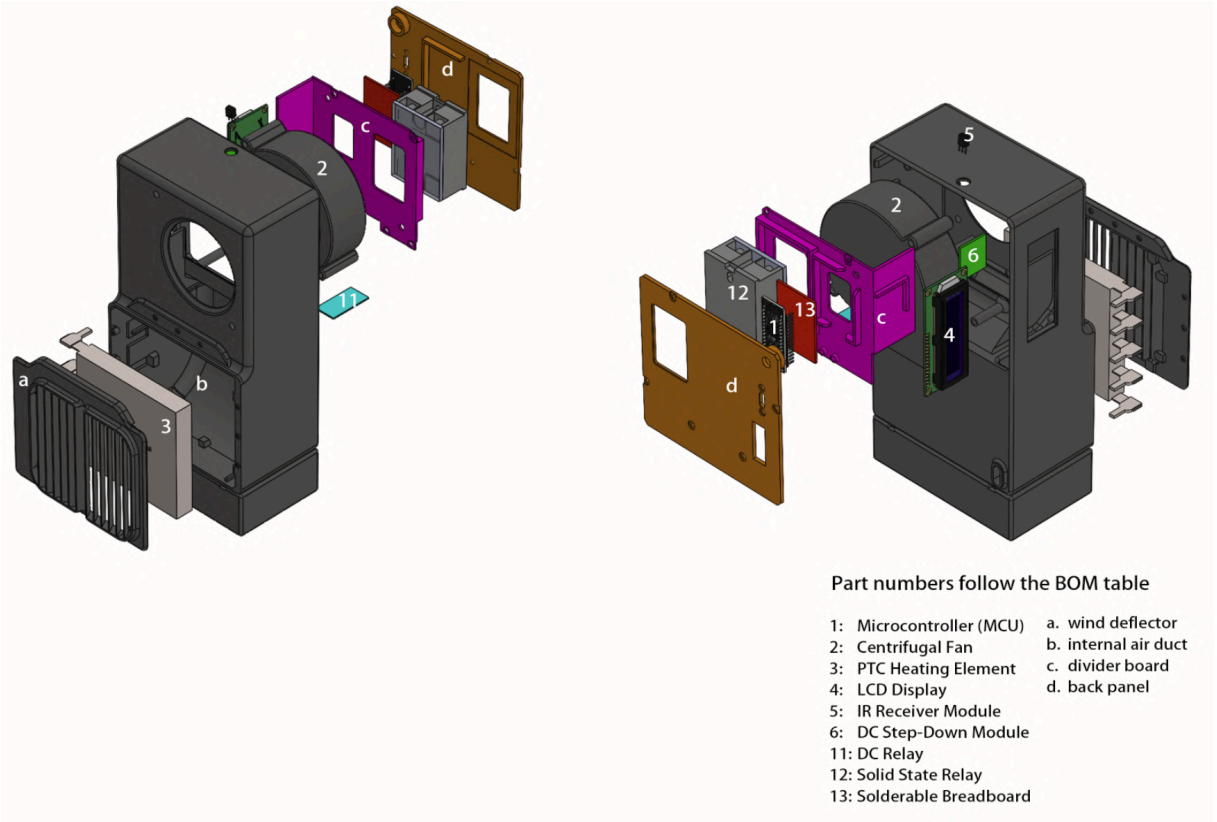

Figure 17. 3D Explosive View of the design

The intake fan mounting slot and the electronic components compartment are separated by a divider panel (Figure 18). Slots and grooves are designed on the back surface of the divider panel for easy installation of electronics. The panel simplifies wiring while minimizing interference from vibrations (to the electronics) caused by direct contact with the fan's surface.

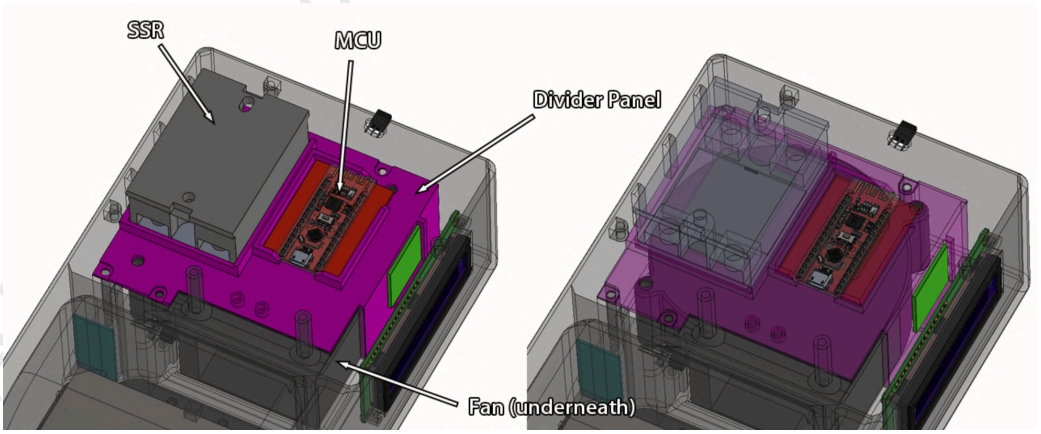

Figure 18. Divider Panel

The design features dedicated brackets on the side panel for other electronic installations (Figure 19). A back panel is added to encapsulate and protect the internal parts (Figure 20).

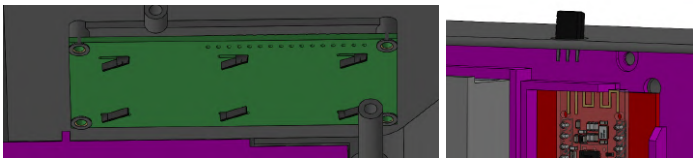

Figure 19. LCD Display mounting bracket and IR module bracket

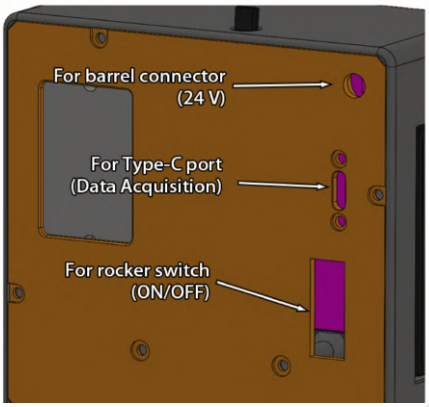

Figure 20. Back Panel

The entire enclosure is constructed from PA6-CF (carbon fiber reinforced PA6) and 3D printed on a BambuLab P1S FDM printer, offering superior thermal resistance (critical heat deflection temperature up to 186°C) to mitigate the high temperatures generated by PTC element (Appendix E). Associated engineering drawings and STEP files for all customized components are listed in Appendices F and G.

3.6 Design Features for Thermal Insulation and Protection - Mechanical

Since the PTC heater not only transfers heat to the airflow and subsequently into the printer chamber but also radiates heat to neighboring regions inside the enclosure, it is of **utmost importance that the team ensures sufficient thermal insulation** between the PTC heater and the interior walls of the enclosure as well as electronics housed inside. In addition to the high heat tolerance of the enclosure material, the team implemented the following design improvements:

1. The maximum operating temperature for the centrifugal fan is 70 °C. To ensure the absolute thermal stability of all components, **the maximum allowable chamber target setpoint is limited to 65°C**. All components have been selected to ensure long-term reliability at this temperature.

2. All electronics are placed at the top of the enclosure, away from the direct heat of the air duct further isolates these components from the heat source (Figure 21). Measurements confirmed that the maximum temperature in the electronics zone (°C) is slightly below 70°C, well within the recommended long-term operating limit of 85°C for all electronics (Appendix H).

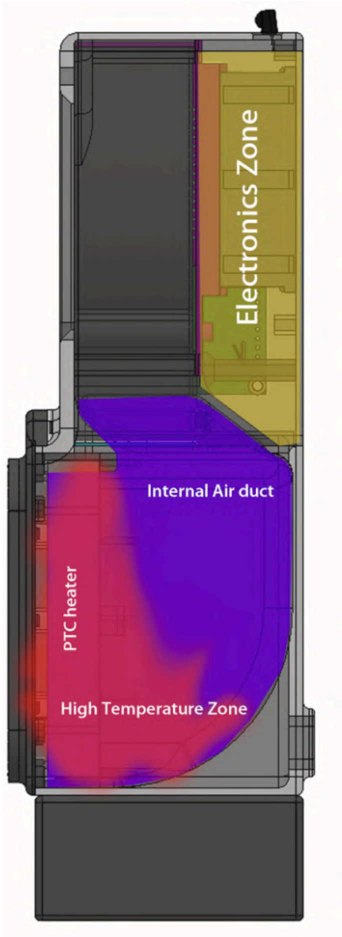

Figure 21. Electronics zone

3. If the service temperature exceeds 75°C, the system will automatically trigger its self-protection mechanism, resulting in an automatic shutdown that ensures the temperature within the enclosure is never near the operating limit of 85°C for electronics.

3.7 Sensing and Communication - Controller Hardware

With the heating process started and appropriate thermal insulation and protection in place, the stream of heated air quickly heats up the entire chamber. The device must continuously monitor chamber temperature and adjust based on the error from the target to maintain ±1°C accuracy (see Section 2.2). This sets the controller in motion. In terms of choice of hardware, the Arduino Nano is selected as the microcontroller unit due to its compact size, ease of programming, and rich set of interfaces that meet all peripheral needs.

The MCU uses its digital GPIO pins (D8 and D9) to drive two relay modules separately: D8 connects to the SSR's trigger terminal (terminal 3) to control the PTC heater (Section 3.2), while D9 connects to another DC relay's trigger terminal to control the fan (Figure 7). When the relay's trigger input is high, the respective hardware (fan or PTC heater) runs at full power; when it's low, they are turned off.

A thermal sensor is mounted at the inner wall of the air duct's inlet (Figure 22) to measure the current chamber temperature. The system uses a semiconductor temperature sensor (TSIC 306) with an accuracy of ±0.3°C to monitor the current chamber temperature, sufficient for the objective of ±0.5°C.

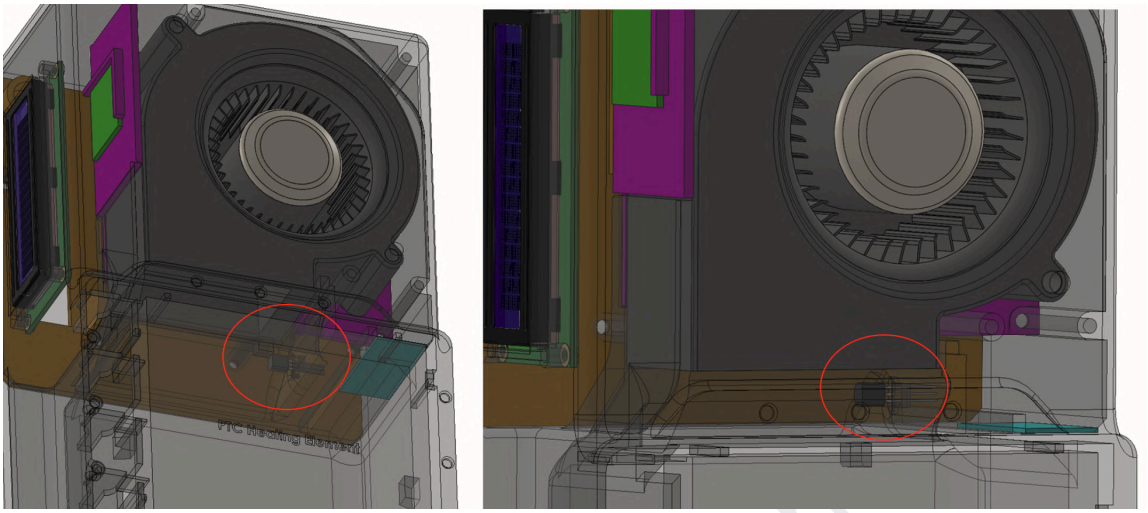

Figure 22. Thermal Sensor Installation Position

The sensor's analog output is being converted to digital signal by MCU's built-in ADC (Analog-Digital Converter). Using the Arduino TsicSensor library (Appendix I), this digital value is directly converted into a Celsius reading, allowing the system to accurately monitor the temperature inside the chamber. This hardware configuration enables the control algorithm outlined in the following section.

3.8 Controller Design - Control Algorithm

The controller algorithm is the primary component for control accuracy. It is implemented on Arduino Nano and programmed in Arduino IDE. The following discussion provides a detailed explanation of the controller's design and control principles. The explanation is divided into two levels: the high level, which outlines the overall operating principle of the controller, and the low level, which delves into more detailed aspects (control codes available in Appendix J).

3.8.1 Controller High-Level Design

A feedback controller is a device or algorithm that continuously monitors a system's output and compares it with a desired setpoint. It computes the error and generates the control signals that directly adjust the system's input (Figure 23).

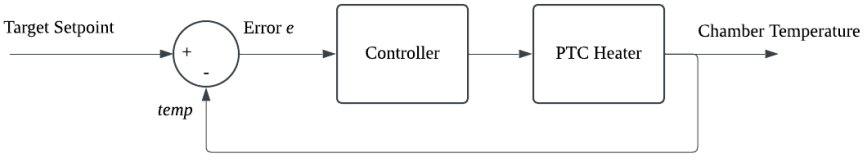

Figure 23. High-Level Control System Diagram

In this design, the error term, e, is formulated as the difference between the target setpoint ($Target\ Temperature$) and the current chamber temperature ($temp$).

$$e = Target\ Temperature - temp$$

Conventional PD (Proportional-Derivative) controllers adjust the system input based on both the error and its rate of change, typically requiring continuous power modulation and a more complex hardware design. To prioritize hardware simplicity, the team chose a heater that supports only on/off operation, sacrificing fine-tuned power control. To address this limitation, a PD-like controller is designed that **adjusts the heater status based on both the error and its rate of change.**

$$threshold_t = base\_threshold + k[\,temp_t - temp_{t-1}]$$

(where " t " indicates at current time step)

At a fixed frequency of 20 Hz, the error term is continuously computed and compared to the $threshold_t$. If the error is greater than the $threshold_t$, the heater will be activated. Otherwise, it will be deactivated.

Two key parameters govern the controller's behavior: $base\_threshold$ and k. The $base\_threshold$ establishes the baseline for the magnitude of $threshold_t$. With the second term (in the formula) constant, a higher value $base\_threshold$ causes a higher value $threshold_t$. This implies that during heating, the maximum allowable error between the chamber temperature and the target temperature is larger, prompting an earlier shut-off of the PTC heater to prevent overshoot. Meanwhile, k determines the sensitivity of the $threshold_t$ to instantaneous change in chamber temperature $[\,temp_t - temp_{t-1}]$. That is, a higher value k causes a higher increase in $threshold_t$ for the same instantaneous change in chamber temperature, causing an earlier shutoff as well.

3.8.2 Controller Low-Level Design

3.8.2.1 Sensor Correlation Function

The design incorporates a built-in TSIC 306 semiconductor temperature sensor to measure the current chamber temperature ($temp$), which is fed directly into the controller to regulate the heater.

However, a single sensor mounted onto the device is only capable of capturing the current temperature next to the sidewall of the printer chamber. Because the temperature distribution is not perfectly uniform, there exists a slight error from the true (spatial) average temperature of the chamber, resulting in imprecise control. Therefore, **a correlation function that maps the sensor's measured temperature to the true average temperature of the chamber proves imperative.**

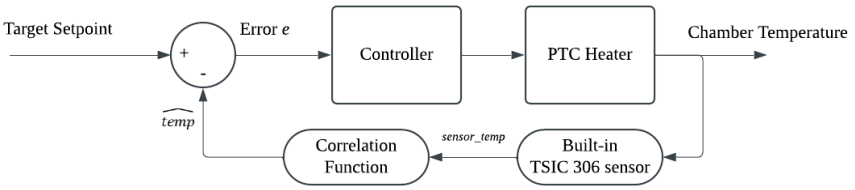

Figure 24. Low-Level Control System Diagram

$$\widehat{temp} = 1.0523 \times sensor\_temp - 6.6486 + Compensation\left(\widehat{temp}, t\right)$$

$$Compensation\left(\widehat{temp}, t\right) = \begin{cases} 0, & \text{if } \widehat{temp} < (\text{Target Temp} - 1.5), \\ a + b\,e^{-ct}, & \text{if } \widehat{temp} \geq (\text{Target Temp} - 1.5). \end{cases}$$

(where " t " indicates the elapsed time after the temperature has reached (Target Temp - 1.5))

where,

$$a(\text{Target Temp}) = 0.7109 \times \left(\frac{\text{Target Temp}}{20}\right) - 0.7443,$$

$$b(\text{Target Temp}) = 1.036 \times \left(\frac{\text{Target Temp}}{20}\right)^2 - 5.2968 \times \left(\frac{\text{Target Temp}}{20}\right) + 5.5476,$$

$$c(\text{Target Temp}) = -0.0578 \times \left(\frac{\text{Target Temp}}{20}\right)^2 + 0.2877 \times \left(\frac{\text{Target Temp}}{20}\right) - 0.3278.$$

The optimized correlation correction function that maps raw sensor reading $sensor\_temp$ into the estimated chamber temperature ($\widehat{temp}$) is presented above (Figure 24). The formulation of the function is experimental-based and explained in Section 6.2.4.1 and 6.2.4.4. At every time step, the error will be computed using $\widehat{temp}$ and fed into the controller.

3.8.2.2 Controller Parameters: Dynamic Baseline and k

As discussed in Section 3.8.1, the $base\_threshold$ provides the baseline that directly regulates the heater status. A dynamic $base\_threshold$, as a function of the target setpoint is implemented as follows.

$$\text{base\_threshold}_{\text{dynamic}} = 1 - 1.6973\,x^3 + 13.354\,x^2 - 37.765\,x + 37.796,$$

$$\text{where } x = \frac{\text{Target Temperature}}{20}.$$

The design process of this mechanism is iterative and experimental-based, explained in detail in Section 6.2.4.2. In the controller, k is set to 75, a value optimized via experiment (Section 6.2.4.3).

In summary, at each time step the raw sensor reading $sensor\_temp$ is converted to an estimated chamber temperature $\widehat{temp}$, from which the error (e) is computed. The controller then compares e to a dynamic threshold — derived from the base threshold ($base\_threshold_{dynamic}$) and the k (set to 75) — to

decide whether to activate the heater. This process is presented as the pseudocode shown in Figure 25:

Algorithm 1: PD-like Temperature Control with Integrated Compensation

Input: T_{target}, Δt, k
Output: Heater status (ON/OFF)

Initialize:
heater $\leftarrow$ OFF;
$\widehat{temp}_{\text{prev}} \leftarrow 0$;
$elapsed\_time \leftarrow 0$;

while *system is running* **do**
  $sensor\_temp \leftarrow$ ReadSensor();
  $\widehat{temp} \leftarrow 1.0523 \times sensor\_temp - 6.6486 + \text{Compensation}(\widehat{temp}, elapsed\_time, T_{\text{target}})$;
  $e \leftarrow T_{\text{target}} - \widehat{temp}$;
  $x \leftarrow \frac{T_{\text{target}}}{20}$;
  $base\_threshold \leftarrow 1 - 1.6973\,x^3 + 13.354\,x^2 - 37.765\,x + 37.796$;
  $threshold \leftarrow base\_threshold + k \times (\widehat{temp} - \widehat{temp}_{\text{prev}})$;
  if $e > threshold$ **then** `// Compare error with threshold`
    $heater \leftarrow$ ON;
  else
    $heater \leftarrow$ OFF;
  $\widehat{temp}_{\text{prev}} \leftarrow \widehat{temp}$;
  $elapsed\_time \leftarrow elapsed\_time + \Delta t$;
  `// Wait for the sampling interval`
  wait Δt;

`Compensation`$(\widehat{temp}, elapsed\_time, T_{target})$ **if** $\widehat{temp} < (T_{target} - 1.5)$ **then**
  $elapsed\_time \leftarrow 0$;
  return 0;
else
  return $a + b\,e^{-c \times elapsed\_time}$;

Figure 25. Controller Logic (Pseudocode) where x represents the normalized target temperature

3.9 Specification Sheet

The design features and component sizes mentioned above are summarized in a complete specification sheet listed in Appendix K

4. Bill of Materials (BOM) / Economic Analysis

A complete BOM is made and attached in Appendix L. The unit production cost is estimated to be 235.75 Canadian dollars (before tax). If the product has to be mass-produced and distributed, the cost can be lower.

5. Implementation Plan / User Manual

This chapter presents the manual for end-users. For the manufacturer's assembly guide, please refer to Appendix M. The user should receive a package that consists of 3 items listed in Table 4.

Table 4. Product Package List (Figure 26)

Label	Description	Quantity
①	Temperature Control Unit	1
②	Remote	1
③	120 VAC to 24 VDC Converter	1

Figure 26. Product Package

5.1 Normal Usage Instructions

To ensure proper and safe operation, please strictly follow the steps below:

1. Before using the product, read the safety instruction on the power code (Figure 26). Unplug all cables and conduct a thorough visual inspection, checking for any wear on the enclosure or wire insulation. Do not proceed if any wear is detected.

2. (If data acquisition required) Connect the device to a computer using the USB 3.0 Type-C port on the back panel (Figure 27) and run the serial reading software (detailed setting in Section 5.3).

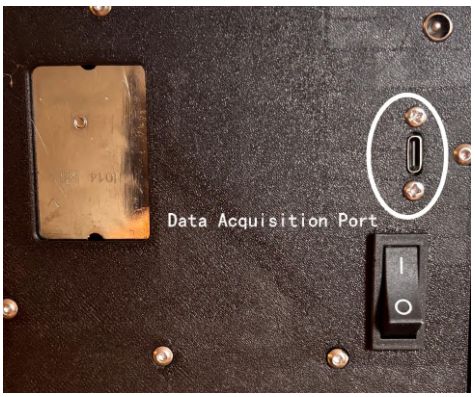

Figure 27. Data Acquisition Port

3. Insert the 24V converter (③) plug into the 5.5 mm barrel jack on the back panel (Figure 28). Turn on the rocker switch and position the device in the center of the printer's side wall (Figure 29).

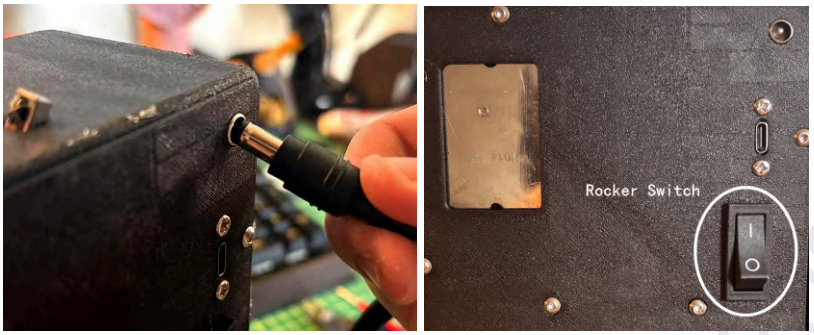

Figure 28. Barrel Jack and Rocker Switch

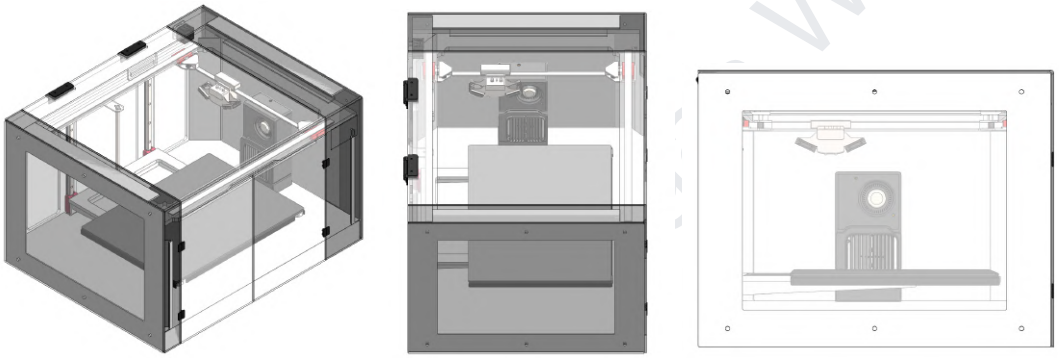

Figure 29. Device Placement Position

4. Close the printer chamber door, then connect the converter and the control unit to an external AC power supply (minimum 850W (Appendices C, K)) to turn on the dual power system.

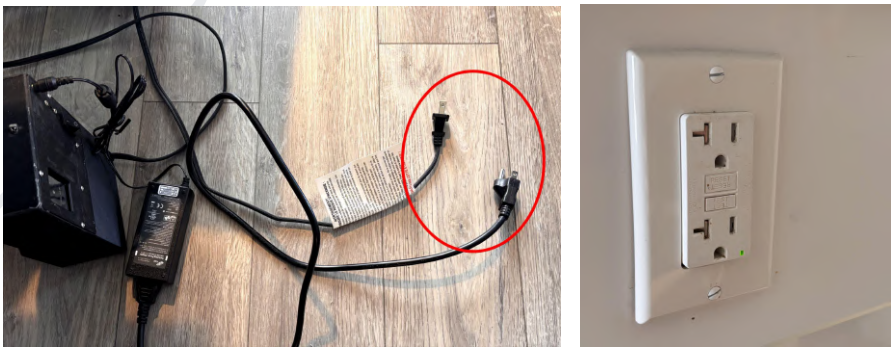

Figure 30. Power the system

5. Once the device is powered on, use the IR remote to set the target temperature. The set and current temperatures will be displayed on the LCD screen (Figure 31). The product will gradually heat to the target temperature, at which point printing tasks may commence. **DO NOT TOUCH THE DEVICE DURING ITS OPERATION.**

Figure 31. LCD Display

6. After use, disconnect **ALL** external power sources before removing the device from the printer.

5.2 Remote Controller

Eleven programmed keypads are presented in the hand-held IR remote. Temperature settings for 9 common 3D printing filaments have been pre-programmed (Appendix N). Other keys on the remote remain undefined, leaving room for future upgrades.

Figure 32. Keypad Definition

When using the remote control, keep the IR receiver (Figure 33) clear of any obstructions. Covering it may block the infrared signals and stop the remote from working properly.

Figure 33. left: IR receiver; right: IR sender

5.3 Data Acquisition

The device uses fixed hardware serial protocol with a default baud rate of 9600 to send data in the following sequential structure at 20Hz:

$$[design\ sensor\ reading,\ target\ setpoint,\ heater\ status\ (1\ means\ ON,\ 0\ means\ OFF)]$$

Users can connect a computer to the data acquisition port and employ any serial port reading software to read and store data. If the users do not have serial reading tools, then can use the MATLAB serial tool provided by the team (Appendix O). The tool reads and saves the complete serial port data (50 Hz) and plots real-time curves of the chamber temperature, heater status, and time. All data will then be automatically saved to an Excel file in the default location (Desktop).

5.4 Reprogrammability and Future Upgrades

The user can connect the computer to the data acquisition port for code uploads. The code needs to be compiled and uploaded using Arduino IDE 1.8.19 or a later version. When uploading the code, please disconnect all power supply cables. Once the upload is complete, the user should follow the manual in Section 5.1, after which the device will automatically resume normal operation.

6. Experiment & Test

The chapter details experiments during the development process, including product optimization, Design of Experiment (DOE), and the final validation.

The primary goal of the design is to achieve stable and uniform temperature distribution within the chamber. To systematically assess the impact of various factors on overall performance, the team developed a Product Functional Decomposition (PFD) diagram (Figure 34). In this diagram, Control Factors (CF) represent the variables that directly and significantly affect product performance, while Specifications (SPEC) denote factors with indirect effects.

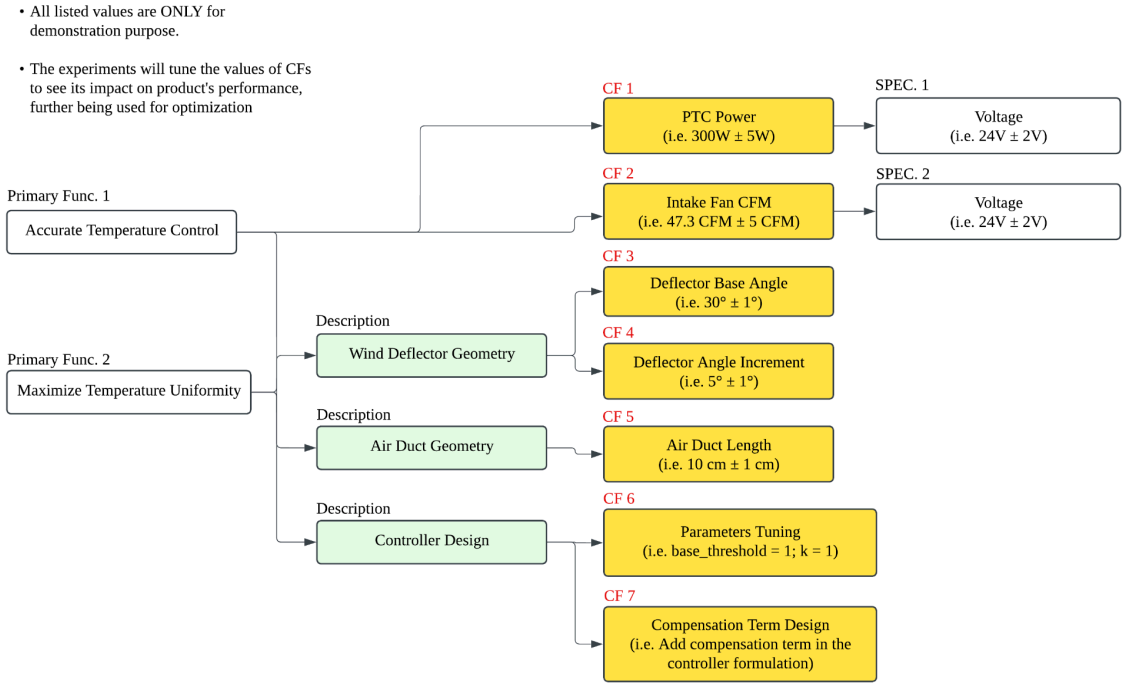

Figure 34. PFD Diagram

(Detailed descriptions of the CFs are provided in the corresponding tuning sections)

Four major experiments were conducted sequentially, **with each one tuning specific CF(s) for verification and refinement.** For clarity, these experiments are labeled as shown in Table 5.

Table 5. Experiment Table

ID	Involved CF(s)	Description
1	CF 1	PTC Heater Selection
2	CF 2	Intake Fan Selection
3	CF 3, 4, 5	Wind Deflector and Air Duct Structural Optimization
4	CF 6, 7	Controller Design, Calibration, Parameter Tuning, and Final Verification

6.1 Test Environment and Setup

Due to the complexity of the system, relying solely on computational-based experiments cannot guarantee the accuracy of the simulation models or the result validity. Consequently, all optimizations are experimental-based in real-world environments.

6.1.1 Testing Chamber, Sensor Matrix

An 1:1 testing chamber with dimensions identical to the original printer (793 mm × 640 mm × 420 mm) (Figure 35) (Appendix P) is constructed and placed in room temperature (25°C). To manage costs, the frame of the chamber was fabricated using 1’ × 1’ wooden planks. The walls incorporated 5 mm thick acrylic planks (Appendix Q), identical to the original printer.

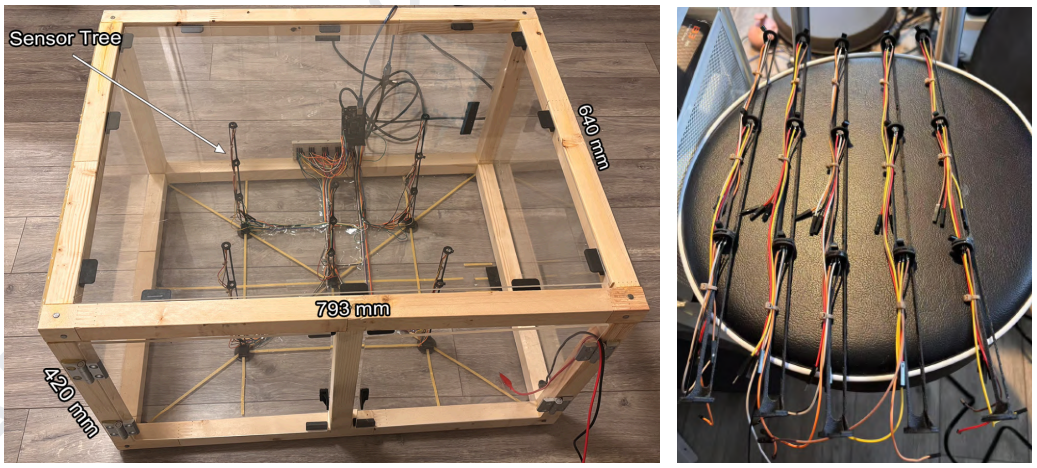

Figure 35. Testing Chamber (left); Sensor Tree (right)

A total of 15 *LM35 semiconductor temperature sensors* (±0.5°C; later referred to as “***sensor matrix***”) were deployed to form a sensor matrix, serving as a “ground truth” measurement of the chamber temperature. The sensor matrix is primarily composed of five “sensor trees” (Figure 36; Appendix R). Each sensor tree incorporates three sensors, installed at heights of 11 cm, 22 cm, and 33 cm, respectively. This arrangement enables the measurement of the three-dimensional temperature distribution, allowing the team to evaluate both the chamber’s spatial average temperature and uniformity.

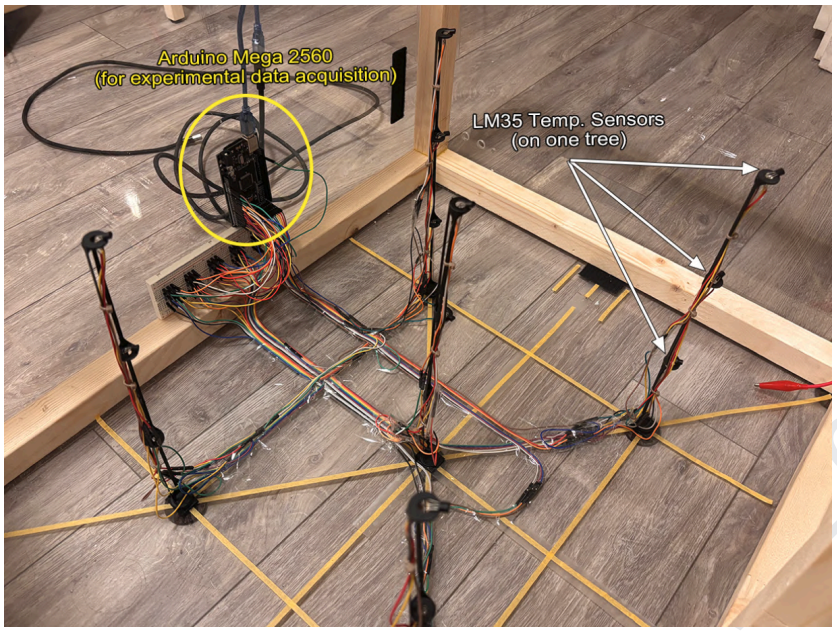

Figure 36. Sensor Tree

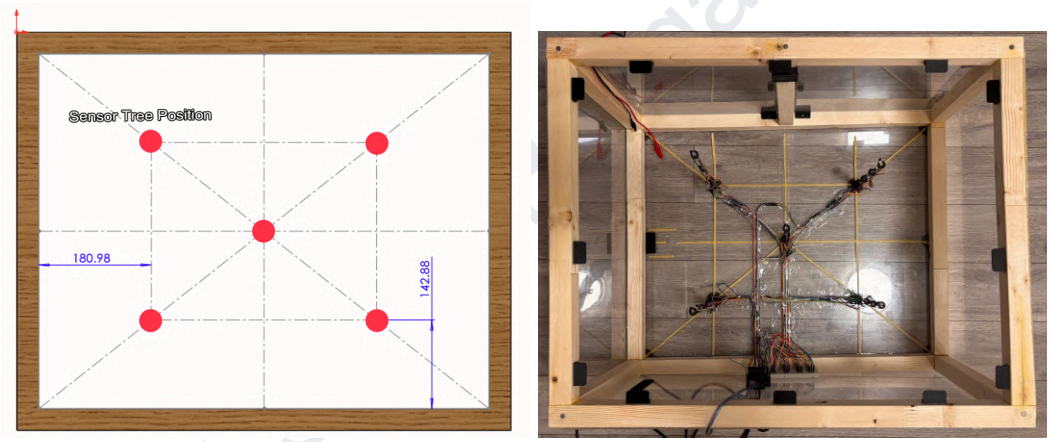

Figure 37. Sensor Tree Placement

Sensor matrix was connected to an Arduino Mega 2560, dedicated to experimental data acquisition (Figure 36). The Arduino Mega recorded temperature readings from all 15 sensors (at 1 Hz) and transmitted the complete sensor matrix readings to a computer via the serial port, where it was saved into an Excel spreadsheet stored locally.

A MATLAB program was used to process and visualize the real-time data (Appendix S), capturing and plotting individual sensor readings, as well as computing the average and standard deviation across all 15 sensors of the matrix. All data were mapped onto a 1:1 digital twin (Figure 38), providing an intuitive real-time visualization of the temperature distribution.

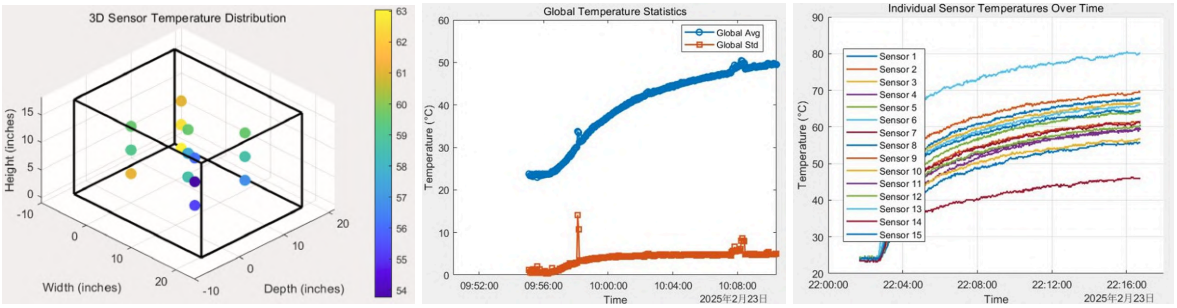

Figure 38. Digital Twin, Data Plot

The real-time spatial average temperature (*Global Avg.*) serves as a measure metric for the current chamber temperature, while the standard deviation (*Global Std.*) is used to assess chamber temperature uniformity. A substantial gap between the spatial average and the target setpoint indicates suboptimal control precision, while an elevated standard deviation points to a non-uniform distribution.

6.1.2 Mounting Bracket

Experiments 1 – 3 (Table 5) focused on optimization of the hardware design. Since the final design dimensions had not been finalized during this iteration, various hardware configurations were tested, making it impractical to use an enclosure with fixed dimensions. The team thus developed two modular brackets to mount various PTC heaters, fans, and wind deflectors.

Both brackets mount the fan at the top, drawing air into the duct, forcing it through the PTC heater, and expelling it from the bottom (Appendix T). For DC-powered heaters with lower power ratings (≤ 300W), the heaters were mounted on Bracket A (Figure 39). For AC-powered heaters with higher power ratings (> 300W), the heaters were mounted on Bracket B (Figure 40). (Appendices U, V)

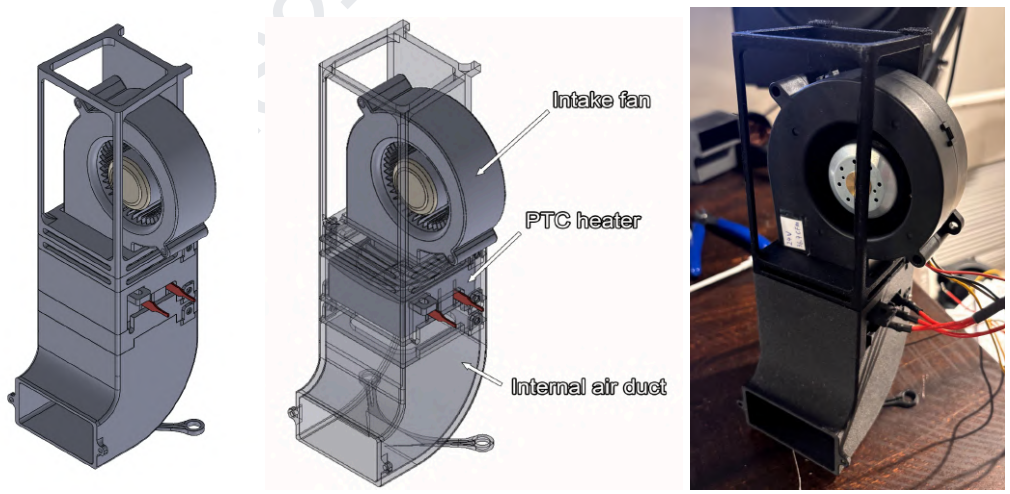

Figure 39. Bracket A

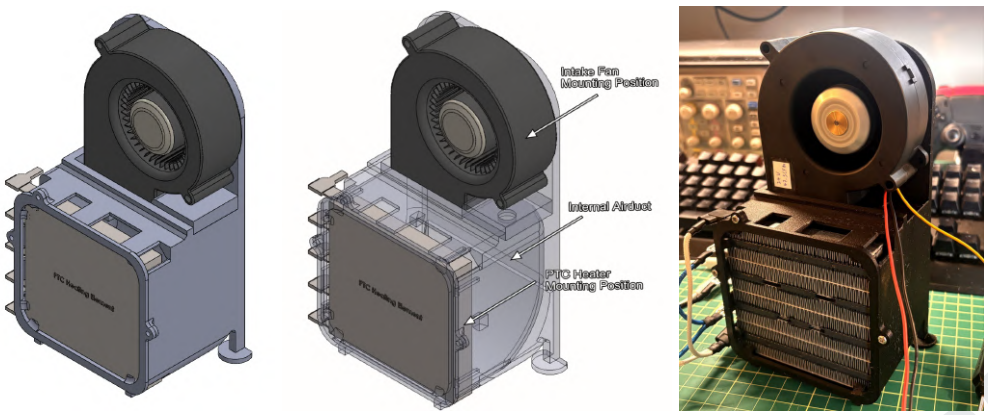

Figure 40. Bracket B

6.2 Analysis, Optimization, Experimental Validation (AOE)

This chapter detailed experiments listed in Table 5. Experiments 1 and 2 use a trial-and-error approach to determine the hardware configurations, while experiments 3 and 4 apply a data-driven model for systematic optimization.

6.2.1 PTC Heater Selection (Experiment ID 1)

***Objective**: Select the PTC model that can heat the chamber to 65°C while having minimum time.*

***Involved CF(s):** CF 1*

To achieve rapid heating, selecting an appropriate PTC heater is crucial, as its performance directly determines the heating rate. The tests began with a 100W unit, followed by 180W and 300W (24 VDC) models. All tests were conducted at 25°C with a 36 CFM for force convection.

Evaluation Metric: For each PTC model, it will be tested to heat the chamber from 25°C to 65°C. The time for the entire heating up process is recorded. If 65°C is not reached, the steady-state temperature is recorded.

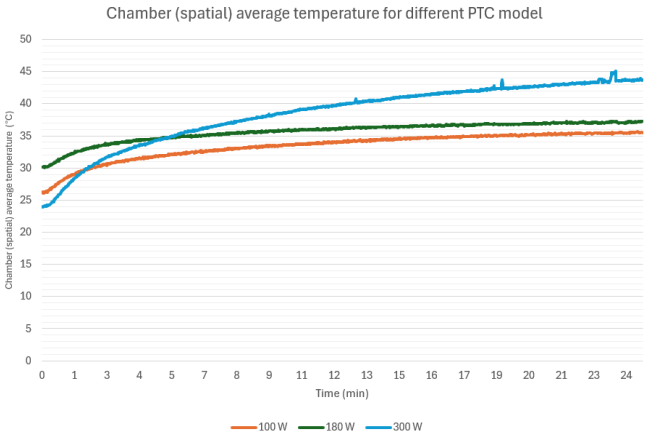

Figure 41. Chamber temperature profile for different PTC models (24 VDC)

***Results**:* Three DC heaters approached steady-state temperatures of 35.4°C, 37.2°C, and 43.7°C, respectively, falling short of the 65°C target (Figure 41).

A higher power PTC element is needed. However, most heaters above 300W operate on 120 VAC, posing safety risks during assembly. Although some DC models exist (＞300W), the superior high currents complicate the selection of power supplies and wire connectors (Appendix W). In contrast, AC-driven heaters can be directly connected to wall power, which simplifies wiring. Given this tradeoff, a PTC heater rated at 1500W was chosen (**However, tests revealed its actual maximum output to be 800W (Appendix X)*).

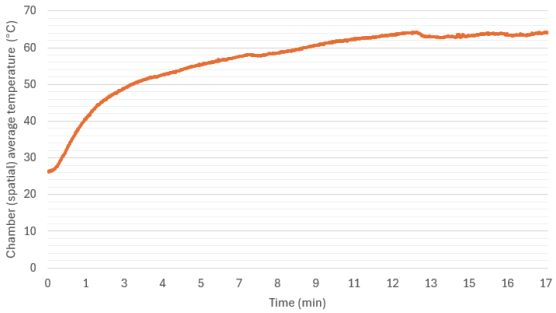

Figure 42. Chamber (spatial) average temperature for 800W AC heater

Experiments show that the enclosure reaches 65°C within ~17 minutes, demonstrating that the 800W PTC heater meets the heating requirements with satisfactory performance. Consequently, the team will select this heater and use it for later experiments.

6.2.2 Intake Fan Selection (Experiment ID 2)

***Objective**: Select the optimal centrifugal fan by comparing airflow performance.*

***Involved CF(s):** CF 2*

Cubic Feet per Minute (CFM) measures fan airflow, directly affecting the air volume passing through the heater and, consequently, the heating speed and temperature uniformity. Due to the system's complexity, calculating the exact required CFM is challenging; therefore, the team adopted a trial-and-error approach to select the fan.

Usually, a larger fan can generate higher airflow more easily, but it also makes the design bulkier. To balance performance and compactness, the team selected four fans (diameter＜10 cm) with CFMs of 18.6, 25.1, 36.7, and 47.3.

Evaluation Metric: Four different fans were installed with the AC PTC heater, and the system was heated from 25°C to 60°C. The heating time and the temperature standard deviation at 60°C were recorded to assess thermal efficiency and uniformity.

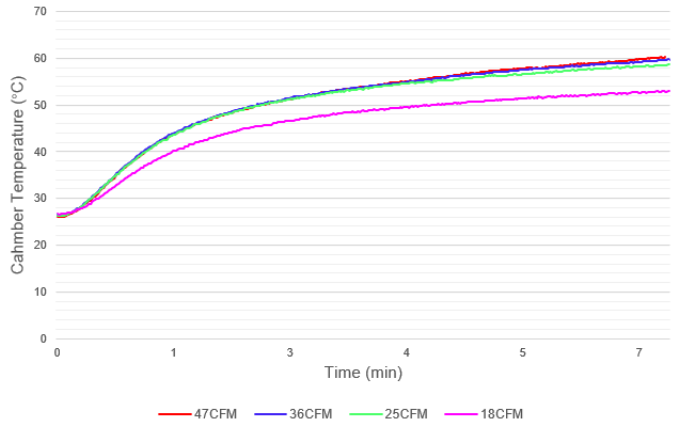

Figure 43. Chamber spatial average temperature profile

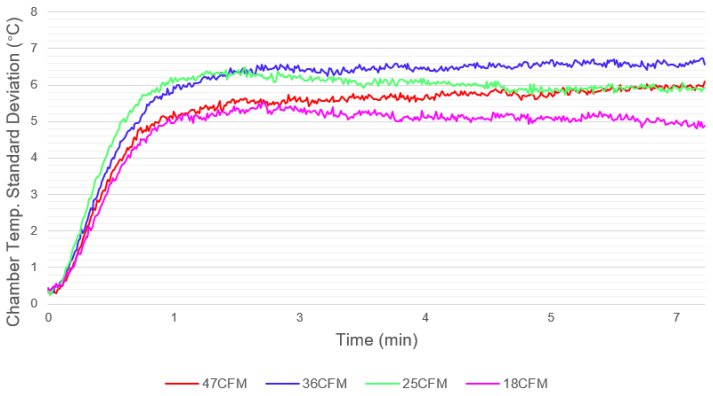

Figure 44. Chamber temperature standard deviation profile

Results: The configuration using the 47.3 CFM fan has the fastest speed to heat up the chamber (Figure 43), confirming that high airflow enhances rapid air movement and more efficient heat exchange.

Although the 18.6 CFM fan performs better in terms of temperature uniformity (Figure 44), its airflow is insufficient for the PTC heater to reach the standard operating power, with a steady-state temperature of only ~ 53°C (Appendix X).

After balancing heating speed and temperature uniformity, the 47.3 CFM fan was chosen and was used in subsequent experiments.

6.2.3 Wind Deflector and Air Duct Structural Optimization (Experiment ID 3)

Objective: *Use the Design of Experiment (DOE) to investigate the interaction between deflector and air duct geometry. Optimized for uniformity.*

Involved CF(s): *CF 3, 4, 5*

Before optimization, the difference between the highest and lowest temperatures inside the chamber was nearly 20°C (Figure 45), leading to localized overheating or underheating and indicating the need for a more uniform temperature distribution.

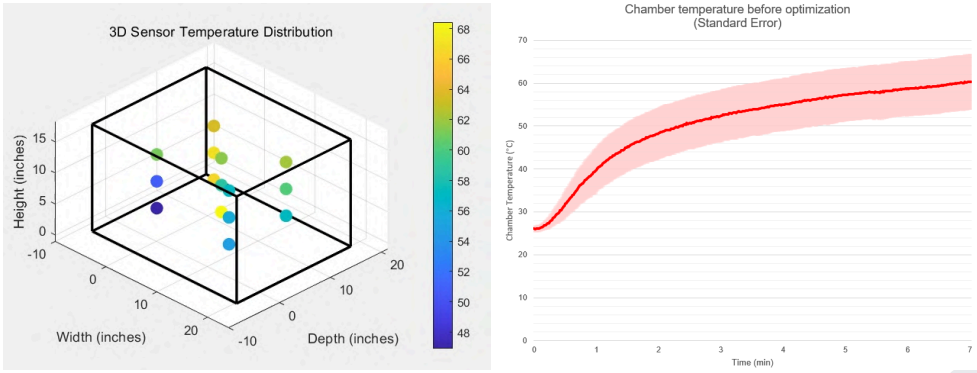

Figure 45. Chamber temperature profile before optimization

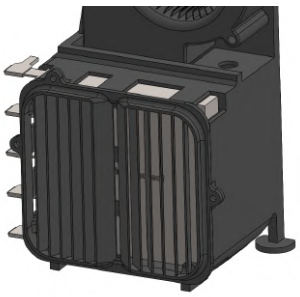

Figure 46. Deflector at the air outlet

Figure 45 shows that hot air primarily accumulates at the center of the enclosure. The team decided to design a deflector (Figure 46) to disperse the hot air toward the sides to increase uniformity. Moreover, the length of the air duct may influence the temperature distribution. A longer duct can draw air from the upper region, potentially affecting overall airflow uniformity. Given the potential interactions between these factors, the team defined three CFs corresponding to CF 3, 4, and 5 in the PFD diagram (Figure 34).

1. CF A - Deflector Base Angle (θ): The angle between the first blade and the vertical axis (Figure 47). The discrete levels are 0°, 10°, 30°, 50°, and 70°.

2. CF B - Deflector Angle Increment (Δθ): The angular difference between adjacent blades (Figure 48), which determines the relative direction of airflow. The discrete levels are -8°, 0°, and 5°.

3. CF C – Air Duct Length (*L*): The vertical distance from the intake fan to the heater fins (Figure 49). The discrete levels are 10 cm, 18.6 cm, and 27.2 cm.

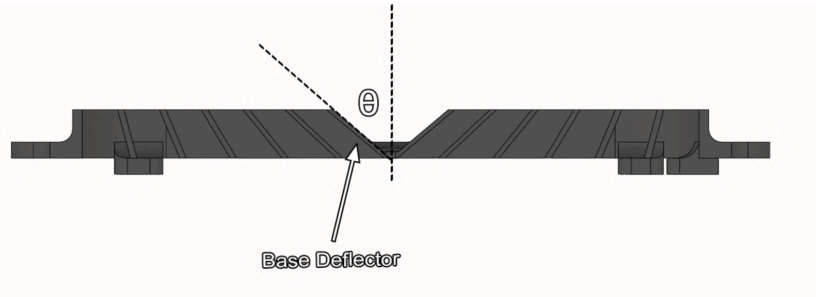

Figure 47. Cross-sectional view of the deflector. Deflector Base Angle (θ = 70°)

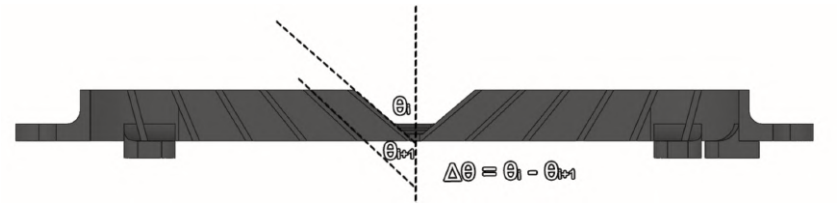

Figure 48. Cross-sectional view of the deflector. Deflector Angle Increment (Δθ = 5°)

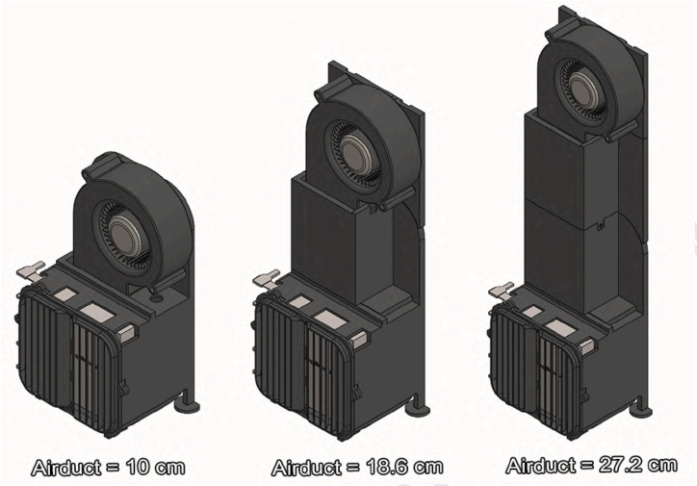

Figure 49. Air Duct Length

To systematically study the effect of the three control factors on temperature uniformity, the team employed a full factorial DOE. **The originally continuously adjustable ranges of three factors were converted into multiple discrete levels, and all combinations of these levels were tested, resulting in 36 different configurations** (Table 6).

Table 6. Full Factorial DOE setup (complete version see Appendix Y)

Config. ID	CF A (θ)	CF B (Δθ)	CF C (*L*)
1	0	0	10.0
2	10	0	10.0
3	10	8	10.0
4	10	-5	10.0
…	…	…	…
36	70	8	27.2

The team 3D printed 12 distinct wind deflector models along with corresponding wind duct extension components, which were then installed on Mounting Bracket B (Figure 50, 51) and placed at the side wall of the chamber.

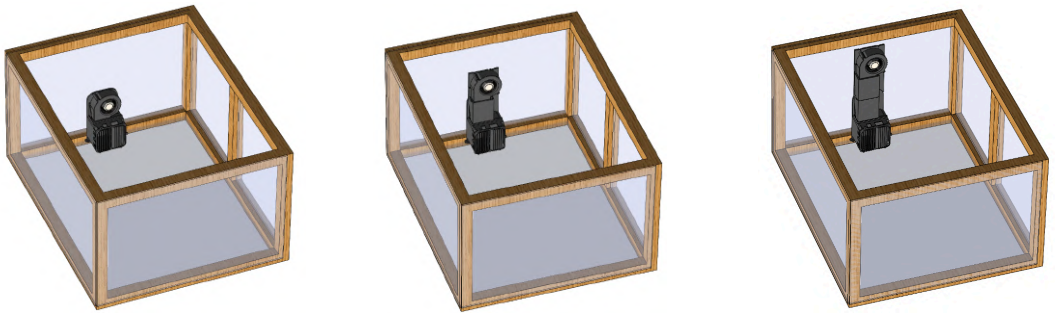

Figure 50. Full factorial experiment setup demonstration

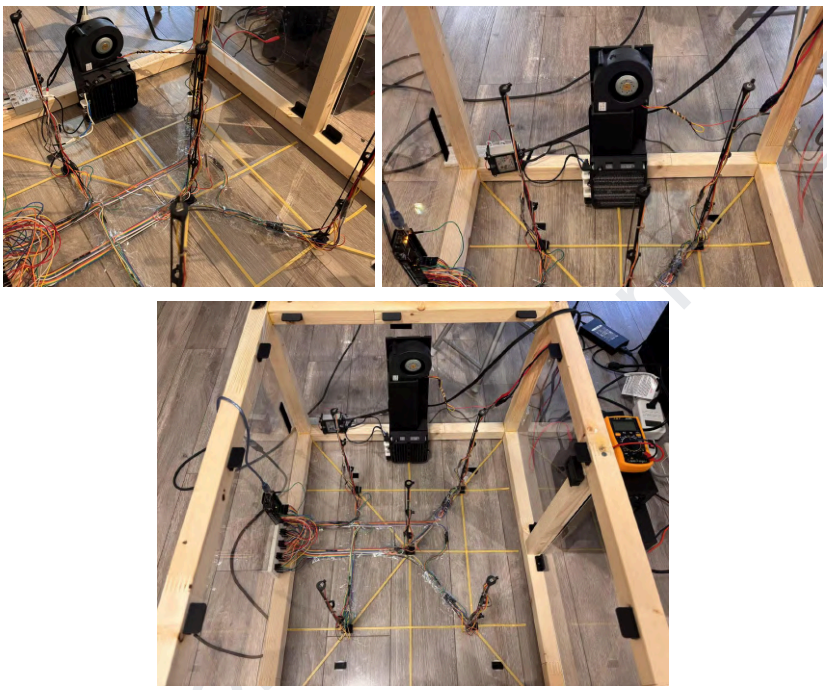

Figure 51. Three examples from the full factorial experiment setup
(top left: CF A = 30°, CF B = 0°, CF C = 10.0 cm;
top right: CF A = 0°, CF B = 0°, CF C = 18.6 cm;
bottom: CF A = 30°, CF B = 0°, CF C = 27.2 cm)

Evaluation Metric: Each configuration underwent a heating experiment starting from room temperature (25°C) with a target of 60°C. The temperature standard deviation at 60°C was measured and compared.

Table 7 - DOE result (complete data in Appendix Y)

Config. ID	Standard Deviation @ 60°C
1	5.946113817
2	2.760555346
3	6.430388196
…	…
36	4.854736641

***Modeling**:* Full factorial experimental data (Appendix Y) shows that extending the wind deflector outward results in a gradual decrease in temperature uniformity, and similarly, increasing the duct length makes the temperature less uniform. To precisely quantify the influence of these factors, the team employed **Response Surface Methodology (RSM)** to perform a regression analysis. The fitted model, detailed in Appendix Z, predicts the chamber temperature's standard deviation as a function of the deflector geometry and duct length. The optimization goal is to minimize this standard deviation—ideally reducing it to zero—to achieve perfectly uniform temperature distribution across the chamber.

$$\text{Chamber Temp. StDev.} = 3.800 - 0.060A + 0.103B + 0.067C + 0.001A^2 + 0.023B^2 - 4\times10^{-5}C^2 - 0.005\,AB - 0.001\,AC + 0.004\,BC$$

In the formula, A, B, and C represent the numerical values for each CF. To prevent overfitting, only the main effects and two-factor interaction terms were included in the regression analysis. The fitted model is visualized as a contour plot in Figure 52.

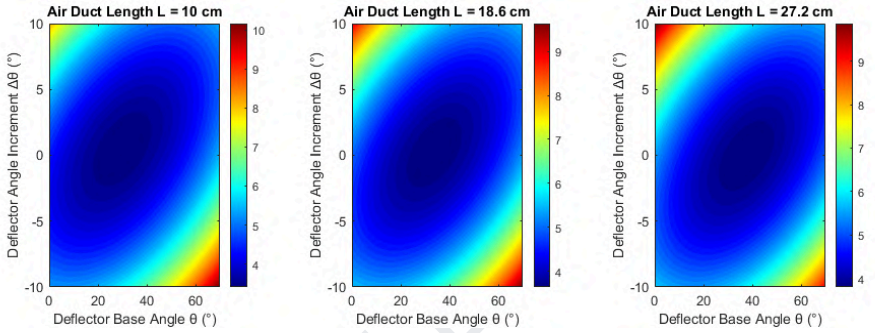

Figure 52. Regression Model Visualization
(contour level: temperature standard deviation at 60°C)

A GRG (generalized reduced gradient) optimization (Appendix AA) is applied to the model, to extrapolate the fitted function and identify the optimal CF levels. The result predicted that the best performance would be achieved when the **deflector base angle (*θ*) was set to 29.87°, the deflector angle increment (*Δθ*) to 0.48°, and the air duct length (*L*) to 10 cm** (Figure 53).

Predicted Temp. Std.	3.412863969
Parameters	
A	29.86776112
B	0.481909008
C	10
A^2	892.0831542
B^2	0.232236292
C^2	100
AB	14.39354312
AC	298.6776112
BC	4.819090076

Figure 53. GRG Optimization Result

Figure 54. Chamber temperature profile vs. time
(solid curves indicate chamber average temperature; lighter region indicates the variance)

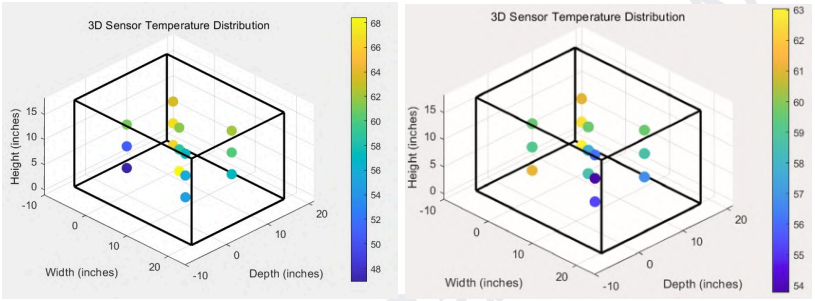

Figure 55. Chamber temperature profile (average temp. = 60°C)
(left: no optimization; right: optimized)

Verification & Conclusion*:* One additional verification run using optimized parameters is conducted. The results proved that the optimal configuration reduced the standard error from **~10°C to ~5°C** (Figure 54, 55), standard deviation (@ 60°C) from **5.93 to 2.20**, improving temperature uniformity by **62.9%**.

Although one evident trade-off is that the optimized system heats up at a slower rate, the additional time to reach 60°C is only three minutes — an interval that is negligible relative to the several-hour duration of a typical printing task. Consequently, the team opted to prioritize enhanced temperature uniformity over a faster heating rate. The optimized deflector and air duct structure is applied to the final design and is being used in later experiments.

6.2.4 Controller Design, Calibration, and Parameter Tuning (Experiment ID 4)

Involved CF(s): *CF 6, 7*

This chapter details the design, calibration, and parameter-tuning process of the controller. To achieve a high-precision, stable temperature control system, the team conducted 5 sequential sub-experiments (Sections 6.2.4.1–6.2.4.5) to progressively optimize the controller:

1. Preliminary Correlation Function Establishment
2. Dynamic Baseline Design

3. Parameter Tuning (k)
4. Long-Term Temperature Control, Augmented Correlation Function, Final Verification

Figure 56. Setup in controller tuning tests

6.2.4.1 Preliminary Correlation Function Establishment

***Objective**: Obtain the preliminary correlation between the in-built temperature sensor and the actual chamber average temperature.*

As elaborated in Section 3.8.2.1, a single built-in TSIC 306 sensor may not accurately reflect the spatial average of the chamber temperature, further affecting the error term e calculation and control accuracy.

$$e = Target\ Temperature - \widehat{temp}$$

$$\widehat{temp} = f(sensor\_temp)$$

A preliminary correlation function, f, is established that takes sensor raw data and converts it to the estimated chamber temperature ($\widehat{temp}$). To model the function, the team conducted a correlation experiment for 3 trials with the same setup. In each trial, the chamber was ramped from 25°C to 65°C. At each time step, the reading from the design's built-in TSIC 306 sensor was recorded, along with the average value from the sensor matrix (served as a ground truth, $temp$) (Figure 57).

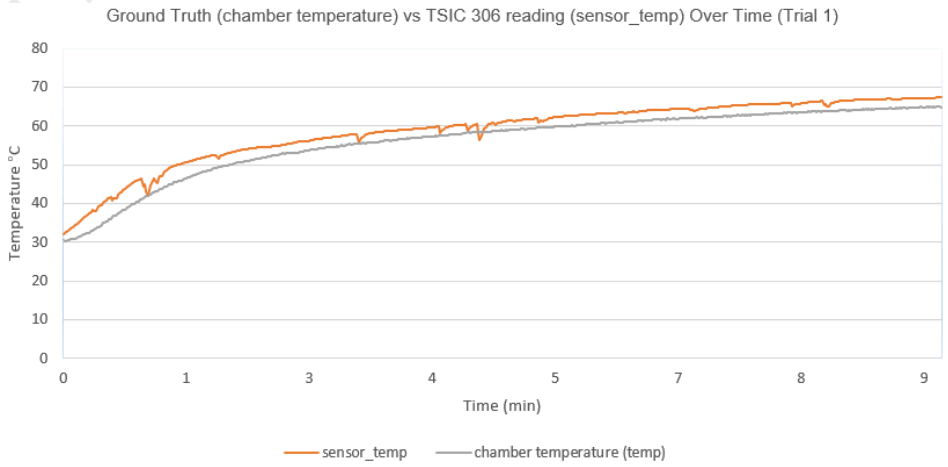

Figure 57. Ground Truth ($temp$), TSIC 306 reading ($sensor\_temp$) vs. time

For each trial's result (Appendix AB), a first-order (linear) fit was applied to correlate the TSIC 306 sensor reading with the chamber temperature (Figure 58).

$$\widehat{temp} = k \times sensor\_temp - b$$

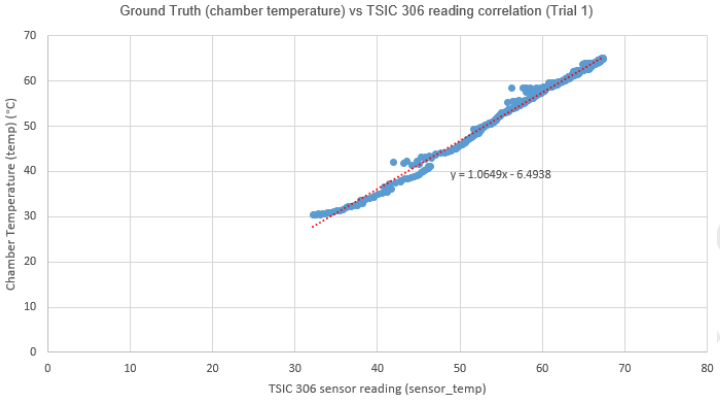

Figure 58. Correlation between sensor reading and chamber temperature
*(*only trial 1 is shown here)*

The results of both parameters k and b of the linear function from the three fits were then averaged, yielding a linear correlation function:

$$\widehat{temp} = 1.0523 \times sensor\_temp - 6.6486$$

This function provides a preliminary correlation between the raw temperature readings from the TSIC 306 sensor and the ground truth chamber (spatial average) temperature. This function served as the baseline correlation model for later tests, and it was subsequently fine-tuned in Section 6.2.4.4.

6.2.4.2 Dynamic Baseline Design

Objective: *Investigate the effect of* $base\_threshold$ *on the controller's accuracy. Design the dynamic* $base\_threshold$ *mechanism to achieve a control accuracy of ±0.5°C.*

As elaborated in Section 3.8.1, at every time step, the controller computes the error term e and compares it to the $threshold$ heater regulation.

$$threshold_t = base\_threshold + k[\,temp_t - temp_{t-1}]$$

(where " t " indicates at current time step)

The focus of this experiment is on assessing the impact of $base\_threshold$ on control accuracy. **By default,** $base\_threshold$ **is designed to be fixed and set to 1.** The team then conducted five experiments at 40, 45, 50, 55, and 60°C ($base\_threshold = 1;\ k = 1$).

In each test, the chamber was heated up and held at the setpoint for a short period (Figure 59). **At each time step, the spatial average of the sensor matrix is calculated, providing a key indicator of the chamber temperature. The temporal average of these spatial averages is then used to assess the steady-state error** (Appendix AC).

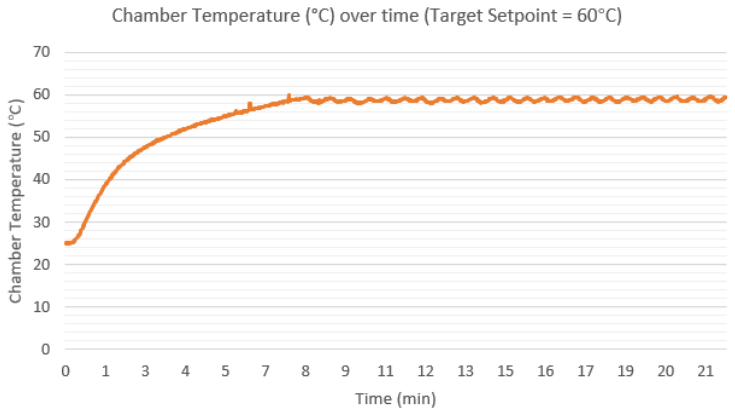

Figure 59. Chamber spatial average temperature profile (setpoint = 60°C)

Table 8 - Chamber temperature at the steady state when $base\_threshold = 1;\ k = 1$

Target Setpoint ($Target\ Temp$) (°C)	**Scaled (Normalized) Target Setpoint (°C)**	**Temporal Average Temp. (°C)**	**Steady State Error (offset) (°C)**
40	2.00	42.10215311	2.102153115
45	2.25	46.11204653	1.112046534
50	2.50	50.30813835	0.30813835
55	2.75	54.65026833	-0.34973167
60	3.00	58.86034654	-1.139653457

Results (Table 8) reveals that at different setpoints, a steady state error ("offset") is consistently observed. This indicates that the heater is deactivated either too late (the "offset" is positive, means the $threshold$ is set too low) or too early relative to the setpoint.

To compensate, the team defined the Dynamic Adjustment Headroom (DAH) as equal to the "offset" itself and incorporated it into the default $base\_threshold$, thereby dynamically adjusting the shutdown timing to remove this steady-state error.

$$base\_threshold_{dynamic} = 1 + Dynamic\ Adjustment\ Headroom$$

DAH can be formulated as a function of the $Target\ Temp$. The offset in Table 8 was modeled using a third-order polynomial fit with respect to the $Target\ Temp$. T**he intended effect is that for a higher steady state, a corresponding higher base threshold causes the heater to shut down proportionally earlier, effectively minimizing the steady-state error.** To mitigate fitting errors caused by differences in scale, all $Target\ Temp$ were scaled by dividing by 20. Figure 60 illustrates the relationship between the normalized $Target\ Temp$ and the DAH.

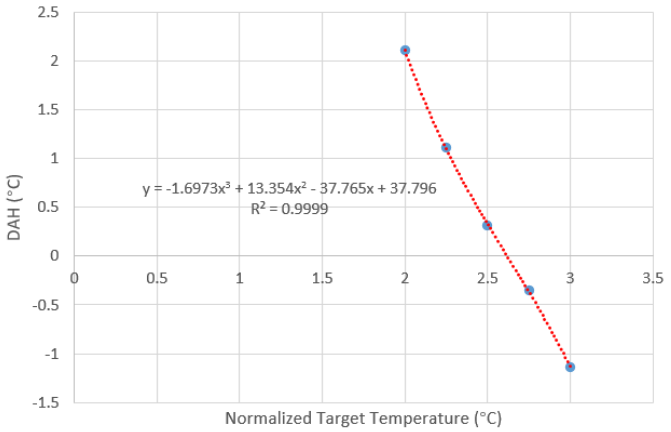

Figure 60. Correlation between normalized target setpoint and DAH

$$base\_threshold_{dynamic} = 1 - 1.6973x^3 + 13.354x^2 - 37.765x + 37.796$$

(where " x " indicates Normalized Target Temperature)

Verified by three additional verification runs at 40°C, 50°C, and 60°C (Table 9; Appendix AD), implementing such dynamic base threshold mechanism can achieve accuracy within ± 0.5°C, reducing the steady state error up to **98.6%** (Figure 61).

Table 9 - Chamber temperature at the steady-state after implementation of dynamic *base_threshold*

Target Setpoint (*Target Temp*) (°C)	**Temporal Average Temp. (°C)**	**Steady State Error (°C)**	**Reduction in Absolute Steady State Error**
40	40.17555858	0.175558576	91.6%
50	50.21341346	0.213413462	30.7%
60	60.01593244	0.015932442	98.6%

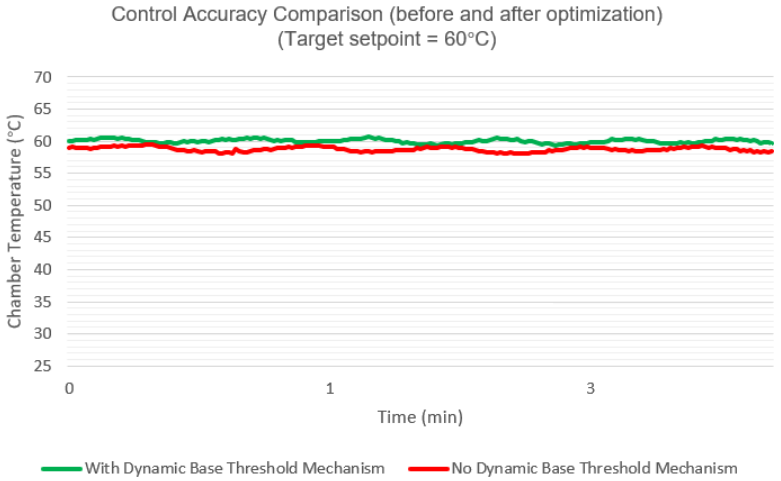

Figure 61. Chamber spatial average temperature profile

6.2.4.3 Sensitivity Tuning for Oscillation Reduction (Controller)

***Objective**: Investigate the effect of k on the controller's sensitivity. Tune the k in the dynamic controller to achieve a steady state oscillation ≤ 0.5°C.*

Severe oscillations still occur around the setpoint (Figure 62). As described in Section 3.8.1, increasing k prompts a faster response to fluctuations, thereby reducing oscillations.

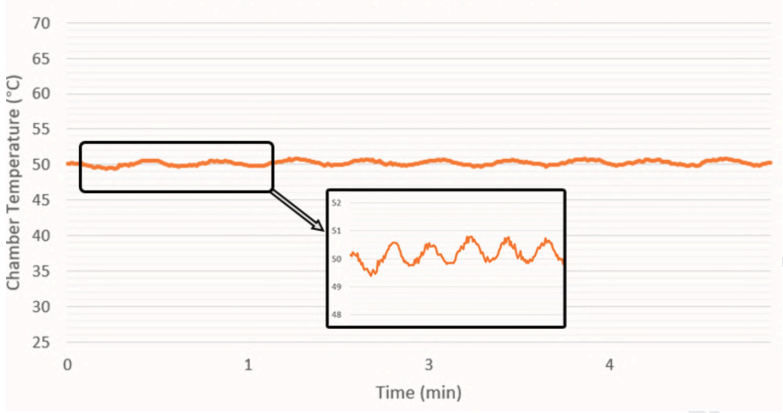

Figure 62. Oscillation at the setpoint when k = 1 (setpoint = 50°C)

The team adopted a trial-and-error method to investigate the optimal k. Eight experiments were conducted with $k \in \{1, 10, 25, 50, 75, 100, 125, 150\}$. In each test, the chamber was heated from 25°C to 50°C (Appendix AE) and held at the setpoint for 5 minutes. At the setpoint, both the temporal average and the oscillation amplitude of the chamber temperature (spatial average) are recorded.

Table 10 - Steady-state error and oscillation for different k values

k	Temporal Average Temp. (°C)	Steady State Error (°C)	Oscillation Amplitude (°C)
1	50.21341346	0.213413462	0.6623
10	50.13166023	0.13166023	0.6221
25	50.05199782	0.051997825	0.5464
50	50.0364652	0.036465201	0.4015
75	49.97041278	-0.029587222	0.2736
100	49.6785119	-0.321488095	0.3667
125	49.87050174	-0.129498258	0.4886
150	49.13662857	-0.863371429	0.1924

An optimal value $k = 75$ is found to best eliminate oscillation amplitude (0.27°C) while still providing a high accuracy (-0.03°C) (Table 10; Appendix AF). Compared to $k = 1$, the oscillation was reduced by **58.6%** (Figure 63). This value is concluded to be a suitable value that was applied to the final controller design.

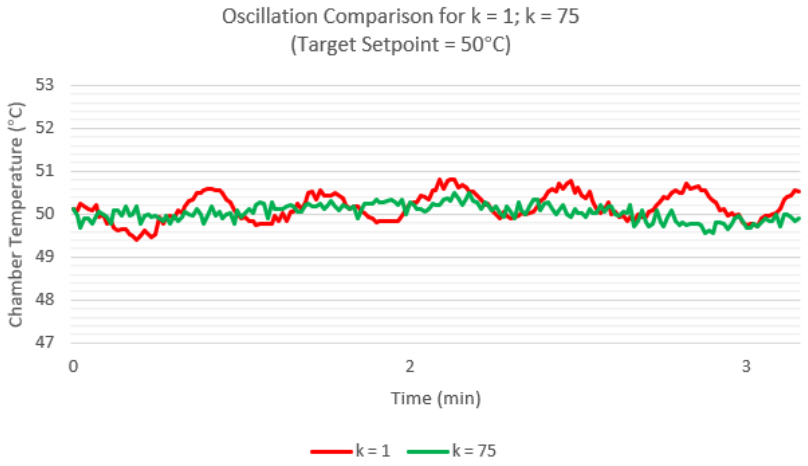

Figure 63. Oscillation Comparison for $k = 1$; $k = 75$

To conclude, the optimized final version of the dynamics error threshold is thus:

$$threshold_t = 1 - 1.6973x^3 + 13.354x^2 - 37.765x + 37.796 + 75\times[\,temp_t - temp_{t-1}]$$

(where "x" indicates Normalized Target Temperature)

6.2.4.4 Long-Term Temperature Control Performance Evaluation and Final Calibration

***Objective**: Evaluate long-term temperature control performance and finalize calibration to ensure product accuracy during extended operation.*

Following the controller parameter tuning in Sections 6.2.4.2 and 6.2.4.3, the product underwent long-term operational testing to verify its performance over extended use. Three sets of experiments were conducted, starting from an ambient temperature of 25°C and held at target setpoint (40°C, 50°C, and 60°C respectively) **for 2 hours** (Appendix AG).

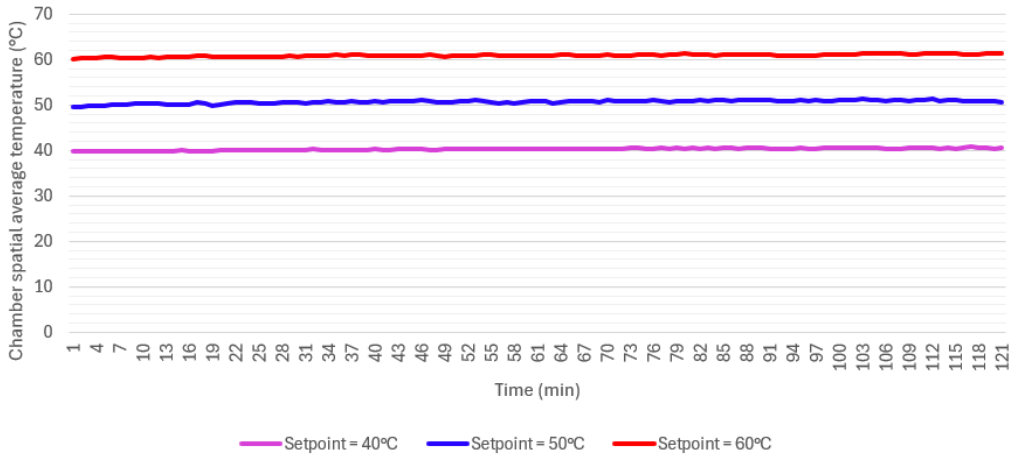

Figure 64. Chamber temperature at the steady state for setpoint = 40, 50, 60°C

Although Figure 64 shows that the error remains small near the setpoint, a closer examination (Figure 65) reveals that all three experiments experienced varying degrees of temperature offset (later referred

to as "***temperature drifting***"). This behavior results in the temperature accuracy gradually drifting beyond the ±0.5°C range during extended heating.

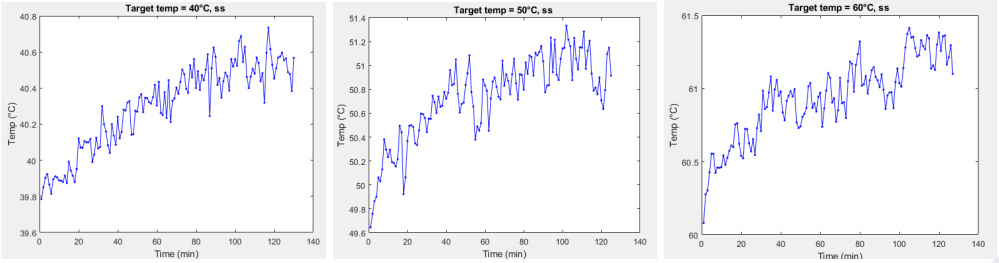

Figure 65. Temperature Drifting (40, 50, 60°C)

One major cause of this issue is the application of the linear sensor correlation function (established in Section 6.2.4.1) to estimate the chamber's real-time temperature, which is then used as the controller's input.

$$\widehat{temp} = 1.0523 \times sensor\_temp \; - \; 6.6486$$

This correlation function was derived from heating experiments ramped from 25°C to 65°C (Section 6.2.4.1), however, as the chamber temperature eventually stabilizes at a fixed target, the air distribution within the chamber changes. Though it can predict chamber temperature during the short-term heating process, **it becomes less precise during extended operation.** This shortcoming causes the built-in temperature sensor to underestimate the actual chamber temperature during extended operation, resulting in continuous heating that gradually drifts away from the set point.

$$\widehat{temp} = 1.0523 \times sensor\_temp - 6.6486 + Compensation\left(\widehat{temp}, t\right)$$

$$Compensation\left(\widehat{temp}, t\right) = \begin{cases} 0, & \text{if } \widehat{temp} < \left(\text{Target Temp} - 1.5\right), \\ a + b\,e^{-ct}, & \text{if } \widehat{temp} \geq \left(\text{Target Temp} - 1.5\right). \end{cases}$$

(where " t " indicates the elapsed time after the temperature has reached (Target Temp - 1.5))

An augmented correlation function is designed. **An exponential compensation term is employed to model the drift**, as its asymptotic behavior reflects the energy input converges to a finite steady state. Since the drift occurs only when the chamber temperature nears the setpoint and is time-dependent, an activation function is employed. Once the chamber temperature reaches Target Temp - 1.5°C, the compensation term is activated.

The coefficients in the exponential compensation: a, b and c are also functions of the target setpoints. For each setpoint, an exponential fit was applied to model the drift (Figure 66), with the results documented in Table 11.

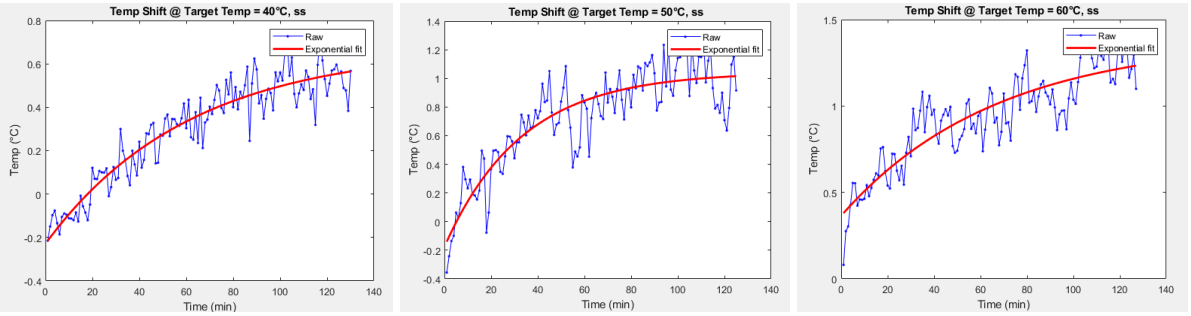

Figure 66. Exponential fit to model the drifting (40, 50, 60°C)

Table 11 - Coefficient for the exponential fit at 40, 50, 60°C

Target Setpoint (*Target Temp*) (°C)	**a**	**b**	**c**
40	0.6725	-0.9020	0.0164
50	1.0431	-1.2194	0.0302
60	1.3834	-1.0188	0.0151

Each coefficient was further individually fitted as a function of the target temperature (normalized) (Figures 67). To mitigate fitting errors caused by differences in scale, all $Target\ Temp$ were normalized by dividing by 20.

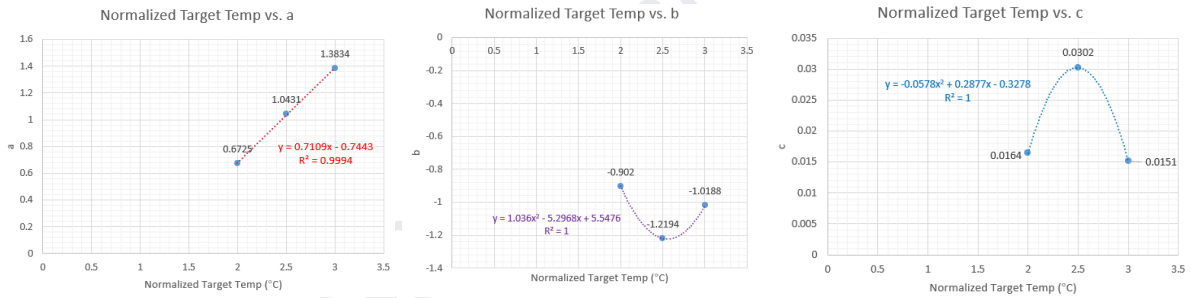

Figure 67. Coefficients as a function of normalized target temperature
(where "x" represents Normalized Target Temperature)

To conclude, the complete correlation function is:

$$\widehat{temp} = 1.0523 \times sensor\_temp - 6.6486 + Compensation\left(\widehat{temp}, t\right)$$

$$Compensation\left(\widehat{temp}, t\right) = \begin{cases} 0, & \text{if } \widehat{temp} < \left(\text{Target Temp} - 1.5\right), \\ a + b\,e^{-ct}, & \text{if } \widehat{temp} \geq \left(\text{Target Temp} - 1.5\right). \end{cases}$$

where,

$$a(\text{Target Temp}) = 0.7109 \times \left(\frac{\text{Target Temp}}{20}\right) - 0.7443,$$

$$b(\text{Target Temp}) = 1.036 \times \left(\frac{\text{Target Temp}}{20}\right)^2 - 5.2968 \times \left(\frac{\text{Target Temp}}{20}\right) + 5.5476,$$

$$c(\text{Target Temp}) = -0.0578 \times \left(\frac{\text{Target Temp}}{20}\right)^2 + 0.2877 \times \left(\frac{\text{Target Temp}}{20}\right) - 0.3278.$$

(where " t " indicates the elapsed time after the temperature has reached (Target Temp - 1.5))

The augmented correlation function was then verified through three additional runs at 40°C, 50°C, and 60°C, each maintaining the target temperature for **one hour**. The results show that the drifting issue was effectively resolved (Figure 68, 69), and the air distribution showed adequate uniformity under steady conditions (Figure 70). For each target setpoint, the control error, oscillation, and temperature standard deviation were recorded in Table 12 and concluded to be the finalization of all experiments.

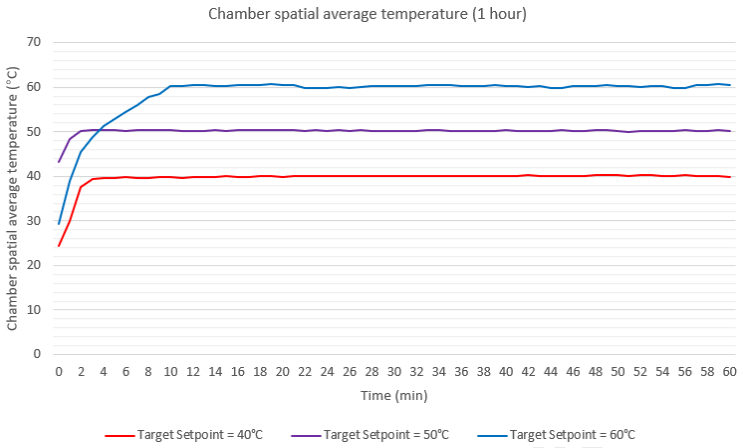

Figure 68. Chamber spatial average temperature profile (setpoint = 40, 50, 60°C)

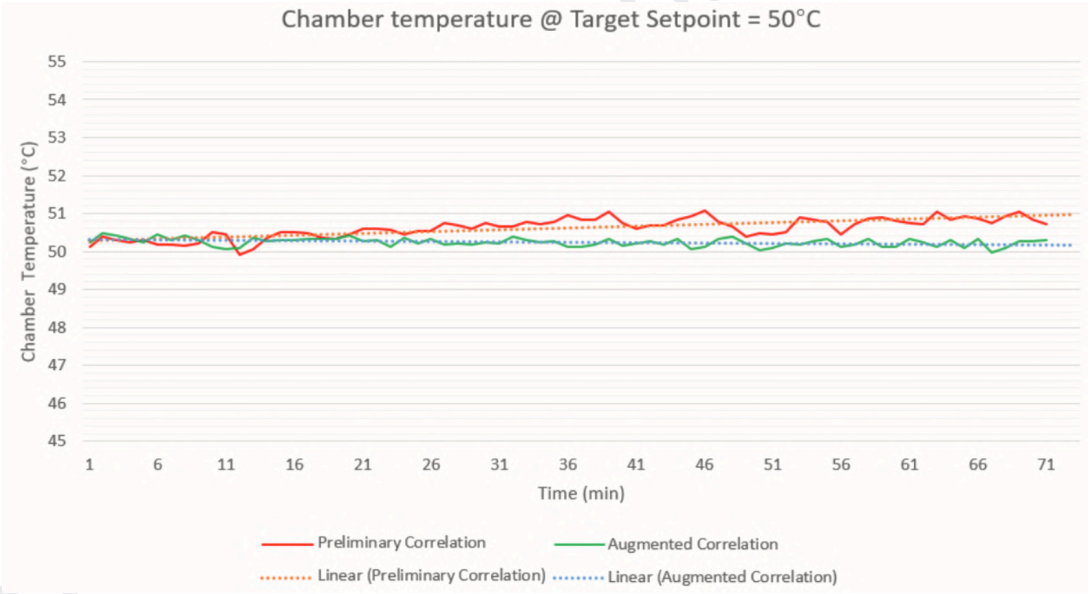

Figure 69. Comparison of the system's performance at steady state with the **preliminary** correlation function vs. with the **augmented** correlation function (with trend lines)
(time in the *x*-axis denotes time elapsed after reaching steady state)

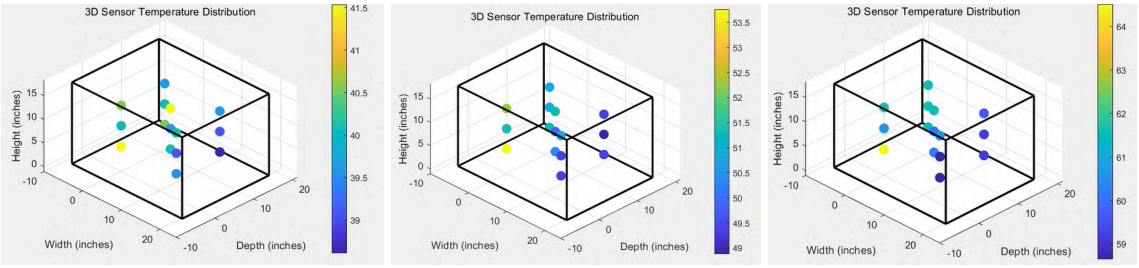

Figure 70. Chamber temperature distribution showing spatial uniformity (setpoint = 40, 50, 60°C)

Table 12 - Temperature Control Error and Stability Metrics (ss: steady-state) (Appendix AH)

Target Setpoint (°C)	Temporal Average Temp. (°C) @ ss	Error (°C)	Oscillation Amplitude (°C)	Chamber Temp. StDev. (°C) @ ss
40	40.10	0.10	0.20	0.75
50	50.25	0.25	0.22	1.31
60	60.28	0.28	0.40	1.85

6.2.4.5 Experiment Conclusion

The team optimized the entire design through a step-by-step tuning process. The final performance is evaluated in terms of accuracy, stability, and uniformity at target temperatures of 40°C, 50°C, and 60°C (Figure 71), with **steady-state error < 0.3 °C**, **oscillation amplitude < 0.5°C, and StDev. < 2°C** across all three cases.

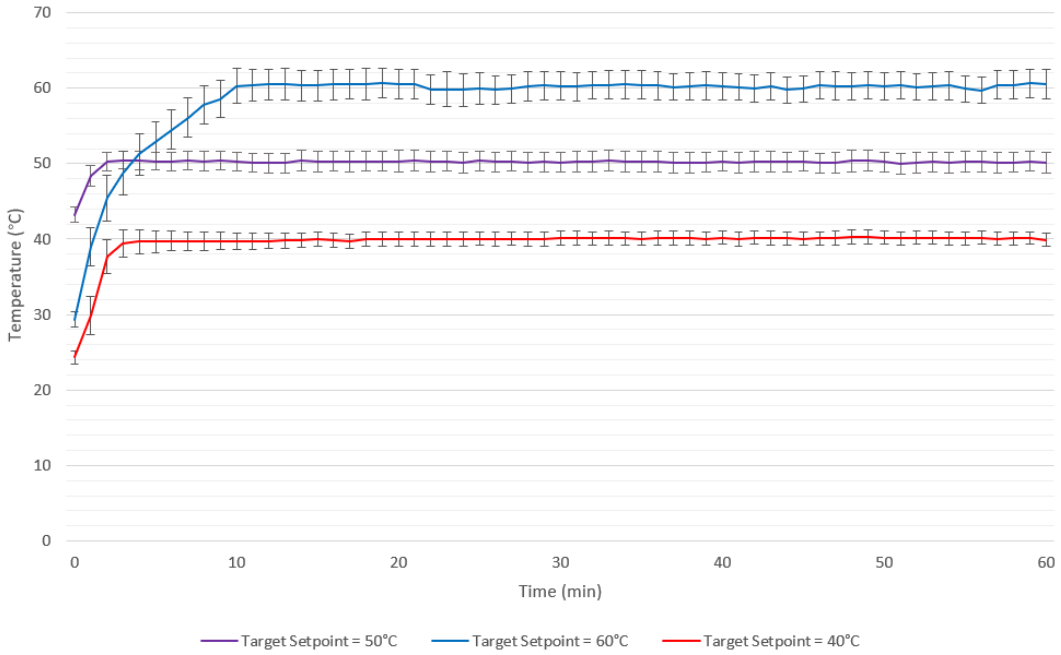

Figure 71. Optimized controller performance

(solid curves represent the chamber's spatial average temperature over time, while the error bars indicate the standard deviation of the temperature.)

The design was further tested at a target setpoint of 65°C for one hour to evaluate its performance under maximum power conditions. Overall, the optimization experiments achieved much elevated performance and the final result is respectable (Table 13, Figure 72).

Table 13 - Temperature Control Error and Stability Metrics (ss: steady-state) @ 65°C

Target Setpoint (°C)	Temporal Average Temp. (°C) @ ss	Error (°C)	Oscillation Amplitude (°C)	Chamber Temp. StDev. (°C) @ ss
65	64.7	0.3	0.44	1.94

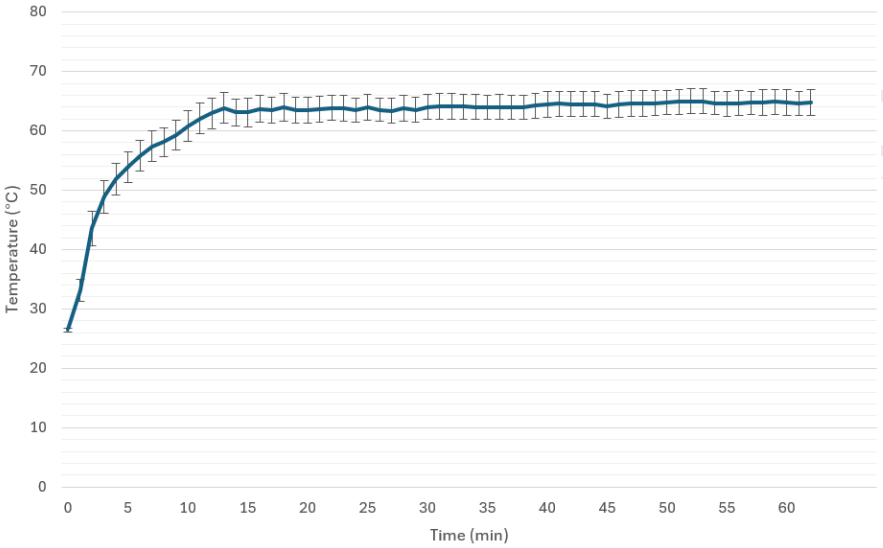

Figure 72. Chamber temperature profile @ setpoint = 65°C

7. Standards and Regulations

The final product is designed for accurate performance, maintainability, robustness, and safety. This consideration is infused in the entire product life cycle, from **design and procurement** to **assembly**, **testing, and implementation**. The team summarized all standards and regulations considered in each phase of the product life cycle.

Table 14 - Applied Standard in **Design and Procurement**

Standard / Regulation	Scope of Application	Design Implementation
IEC 60335-1 [4]	General Safety Requirement of Electrical Appliances Insulation and Fire Hazard Prevention	The design incorporates measures that closely adhere to IEC 60335-1*, key safety measures include: 1. The design contains no exposed wire as all electric connections are sealed with insulating and fireproof materials (i.e. heat-shrink tubings). 2. The enclosure is fabricated with PA6-CF. Its heat deflection temperature (186°C) is above the theoretical maximum source of heat (Appendix E). 3. The controller featured an automatic shutdown trigger at 75°C.

		A fuse (25A) was incorporated into the high-power circuit for overcurrent protection.
IEC 60364-1 [5]	General Voltage and Current Requirements Outline for Household Installations	1. Power and control circuits are wired separately to prevent EMI. 2. All components, at normal operation, do not exceed voltage, current, and total power constraints **.
ASTM F2362-03 [6]	Accuracy and Calibration Requirements for Semiconductor Sensors	The selected TSIC 306 offers an accuracy of ±0.3°C. Sensor calibration was conducted using higher-accuracy sensors during optimization experiments, as per ASTM F2362-03.
VDI 2230 [7]	Design Guide for Bolted Joint General Form Factor Reference	The device uses ISO 4017 socket head cap screw***, Sizes: M3 × 10 mm, M3 × 5 mm, M4 × 35 mm. Ultimately, joint loads are low (≤ 5 kg), and no formal preload calculation is required as per VDI 2230.
RoHS [8]	Environmental Compliance Against Hazardous Substances	Enclosure is 3D printed using PA6-CF, non-volatile and non-toxic at product's operating temperature (max @ 65°C).
IEC 60529 [9]	IP Rating Reference - Enclosure Resistance against the Intrusion of Dust or Liquids	The design offers fully enclosed housing, with inherent insulation and compartmentalization to isolate electrical and heating systems from the external environment (as per IP20 level) with a minimum opening gap of less than 12.5 mm.

** Complete the electrical/thermal adherence discussion in Appendix AI.*
*** Complete voltage, current and power adherence and discussion in Appendix AK.*
**** Detailed discussion on fastening design in Appendix AL.*

Table 15 - Applied Standard in **Assembly, Testing, and Implementation**

Standard / Regulation	Scope of Application	Design Implementation
IEC 61010-1 [10]	General Safety Requirements of Electronic Assemblies	1. Wiring utilized AWG wires based on current load (12 AWG for high-current, 20 – 24 AWG for low-voltage circuits) (Appendix AJ). 2. Wire connections and management closely adhere* to IEC 61010-1 and IPC/WHMA-A-620.
IPC-A-610 [11]	Additional Requirements / Guidelines in addition to IEC 61010-1, for Soldering Requirements	All electrical components are permanently soldered.
ISO/ASTM 52910 [12]	3D Printing Process	Printing parameters (Appendix AP) Drying procedures (Appendix AQ) performed and documented as per ISO/ASTM 52910**.
ISO 2768-1 [13]	General Mechanical Assembly Reference	Design incorporates clearance gaps (2 – 4 mm around PTC heater) and round edge of enclosure to prevent injury.
IEC 60068-1 [14]	Environmental testing: specifically Thermal Cycling Measures	During the optimization tests, the enclosure underwent repeated thermal cycling between 40°C and 65°C, and visual inspections per IEC 60068-1 revealed no fractures or permanent deformations.
ISO 12100 [15]	Generic Risk Assessment Guidelines	All proposed components are assessed under general guidelines for potential hazards***. Safety factor unavailable in ISO 12100(Type-A Standard,) SF=2.0 adopted from IEC 61010-1.

** Complete discussion on conformance regarding electrical assembly in Appendix AM.*
*** Discussion on conformance regarding Additive manufacturing (3D printing of enclosure) in Appendix AN.*
**** Discussion on hazard evaluation as per ISO 12100 general guideline available Appendix AO.*

8. Life-Cycle-Analysis (LCA)

Quantitative and **qualitative** assessments of the environmental impacts over the entire lifecycle of the design have been conducted. The objective of the LCA is to identify and quantify the energy and resource inputs, emissions, and waste treatments at each stage. This evaluation covers the **raw material phase**, **the production and assembly phase**, **the usage phase**, and **the disposal phase**. During the analysis, the functional unit is defined as "one, single device".

8.1 Production and Assembly Phase

Fabrication of one unit consumes 0.461 kg of PA6-CF. 3.35kWh of energy is being input during the 3D printing process (Appendix AR), which amounts to ~7.29 kWh/kg of material. Solid waste (e.g., metal scraps) is generated during the processes of soldering and testing. The manufacturing of certain electronic components (e.g., Arduino Nano, PTC heater) also requires the use of rare metals and valuable materials, thereby consuming non-renewable resources and potentially producing wastewater and exhaust during extraction and processing, which further increases environmental burdens[16].

During the testing phase, the team conducted 72 tests: 65 short-duration tests (each run < 10 minutes), 4 medium-duration tests (1 hour each), and 3 long-duration tests (2 hours each), with a total testing duration of ~20 hours. During all tests, the design operated continuously at 840 W, consuming a total of 16.8 kWh of energy.

8.2 Usage Phase

The usage phase mainly focuses on the continuous power input to maintain stable temperature control. Assuming that in practical application, the device is used 3 times per week, with each session lasting 10 hours, the weekly energy consumption will be ~25.2 kWh (Appendix AS). Although the device itself does not emit direct pollutants during operation, the energy consumed indirectly results in greenhouse gas emissions. Moreover, long-term operation in high-temperature environments poses additional challenges for lifecycle management.

8.3 Disposal and Recycling Phase

In the disposal phase, complex electronics and composite materials can lead to a significant accumulation of e-waste if proper disassembly and resource recovery are not achieved[17]. This not only increases the difficulty of solid waste treatment but also raises the risk of heavy metal leaching and chemical pollution, which may result in long-term ecological toxicity to soil and water bodies, as well as substantially higher costs for waste management and resource recovery. If the design is no longer being used, the team suggests the reuse of any electronics (e.g., LCD display, MCU) if it is possible.

8.4 Overall Assessment

In summary, the project faces several lifecycle challenges. During production, it incurs high energy consumption (~7.29 kWh/kg of raw material), greenhouse gas emissions, resource depletion, and ecological toxicity due to chemical processes. In the usage phase, maintaining a stable temperature (at roughly 25.2 kWh/week) demands significant energy, while the disposal phase is further complicated by the intricate composition of electronic components and composite materials, complicating waste management and elevating environmental risks.

To mitigate these issues, two targeted improvements are recommended. First, optimizing the internal electronic component structure to achieve a more compact design will reduce material usage right from the source. Second, refining the air duct structure to enhance heat exchange efficiency can substantially lower energy consumption during operation. These specific strategies will better align the project with green design principles and sustainable development goals.

9. Future Work

Although the design integrated portability with accuracy, **three** major challenges have been identified:

1. Limited by time and cost, the testing environment did not simulate the heat bed and hot end in the original 3D printer. Since these components are direct heat sources, they can significantly influence the temperature distribution inside the chamber. Consequently, the controller calibrated in the testing environment may not be robust enough for the actual printer, resulting in reduced control accuracy. One solution is to install the design into the printer and redo all correlation experiments, fine-tuning the parameters based on the data. Alternatively, a future CFD modeling of the original 3D printer could result in quantifiable key heat transfer parameters that could be integrated into the control algorithm, potentially removing the need for detailed full factorial and response surface experiments.

2. The ventilation fans in the printer can significantly alter airflow patterns. Thus, the wind deflector design optimized from testing data might not perform effectively in an actual printer. The team believes that a motor-driven, automatic oscillating deflector could enhance temperature uniformity and improve system robustness. However, due to its mechanical complexity, integrating an automatic and oscillating deflector in such a compact space presents further challenges.

3. 3D printing tasks can easily extend to tens of hours. The lack of long-duration (>10 hours) tests makes the design's performance in extended use remain questionable. This validation has to be completed in the future. New issues may arise that require corresponding modifications.

10. Conclusion

At the current stage of product development, the design has achieved an optimal performance in temperature control accuracy (**±0.5°C**), temperature stability (**< 0.5°C**)**,** and spatial temperature standard deviation **(< 2°C)**. However, all parameters were tuned and optimized with an inaccurate replicate of the original Anisoprint A3 model. This leaves much space for future improvements. To ensure performance in the actual printer, both geometric and control parameters need to be recalibrated to account for a different rate of convection to the external atmosphere of the chamber, the heat emitted from the heat bed and the hot end, the presence of the axial cooling fans, and the extended duration of printing sessions. An oscillating axial fan to further distribute chamber air could be designed and implemented in the future as well.

Overall, this design demonstrated adequate integration of mechanical and electrical systems, design of experiment, the proper use of polynomial regression modeling and discrete trials in parameter optimization, control algorithm programming, and proper consideration for user experience and life cycle impacts. Its performance at the current stage is adequate but will likely require additional optimization before being commissioned for service in the Anisoprint A3 printer.

11. References

[1] Waylinl, “How to fix warping in 3D printing,” Qidi Tech Online Store, https://ca.qidi3d.com/blogs/news/fix-3d-printing-warping-guide?shpxid=b594b7de-521e-4a3f-9720-1cab1229ead1 (accessed Mar. 23, 2025).

[2] S. Shahparnia and O. M. Ramahi, "Electromagnetic interference (EMI) reduction from printed circuit boards (PCB) using electromagnetic bandgap structures," in IEEE Transactions on Electromagnetic Compatibility, vol. 46, no. 4, pp. 580-587, Nov. 2004, doi: 10.1109/TEMC.2004.837671.

[3] “IPC/WHMA-A-620 - Revision E - standard only requirements and acceptance for cable and Wire Harness Assemblies,” IPC Store, https://shop.ipc.org/ipcwhma-a-620/ipcwhma-a-620-standard-only/Revision-e/english (accessed Mar. 23, 2025).

[4] Household and similar electrical appliances – Safety – Part 1: General requirements, IEC 60335-1, International Electrotechnical Commission, Geneva, Switzerland, 2020.

[5] Low-voltage electrical installations – Part 1: Fundamental principles, assessment of general characteristics, definitions, IEC 60364-1, International Electrotechnical Commission, Geneva, Switzerland, 2005.

[6] Standard Specification for Temperature Monitoring Equipment, ASTM F2362-03, ASTM International, West Conshohocken, PA, USA, 2003.

[7] Systematic calculation of high duty bolted joints, VDI 2230, Verein Deutscher Ingenieure (VDI), Düsseldorf, Germany, 2003.

[8] Directive on the restriction of the use of certain hazardous substances in electrical and electronic equipment (RoHS), 2011/65/EU, European Union, Brussels, Belgium, 2011.

[9] Degrees of protection provided by enclosures (IP Code), IEC 60529, International Electrotechnical Commission, Geneva, Switzerland, 2013.

[10] Safety requirements for electrical equipment for measurement, control, and laboratory use – Part 1: General requirements, IEC 61010-1, International Electrotechnical Commission, Geneva, Switzerland, 2010.

[11] Acceptability of Electronic Assemblies, IPC-A-610, IPC – Association Connecting Electronics Industries, Bannockburn, IL, USA, 2020.

[12] Additive manufacturing – Design – Requirements, guidelines and recommendations, ISO/ASTM 52910, International Organization for Standardization / ASTM International, Geneva, Switzerland / West Conshohocken, PA, USA, 2018.

[13] General tolerances – Part 1: Tolerances for linear and angular dimensions without individual tolerance indications, ISO 2768-1, International Organization for Standardization, Geneva, Switzerland, 1989.

[14] Environmental testing – Part 1: General and guidance, IEC 60068-1, International Electrotechnical Commission, Geneva, Switzerland, 2013.

[15] Safety of machinery – General principles for design – Risk assessment and risk reduction, ISO 12100, International Organization for Standardization, Geneva, Switzerland, 2010.

[16] U.S. International Trade Commission, “Recovering Rare Earth Elements from E-Waste: Potential Impacts on Supply Chains and the Environment,” U.S. Int. Trade Comm., Washington, DC, 2024. [Online]. Available: https://www.usitc.gov/sites/default/files/publications/332/journals/jice_recovering_rare_earth_elements_from_e_waste.pdf [Accessed: Mar. 23, 2025].

[17] M. A. Khan and J. S. Park, "Efficient disassembly and recycling of electronic waste: Overcoming challenges posed by complex components and composite materials," in Proc. IEEE Int. Conf. on Sustainable Electronics Recycling, New York, NY, USA, Oct. 2023, pp. 123–130

[18] “Arduino Nano,” Arduino Official Store, https://store.arduino.cc/products/arduino-nano (accessed Mar. 23, 2025).

[19] "9BMB24G201," DigiKey Electronics, https://www.digikey.ca/en/products/detail/sanyo-denki-america-inc/9BMB24G201/6192096?_gl=1%2A177nogk%2A_up%2AMQ..%2A_gs%2AMQ..&gclid=Cj0KCQjwzva1BhD3ARIsADQuPnWirRvnwE_gGuiTZ3EM2KpBtCjTHX9od0my8GQJsMLZcroiW96GpJcaAgIFEALw_wcB (accessed Mar. 23, 2025).

[20] TSIC 306 TO92 Innovative Sensor Technology, USA Division | Sensors, transducers | DigiKey, https://www.digikey.com/en/products/detail/innovative-sensor-technology-usa-division/TSIC-306-TO92/13181022 (accessed Mar. 24, 2025).

[21] "LCD1602 16x2 I2C Blue LCD display," ProtoSupplies, https://protosupplies.com/product/lcd1602-16x2-i2c-blue-lcd-display/ (accessed Mar. 23, 2025).

[22] “3D printing temperature: Effects, materials and considerations – Raise3D: Reliable, industrial grade 3D printer,” Raise3D, https://www.raise3d.com/blog/3d-printing-temperature/ (accessed Mar. 23, 2025).

[23] B. O'Neill, "ABS print temperature considerations: Nozzle, bed, enclosure," Wevolver, https://www.wevolver.com/article/abs-bed-temperature#:~:text=A%20heated%20build%20chamber%20is,around%2060%E2%80%9370%20%C2%B0C.(accessed Mar. 23, 2025).

[24]M. Tyson, "Advanced guide to printing PETG filament," 3D Printing Solutions, https://www.3dprintingsolutions.com.au/User-Guides/how-to-3d-print-petg-filament#:~:text=Printing%20PETG%20requires%20a%20heated,PETG%20(80%C2%B0C%20).(accessed Mar. 23, 2025).

[25]IN3DTEC, "How to 3D PRINT TPU a comprehensive guide: IN3DTEC: Prototyping & on-demand manufacturing services," IN3DTEC, https://www.in3dtec.com/how-to-3d-print-tpu-a-comprehensive-guide/#:~:text=TPU%20typically%20prints%20well%20at,and%20type%20of%20TPU%20filament. (accessed Mar. 23, 2025).

[26]"Polycarbonate 3D printing: In-depth guide: Top 3D Shop," Digital Manufacturing Store Top 3D Shop, https://top3dshop.com/blog/polycarbonate-3d-printing-in-depth-guide#:~:text=When%20dealing%20with%20polycarbonate%2C%20ambient,and%20eliminate%20potential%20delamination%20issues.(accessed Mar. 23, 2025).

[27] IN3DTEC, "The best ASA 3D printing settings achieving optimal results: IN3DTEC: Prototyping & on-demand manufacturing services," IN3DTEC, https://www.in3dtec.com/the-best-asa-3d-printing-settings-achieving-optimal-results/#:~:text=To%20mitigate%20these%20issues%2C%20it,and%20promote%20better%20layer%20bonding. (accessed Mar. 23, 2025).

[28] I. Peter, "From experiment to final print: Understanding self-regulation PTC Heaters," TechBlick, https://www.techblick.com/post/from-experiment-to-final-print-understanding-self-regulation-ptc-heaters (accessed Mar. 23, 2025).

[29] American wire gauge conductor size table, https://www.solaris-shop.com/content/American Wire Gauge Conductor Size Table.pdf (accessed Mar. 24, 2025).

[30]**Arduino Nano 3.0 Dev Board**, Arduino. [Online]. Available: https://store.arduino.cc/products/arduino-nano?srsltid=AfmBOopqtVmzMhrBjRfxZrsG-3D2PJYuGdZpN-oA0GNkNUuHFR5DUrd1. [Accessed: Mar. 23, 2025].

[31]**1688-1380-ND**, Digi-Key. [Online]. Available: https://www.digikey.ca/en/products/detail/sanyo-denki-america-inc/9BMB24G201/6192096. [Accessed: Mar. 23, 2025].
[32]**JKFTP-120-1500**, Sun-Zone. [Online]. Available: https://www.sun-zone.com.cn/productdetail/ptcheatingelem008.html. [Accessed: Mar. 23, 2025].

[33]**FNK0079**, Freenove. [Online]. Available: https://store.freenove.com/products/fnk0079. [Accessed: Mar. 23, 2025].

[34]**HW-477**, Amazon India. [Online]. Available: https://www.amazon.in/Intensity-Sensor-HW-477-V0-2-Effect/dp/B0CPTB6XMM?th=1. [Accessed: Mar. 23, 2025].

[35]**MP1584EN DC-DC 3A**, Amazon Canada. [Online]. Available: https://www.amazon.ca/DZS-Elec-Converter-Adjustable-Regulator/dp/B07JWGN1F6. [Accessed: Mar. 23, 2025].

[36]**TSIC 306 TO92**, Digi-Key. [Online]. Available: https://www.digikey.ca/en/products/detail/innovative-sensor-technology-usa-division/TSIC-306-TO92/13181022. [Accessed: Mar. 23, 2025].

[37]**FSP040-DAAN3**, Digi-Key. [Online]. Available: https://www.digikey.com/en/products/detail/fsp-technology-inc/FSP040-DAAN3/15713222. [Accessed: Mar. 23, 2025].

[38]**Dual High-Power FET Trigger Switch Driver Module**, Amazon Canada. [Online]. Available: https://www.amazon.ca/MOSFET-Trigger-Adjustment-Electronic-Control/dp/B0D2XTC6XC. [Accessed: Mar. 23, 2025].

[39]**SSR-25DA**, Amazon Canada. [Online]. Available: https://www.amazon.ca/SSR-25-DC-AC-Solid-State-Relay/dp/B07FW16J9H?th=1. [Accessed: Mar. 23, 2025].

[40]**GK1009C**, Amazon Canada. [Online]. Available: https://www.amazon.ca/Gikfun-Solder-able-Breadboard-Arduino-Electronic/dp/B0778G64QZ. [Accessed: Mar. 23, 2025].

[41]**CAB-15455**, Digi-Key. [Online]. Available: https://www.digikey.ca/en/products/detail/sparkfun-electronics/CAB-15455/10819694. [Accessed: Mar. 23, 2025].

[42]**ATC25-25**, Amazon Canada. [Online]. Available: https://www.amazon.ca/Conext-Link-ATC25-25-Fuse-Pack/dp/B01DELSTCM. [Accessed: Mar. 23, 2025].

[43]**FHAC0002XP**, Digi-Key. [Online]. Available: https://www.digikey.ca/en/products/detail/littelfuse-commercial-vehicle-products/FHAC0002XP/3427040. [Accessed: Mar. 23, 2025].

[44]**07112 Barrel Connector**, Amazon Canada. [Online]. Available: https://www.amazon.ca/GOSONO-Female-Connector-Security-5-5x2-5mm/dp/B07V4F9NDK?th=1. [Accessed: Mar. 23, 2025].

[45]**CA-KCD3-101**, Finglai. [Online]. Available: https://www.finglai.com/products/switches/rocker-switches/KCD3-KCD8-26x11/KCD3-101-B.html?srsltid=AfmBOopvqxHwKfb9YfO132GjTdXwHS5UsJFJZx3VwTC2Vlq5n5eENmi5. [Accessed: Mar. 23, 2025].

[46]**B3601**, PartSource. [Online]. Available: https://partsource.ca/products/b3601-certified-22-14-awg-automotive-closed-end-connector-6-pk. [Accessed: Mar. 23, 2025].

11. Appendices

Appendix A - Attribution Table

Project Title:	Chamber Temperature Control System for the 3D printer	Supervisor:	Dr. Kamran Behdinan
Document Name:	Final Design Specification	Date:	Mar. 23rd 2025

This form must be filled out and signed for each team-written document. The completed form must be attached to the document, though not included as part of the document (not included in the table of contents, page numbers, or word count limits). It should accurately reflect each team member's contribution to the document and in what way they contributed.

If there are irreconcilable differences that are preventing all team members from signing the attribution table, then each team member must write a letter (max 800 words) explaining their position on the difference and suggest a solution.

Making fraudulent claims in an attribution table displays intent to deceive and is a serious academic offence.

Section	Student Names					
	Bangan Wang	Zidong Han	Liang Yan	Lurui Wang		
Executive Summary		**RD**	**RD**			
1. Introduction		**FP**	**RD**			
2. PR (FOCs)	**ET, FP**		**RD ET**			
3.1	**RD, MR**	**ET, FP**	**MR ET**			
3.2	**RD, MR**	**ET, FP**	**MR ET**			
3.3	**ET, MR**	**ET. FP**	**MR ET**			
3.4	**ET, MR**		**MR ET**			
3.5	**ET, MR, FP**		**MR ET**			
3.6	**ET, MR**		**MR ET**			
3.7	**RD**		**MR ET**			
3.8	**RD, MR, FP**	**RS, RD**	**MR ET**	**ET**		
3.9	**RD**	**RS, RD**		**ET**		
4. BOM	**RD, MR**	**ET**		**MR,RD**		
5. Implementation Plan	**RD, MR, FP**			**MR,RD**		
6. Experiment&Test	**RD, MR, FP**	**RS, RD**	**MR ET**	**MR,RD**		
7. Standards and Regulations		**RD, ET**				
8. Life Cycle Analysis(LCA)		**ET**		**MR, ET**		
9. Future Works	**RD**			**ET**		
10. Conclusion	**FP**	**FP**	**RD, MR**	**FP**		
11. References		**RD, ET**		**RD, ET**		
12. Appendices	**RD, MR, ET**	**RD,MR, ET**		**RD, MR,ET**		
ALL						

Fill in abbreviations for roles for each of the required content elements. You do not have to fill in every cell. The "all" row refers to the complete report and should indicate who was responsible for the final compilation and final read through of the completed document.

RS - research

RD – wrote first draft

MR - major revision

FP – final read through of complete document for flow and consistency

CM - responsible for compiling the elements into the complete document

OR - other

ET - edited for grammar and spelling

If you put OR (other) in a cell please put it in as OR1, OR2, etc. Explain briefly below the role referred to:

OR1: _____
OR2: _____

By signing below, you verify that you have:

- Read the attribution table and agree that it accurately reflects your contribution to the associated document.
- Written the sections of the document attributed to you and that they are entirely original.
- Accurately cited and referenced any ideas or expressions of ideas taken from other sources according to an accepted standard.
- Read the University of Toronto Code of Behaviour on Academic Matters and understand the definition of academic offense includes (but is not limited to) all forms of plagiarism. Additionally, you understand that if you provide another student with any part of your own or your team's work, for whatever reason, and the student having received the work uses it for the purposes of committing an academic offence, then you are considered an equal party in the offence and will be subject to academic sanctions.
-

Print Name:	Bangan Wang	Signature:	BANGAN WANG
Print Name:	Zidong Han	Signature:	ZIDONG HAN
Print Name:	Liang Yan	Signature:	LIANG YAN
Print Name:	Lurui Wang	Signature:	LURUI WANG

Appendix B - PTC Element Circuit Model (Internal)

The PTC heater itself can be modeled as a resistor circuit that generates heat when connected to the power supply. Measured by a multimeter, the PTC can be modeled as the equivalent circuit shown below.

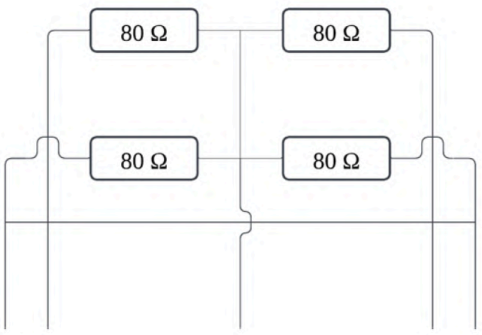

Figure B1. PTC equivalent circuit

Appendix C - Power Consumption Estimation for Control Circuit

The control circuit consists of an MCU, a centrifugal fan, a temperature sensor, an LCD, and an IR remote module. These components are powered by a DC converter that steps down from 120 VAC to 24 VDC. A suitable converter is selected to ensure that its power rating meets the total power consumption of the circuit. The power consumption for each component is summarized below.

Table C1 - Power Consumption Estimation (Control Circuit)

Component	Power (W)
MCU (Arduino Nano)	0.095 [18]
Centrifugal Fan	19.9 [19]
Temperature Sensor	0.000175 [20]
LCD Display	0.15[21]
IR remote receiver	0.025 (estimated)
TOTAL	**20.17**

The team thus selected a 40W power supply for the control circuit to have extra headroom for 50%.

Appendix D - MCU (Arduino Nano) Supply Voltage Requirement

The Arduino Nano has an onboard voltage regulator that steps down the input voltage to a stable 5V (stable working voltage). However, this onboard regulator has a dropout voltage, meaning it needs the input to be a few volts higher than 5V (i.e. 7V) to function properly. Without this extra voltage, the regulator may not provide a stable 5V output, which can lead to unreliable operation of the board. Thus, the DC step-down convertor's output is 7V and powers the MCU via its V-in pin.

Appendix E - PTC Maximum Surface Temperature

To ensure that the enclosure would not melt during operation, the team directly measured the maximum surface temperature of the PTC heater. The heater was activated without **any** external forced convection so that its maximum surface temperature (the "extreme condition") could be reached and measured. After powering on, the surface temperature of the PTC heater increased until the output power eventually stabilized at 670W (indicating that the high temperature reduced the heater's internal impedance, thereby lowering the supplied power). Using a temperature gun with an accuracy of ±1.5°C, the team recorded a surface temperature of approximately 150°C.

Figure E1. PTC Heater Surface Temperature

Appendix F - Design Engineering Drawings (mechanical)

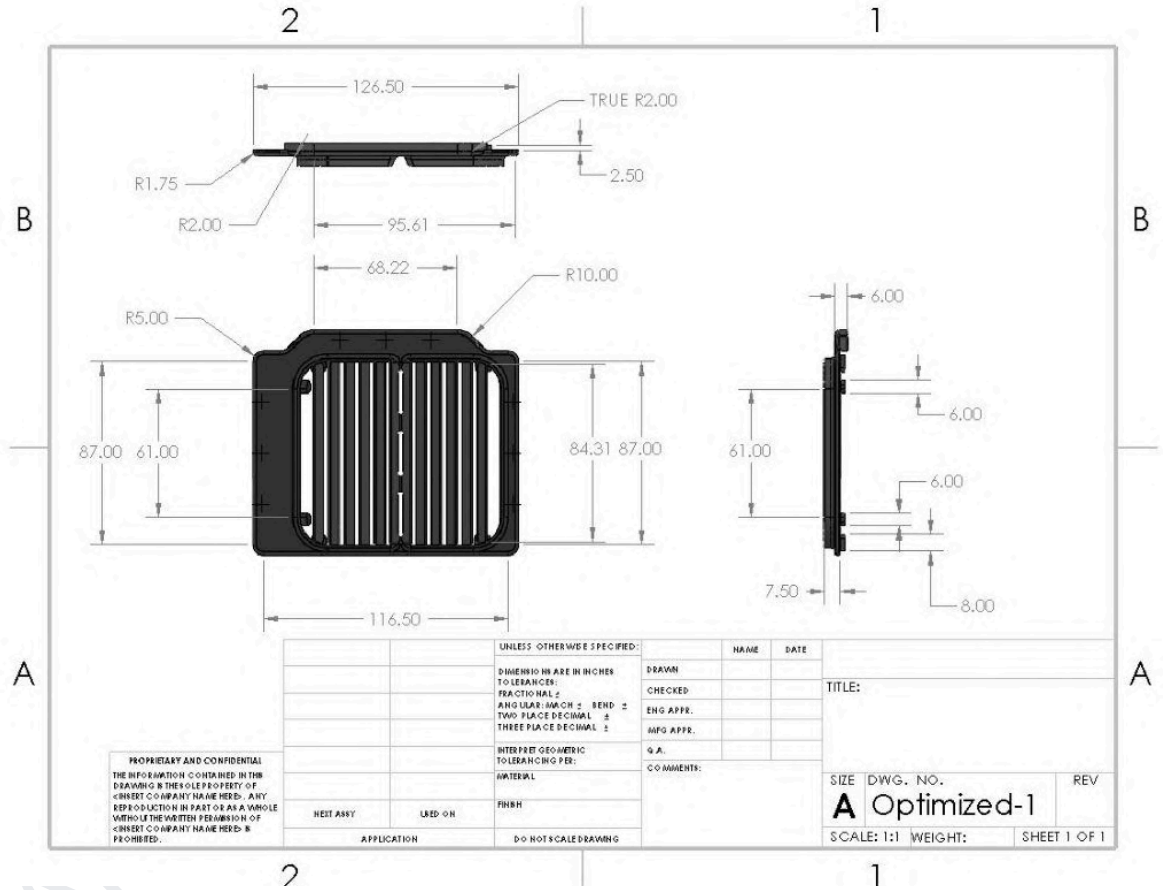

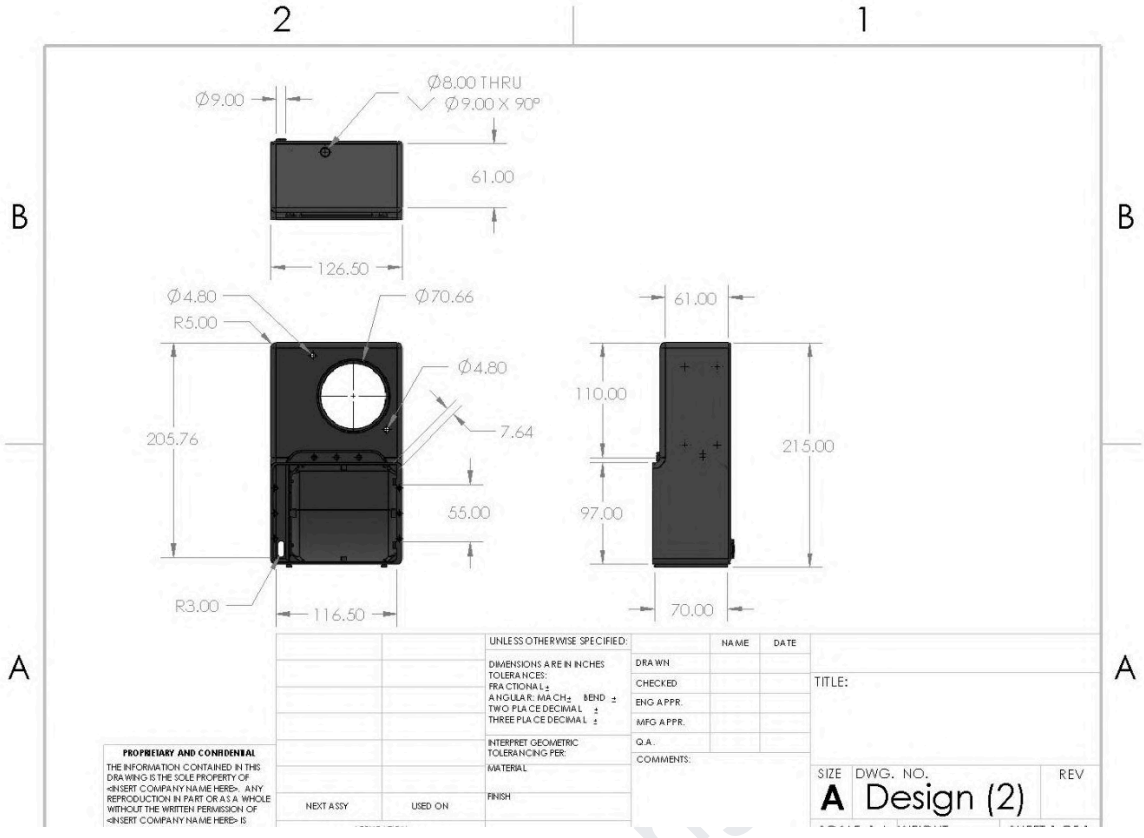
2
1
B
A
Ø9.00
Ø8.00 THRU
Ø9.00 X 90°
61.00
126.50
Ø4.80
R5.00
Ø70.66
Ø4.80
7.64
205.76
55.00
R3.00
116.50
61.00
110.00
215.00
97.00
70.00
UNLESS OTHERWISE SPECIFIED:
DIMENSIONS ARE IN INCHES
TOLERANCES:
FRACTIONAL ±
ANGULAR: MACH ± BEND ±
TWO PLACE DECIMAL ±
THREE PLACE DECIMAL ±
INTERPRET GEOMETRIC TOLERANCING PER:
MATERIAL
FINISH
NEXT ASSY
USED ON
NAME
DATE
DRAWN
CHECKED
ENG APPR.
MFG APPR.
Q.A.
COMMENTS:
TITLE:
SIZE
DWG. NO.
REV
A
Design (2)
PROPRIETARY AND CONFIDENTIAL
THE INFORMATION CONTAINED IN THIS DRAWING IS THE SOLE PROPERTY OF <INSERT COMPANY NAME HERE>. ANY REPRODUCTION IN PART OR AS A WHOLE WITHOUT THE WRITTEN PERMISSION OF <INSERT COMPANY NAME HERE> IS

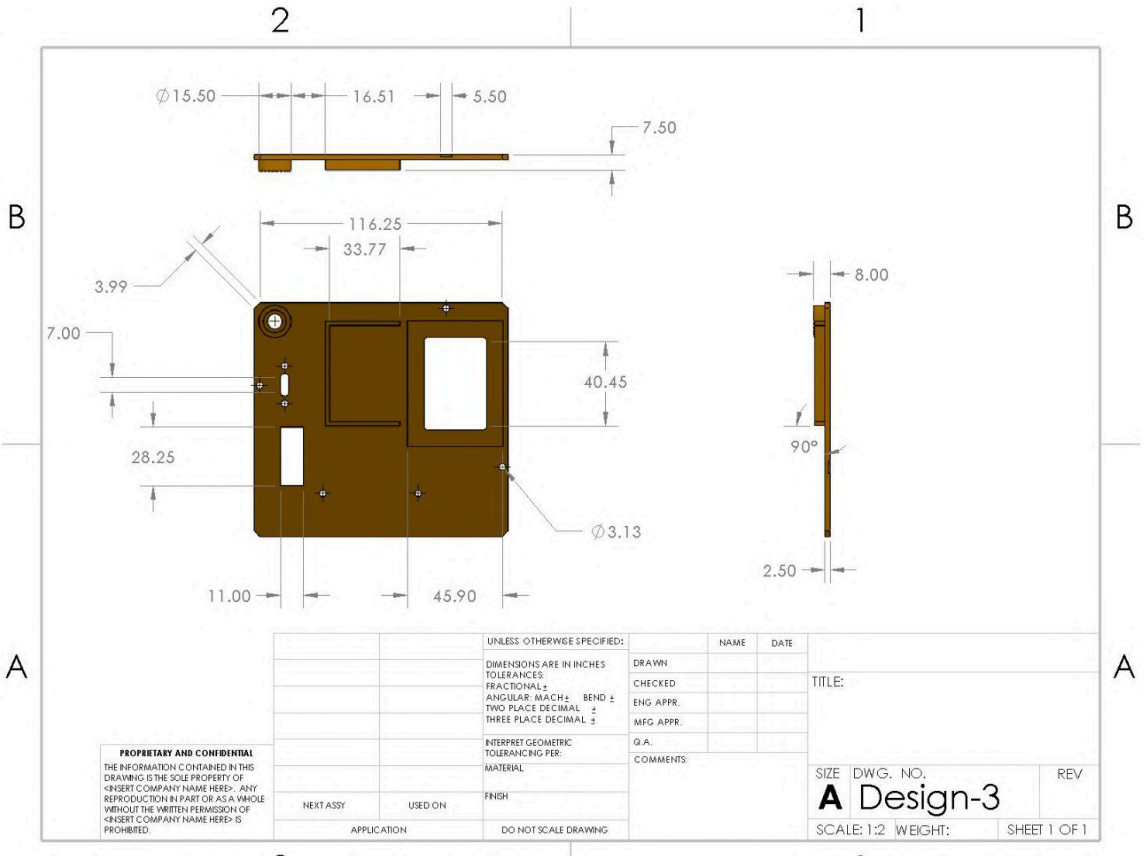
2
1
B
A
Ø15.50
16.51
5.50
7.50
116.25
33.77
3.99
7.00
40.45
28.25
Ø3.13
11.00
45.90
8.00
90°
2.50
UNLESS OTHERWISE SPECIFIED:
DIMENSIONS ARE IN INCHES
TOLERANCES:
FRACTIONAL ±
ANGULAR: MACH ± BEND ±
TWO PLACE DECIMAL ±
THREE PLACE DECIMAL ±
INTERPRET GEOMETRIC TOLERANCING PER:
MATERIAL
FINISH
NEXT ASSY
USED ON
APPLICATION
DO NOT SCALE DRAWING
NAME
DATE
DRAWN
CHECKED
ENG APPR.
MFG APPR.
Q.A.
COMMENTS:
TITLE:
SIZE
DWG. NO.
REV
A
Design-3
SCALE: 1:2
WEIGHT:
SHEET 1 OF 1
PROPRIETARY AND CONFIDENTIAL
THE INFORMATION CONTAINED IN THIS DRAWING IS THE SOLE PROPERTY OF <INSERT COMPANY NAME HERE>. ANY REPRODUCTION IN PART OR AS A WHOLE WITHOUT THE WRITTEN PERMISSION OF <INSERT COMPANY NAME HERE> IS PROHIBITED.

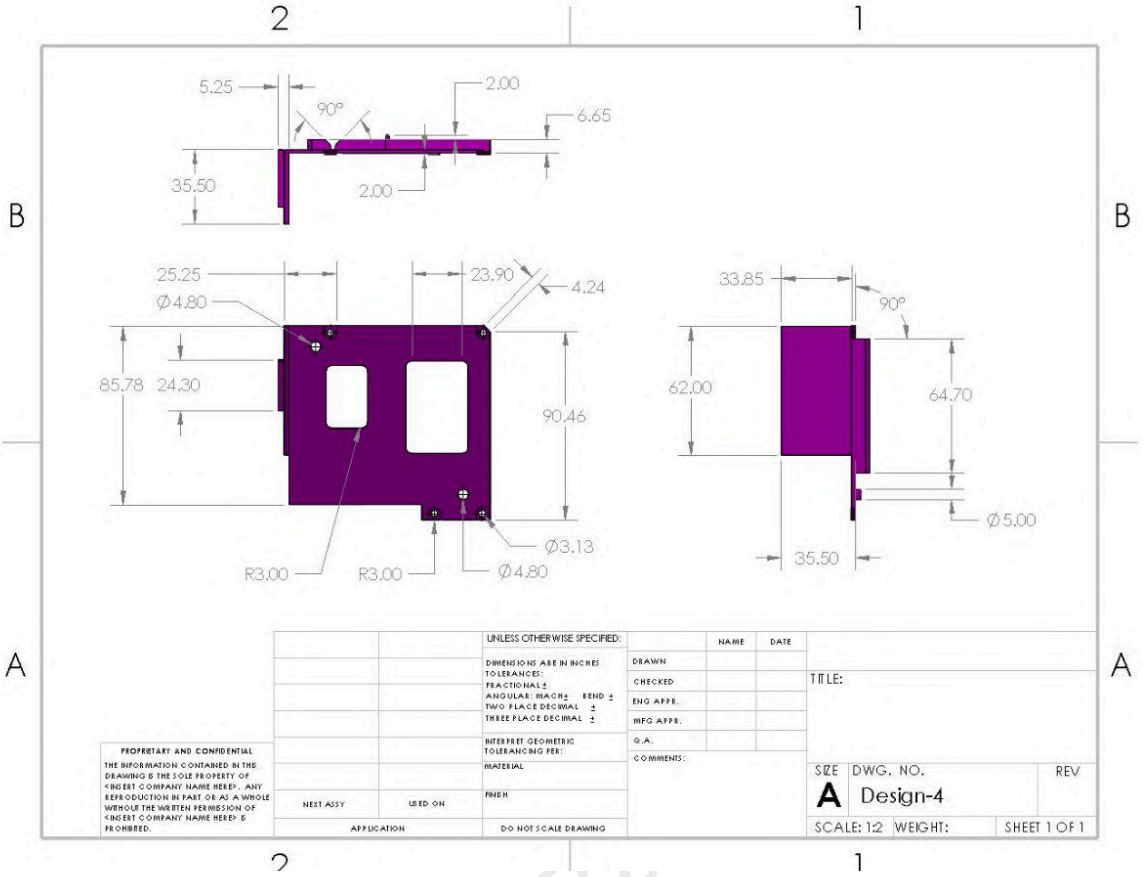
5.25
90°
2.00
6.65
35.50
2.00
25.25
23.90
4.24
Ø4.80
85.78
24.30
90.46
R3.00
R3.00
Ø3.13
Ø4.80
33.85
90°
62.00
64.70
Ø5.00
35.50
UNLESS OTHERWISE SPECIFIED:
DIMENSIONS ARE IN INCHES
TOLERANCES:
FRACTIONAL ±
ANGULAR: MACH ± BEND ±
TWO PLACE DECIMAL ±
THREE PLACE DECIMAL ±
INTERPRET GEOMETRIC TOLERANCING PER:
MATERIAL
FINISH
NEXT ASSY
USED ON
APPLICATION
DO NOT SCALE DRAWING
NAME
DATE
DRAWN
CHECKED
ENG APPR.
MFG APPR.
Q.A.
COMMENTS:
TITLE:
PROPRIETARY AND CONFIDENTIAL
THE INFORMATION CONTAINED IN THIS DRAWING IS THE SOLE PROPERTY OF <INSERT COMPANY NAME HERE>. ANY REPRODUCTION IN PART OR AS A WHOLE WITHOUT THE WRITTEN PERMISSION OF <INSERT COMPANY NAME HERE> IS PROHIBITED.
SIZE
A
DWG. NO.
Design-4
REV
SCALE: 1:2
WEIGHT:
SHEET 1 OF 1

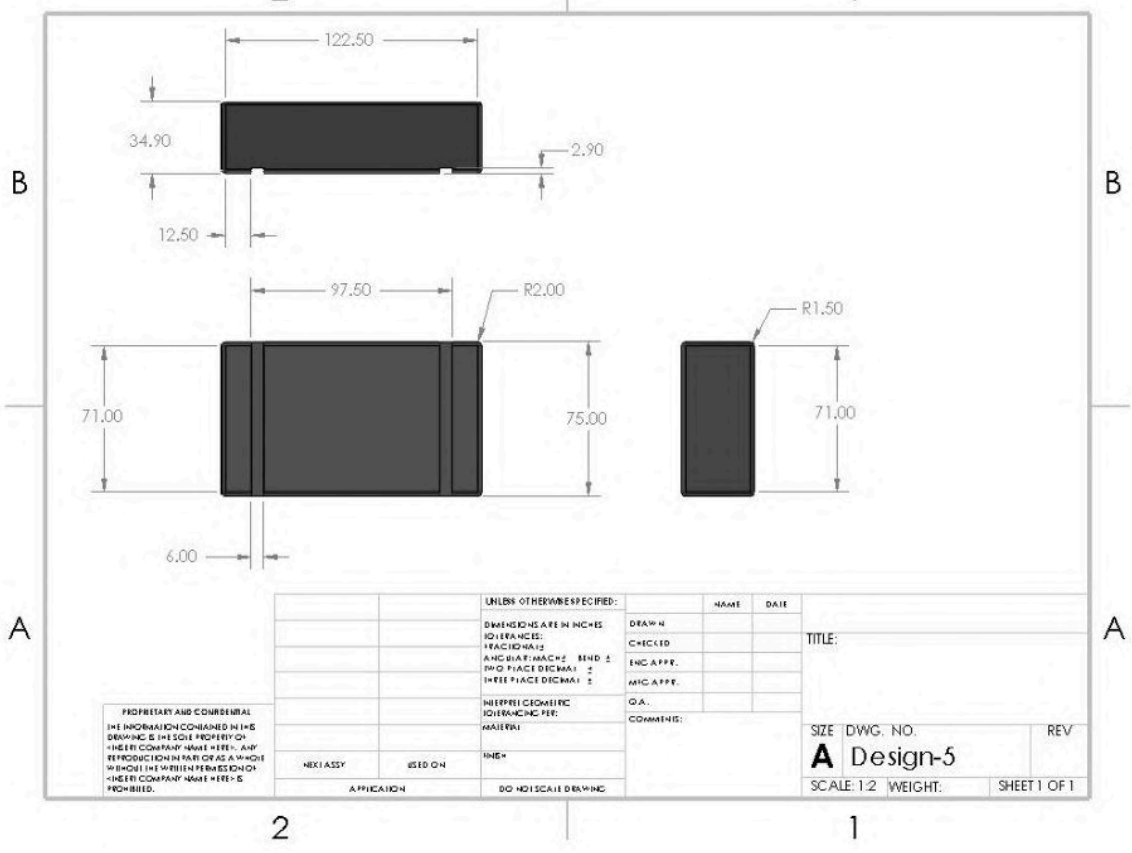
122.50
34.90
2.90
12.50
97.50
R2.00
R1.50
71.00
75.00
71.00
6.00
UNLESS OTHERWISE SPECIFIED:
DIMENSIONS ARE IN INCHES
TOLERANCES:
FRACTIONAL ±
ANGULAR: MACH ± BEND ±
TWO PLACE DECIMAL ±
THREE PLACE DECIMAL ±
INTERPRET GEOMETRIC TOLERANCING PER:
MATERIAL
FINISH
NEXT ASSY
USED ON
APPLICATION
DO NOT SCALE DRAWING
NAME
DATE
DRAWN
CHECKED
ENG APPR.
MFG APPR.
Q.A.
COMMENTS:
TITLE:
PROPRIETARY AND CONFIDENTIAL
THE INFORMATION CONTAINED IN THIS DRAWING IS THE SOLE PROPERTY OF <INSERT COMPANY NAME HERE>. ANY REPRODUCTION IN PART OR AS A WHOLE WITHOUT THE WRITTEN PERMISSION OF <INSERT COMPANY NAME HERE> IS PROHIBITED.
SIZE
A
DWG. NO.
Design-5
REV
SCALE: 1:2
WEIGHT:
SHEET 1 OF 1

Appendix G - Design 3D Models (mechanical)

To download the 3D SOLIDWORKS model, please click the link below:
https://drive.google.com/file/d/12gVZH8mJOfofzbYcT9i6_ZFe7pgv5eS-/view?usp=sharing
(Please use SOLIDWORKS 2023 or a later version to open the file).

Appendix H - Electronics Compartment Temperature

To prevent the electronics from being damaged during prolonged exposure to high heat, the team placed the design into a testing chamber, heated from 25°C to 65°C. At the chamber temperature (spatial average) = 65°C, the temperature within the electronics compartment reached 70°C, below the recommended long-period operating temperature of 85°C for all electronics with a safety factor of 1.21.

Figure M6. Electronics Compartment

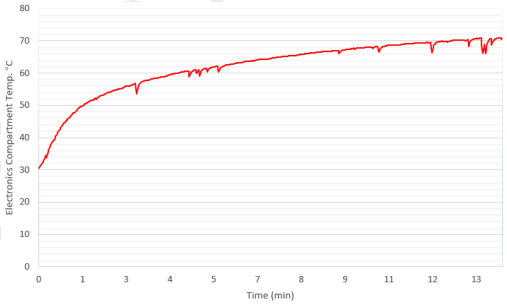

Figure M6. Temperature in the electronics compartment
(from room temperature to 65°C service temperature)

Appendix I - *TsicSensor* Library Description

TsicSensor is an Arduino library for reading TSIC temperature sensors. This library reads temperature values from several TSIC sensor types (TSIC 206/306/506/516/716). It uses interrupts to decode the ZACwire protocol used by the sensors and supports methods for reading temperature values in several scales (Celsius/Fahrenheit/Kelvin)
Details here: https://github.com/tripplefox/TsicSensor

Appendix J - Controller Code for Arduino Nano

To download the complete controller code for the system's MCU, please use the link below:
https://drive.google.com/file/d/166kpVEMYXF6j96-r5fREq5num95BHTkA/view?usp=sharing

Please use Arduino IDE 1.8.19 or a later version. Please download the corresponding library before uploading the code. To download the libraries:
<LiquidCrystal_I2C.h>: https://docs.arduino.cc/libraries/liquidcrystal-i2c/#Releases
<IRremote.h>: https://docs.arduino.cc/libraries/irremote/
<TSIC.h>: https://docs.arduino.cc/libraries/tsic/

The complete code in C is as follows:

```
#include <LiquidCrystal_I2C.h>
#include <IRremote.h>
#include <TSIC.h>

// Pin definition & hardware config.
const int IR_RECV = 2;
const int FAN_PWM_PIN = 9;
const int HEATER_PIN = 8;
TSIC Sensor1(A1);
LiquidCrystal_I2C lcd(0x27, 16, 2);


// Material Preset
const int PLA = 55;
const int ABS = 65;
const int PETG = 65;
const int TPU = 50;
const int PP = 60;
const int ASA = 65;
const int CFGF = 55;
const int PC = 65;
const int PA = 60;

// IR recv.
IRrecv irrecv(IR_RECV); // create object receiver
decode_results results;

// System Settings.
int TEMP = 50; // target temp.
int TEMP_MIN = 25;
int TEMP_MAX = 65; // maximum target temp
unsigned long key_val = 0; // IR Recv. default

// Filter Parameters.
const float Q = 0.01;
const float R = 0.1;
bool firstRead = true;

// Parameters default
uint16_t temperature1 = 0;
float temp;
float previous_temp = 0.0;
float current_temp;
float diff_temp;
float last_temp = 0.0;
int heater_status = 0; // 0: off, 1: on

// P Controller Parameters
static double error_integral = 0.0;


// Threshold definition
const double base_threshold = 1;
const double k = 75;
static bool heaterOn = false;

// Temperature Conversion Constant
const double X_Var = 1.052342884;
const double intercept = -6.648611246;
float Correlated_temp;
```

```
unsigned long calib_start_time = 0;
bool calibration_started = false;
float corr_bias;
float elapsed;
float t;
float corr_a;
float corr_b;
float corr_c;
float TEMP_Scaling;
//float lev4_cali;


// --------------------------- Helper Functions ---------------------------------

// sensor noise reduction
float smoothTempRead(float rawTemp){
  static float x_est = 0.0;
  static float P = 1.0;

  if(firstRead){
    x_est = rawTemp;
    firstRead = false;
  }

  float K = P / (P + R);
  x_est = x_est + K * (rawTemp - x_est);
  P = (1 - K) * P + Q;

  return x_est;
}

// data acquire, sanitation, noise reduction
void get_temp(){

  // data acquisition
  if(Sensor1.getTemperature(&temperature1)){
    current_temp = Sensor1.calc_Celsius(&temperature1);
  }

  // sanitation
  if(previous_temp == 0.0){
    previous_temp = current_temp;
  }
  diff_temp = abs(current_temp-previous_temp);

  if(diff_temp > 5){
    return;
  }

  // noise reduction
  temp = smoothTempRead(current_temp);
  previous_temp = current_temp;
}

// Display func.
void LCDprint(){
  lcd.setCursor(0,0);
  lcd.print("CURRENT:  ");
  lcd.print((int)round(Correlated_temp));
  lcd.print(" C   ");

  lcd.setCursor(0,1);
  lcd.print("TARGET :  ");
  lcd.print(TEMP);
  lcd.print(" C   ");
}

// Transfer sensor reading to the actual average temp.
// calibration func.
void calibrate(){
  float lev3_cali = -1.6973*pow(TEMP_Scaling,3)+13.3544*pow(TEMP_Scaling,2)-37.7647*TEMP_Scaling+37.7959;

  float base_value = intercept + X_Var*temp + lev3_cali;
  Correlated_temp = base_value;
```

```
  // steady state compensation
  if(!calibration_started && fabs(base_value - TEMP) <= 1.3){
    calib_start_time = millis();
    calibration_started = true;
    corr_bias = 0.0;
  }

  if(calibration_started){
    elapsed = (millis()-calib_start_time)/1000.0; // convert ms to sec., float
    t = elapsed/60.0; //convert to min., float
    corr_bias = corr_a + corr_b * exp(-corr_c * t); // compensation function
    Correlated_temp = base_value + corr_bias;
  } else{
    Correlated_temp = base_value;
  }

  // debounce
  static unsigned long condition_start_time = 0;
  const unsigned long debounce_time_threshold = 30000.0; // 30 sec

  if(calibration_started && fabs(base_value - TEMP) >= 2.0){
    if(condition_start_time == 0){
      condition_start_time = millis();
    }
    if(millis()-condition_start_time >= debounce_time_threshold){
      calibration_started = false;
      condition_start_time = 0;
      corr_bias = 0.0;
    }
  } else {
    condition_start_time = 0;
  }
}


// --------------------------- Main Code -------------------------------------

void setup() {
  Serial.begin(9600);
  irrecv.enableIRIn(); // IR input on
  irrecv.blink13(true); // blink effect

  // lcd initialization
  lcd.init();
  lcd.backlight();
  lcd.clear();

  pinMode(HEATER_PIN, OUTPUT);
  digitalWrite(HEATER_PIN, LOW); // turn off the heater by default
  heater_status = 0;

  pinMode(FAN_PWM_PIN, OUTPUT);
  analogWrite(FAN_PWM_PIN, 0); // turn off the fan by default

  // initilizing compensation
  calibration_started = false;
  corr_a = 0.0;
  corr_b = 0.0;
  corr_c = 0.0;

  lcd.setCursor(0,0);
  lcd.print("DEV. BY B.A.G.");
  delay(2000);
  lcd.setCursor(0,0);
  lcd.print("Initializing...");

  delay(2000);
}

void loop() {
  // Acquire data
  TEMP_Scaling = TEMP/20.0;
  corr_a = TEMP_Scaling * 0.7109 - 0.7443;
  corr_b = 1.036*pow(TEMP_Scaling, 2) - 5.2968*TEMP_Scaling + 5.5476;
  corr_c = -0.0578*pow(TEMP_Scaling, 2) + 0.2877*TEMP_Scaling - 0.3278;
```

```
get_temp();
calibrate();

if(last_temp == 0.0){
  last_temp = Correlated_temp;
}

if(Correlated_temp < 75.0){
  // ----------------------- Control ----------------------------------
  double slope = Correlated_temp - last_temp;
  last_temp = Correlated_temp;

  double dynamicThreshold1 = base_threshold;
  double dynamicThreshold2 = base_threshold;

  if(slope > 0){
    dynamicThreshold1 = base_threshold + k*slope;
  } else if (slope < 0){
    dynamicThreshold1 = base_threshold + k*slope; // could be negative somehow
  }

  double error = TEMP - Correlated_temp;

  static int prev_TEMP = TEMP;

  if(TEMP != prev_TEMP){
    error_integral = 0.0; // reset integral term if target being modified.
    prev_TEMP = TEMP;
  }

  if(fabs(TEMP-Correlated_temp) <= 3.0){
    error_integral += error * 0.05;
  }

  double effective_error = error + 0.001 * error_integral;

  // ----------------------- Hardware Implementation -------------------------
  if(slope >= 0){ // rising
    if(effective_error > dynamicThreshold1){
      heaterOn = true;
      heater_status = 1;
    } else {
      heaterOn = false;
      heater_status = 0;
    }
  } else{
    if(effective_error > dynamicThreshold2){
      heaterOn = true;
      heater_status = 1;
    } else {
      heaterOn = false;
      heater_status = 0;
    }
  }

  digitalWrite(HEATER_PIN, heaterOn ? HIGH : LOW);

  // Fan Control.
  analogWrite(FAN_PWM_PIN, 255);

  // IR remote receive
  if (irrecv.decode(&results)){
    if (results.value == 0xFFFFFFFF){
      results.value = key_val;
    }

    switch (results.value){
      case 0xFF906F:
        if(TEMP < TEMP_MAX){
          TEMP += 1;
        }
        break;

      case 0xFFA857:
        if(TEMP > TEMP_MIN){
```

```
          TEMP -= 1;
        }
        break;


      case 0xFF6897:
        TEMP = PLA;
        break;

      case 0xFF30CF:
        TEMP = ABS;
        break;

      case 0xFF18E7:
        TEMP = PETG;
        break;

      case 0xFF7A85:
        TEMP = TPU;
        break;

      case 0xFF10EF:
        TEMP = PP;
        break;

      case 0xFF38C7:
        TEMP = ASA;
        break;

      case 0xFF5AA5:
        TEMP = CFGF;
        break;

      case 0xFF42BD:
        TEMP = PC;
        break;

      case 0xFF4AB5:
        TEMP = PA;
        break;

      // case 0xFF52AD:
      //   TEMP = PLA;
      //   break;

    }
    key_val = results.value;
    irrecv.resume();
  }

  // Display to LCD
  LCDprint();
  Serial.print(Correlated_temp); //predicted chamber temperature
  Serial.print(",");
  Serial.print(TEMP);
  Serial.print(",");
  Serial.print(heater_status);
  Serial.println();
  delay(50);

 } else {
  heaterOn = false;
  heater_status = 0;
 }

}
```

Appendix K - Product Specification Sheet

Table K. Specification Sheet

Mechanical Spec.			
Size (L x W x H)			247 mm × 126.5 mm × 85.5 mm
Weight			0.97 kg
Enclosure Material			PA6-CF (carbon fiber-reinforced PA6 (Nylon 6), 3D printed)
Installation Type			Freestanding
Power Supply			
Inputs	Input Type		Cord
	Voltage Range	Power System 1 (Power Circuit)	120 VAC
		Power System 2 (Control Circuit)	90 – 264 VAC
	Frequency		47 – 63 Hz
	Current	Power System 1 (Power Circuit)	6.70 A*
		Power System 2 (Control Circuit)	1.67 A
Total Power Consumption			840 W **
Temperature Measurement			
Inputs			Semiconductor Temperature Sensor (TSIC 306 TO92)
Resolution			± 0.3 °C
Temperature Unit			°C
Sampling Time			50 ms
Control & Performance			
Control Action			PD-like Controller
Control Temperature Range			40 – 65 °C
Accuracy (at setpoint)			± 0.5 °C (average temperature measured at multiple points within the chamber remains within ±0.5 °C of the target setpoint)
Oscillation (at setpoint)			＜0.5 °C (fluctuation of the spatial average temperature within the chamber at the setpoint ＜0.5 °C)
Temperature Uniformity (after 1-hour operation)			(Highest vs. Lowest Chamber Temperature) Max. - Min. ≤ 2.5 °C (40°C setpoint) Max. - Min. ≤ 4.5 °C (50°C setpoint) Max. - Min. ≤ 5.0 °C (60°C setpoint) Chamber Temp. (spatial) Standard Deviation (StDev.): StDev. ≤ 0.75 (40°C setpoint) StDev. ≤ 1.31 (50°C setpoint) StDev. ≤ 1.85 (60°C setpoint)

Heat up Speed	17 min (25°C – 65°C)
Communication & Connectivity	
Remote Control	Infrared Remote (IR) Control
Display	16 × 2 LCD Display
USB (Data Acquisition)	USB 3.0, Type-C Serial Communication (baud rate = 9600)
Auxiliary Spec.	
Air Intake	47.3 CFM
Environment Spec.	
Working Temperature	0°C – 70°C***

* The current for the power circuit (PTC heater) is 6.70A. The peak power of the PTC element (during normal operation) is measured to be 800W by using an electricity usage monitor. Given the operation voltage for the heater is 120VAC, the maximum current is calculated to be 6.70A.

** The design's maximum power consumption is 840W, consisting of the PTC heater (800W), control circuit (~ 20W, Appendix C), plus an extra 20W for safety headroom.

*** The theoretical maximum working temperature for the design is 70° as the intake fan's maximum suggested operation temperature is 70°C, even though all other electronics have a maximum operation temperature of up to 85°C.

Appendix L - Bill of Material (BOM)

Table L1. Design Components BOM

Item No.	Name	Manufacturer/Brand	Type/Model	*Tech. Spec.	Quantity (QTY.)	Unit Price (in CAD)
1	Microcontroller (MCU)	IoTCrazy	Arduino Nano 3.0 Dev Board	ATmega328P, 5VDC, 16MHz, -40°C~85°C, USB Type-C	1	12.99
2	Centrifugal Fan Blower	Sanyo Denki America Inc.	1688-1380-ND	97.1mm X 33mm, 12~26.4VDC, 19.9W, 47.3CFM, -20°C~70°C, 760Pa Static Pressure, 40000 Hrs@60°C	1	53.75
3	PTC Heating Element	SHENZHEN JINKE SPECIAL MATERIALS CO. LTD.	JKFTP-120-1500	95mm X 88mm X 14.5mm, 120VAC, 60Hz, 1500W	1	9.50
4	LCD Display	Freenove	FNK0079	5VDC, I2C LCD 1602 Module, 16x2 Display	1	8.50
5	IR Receiver Module (with remote)	ACEIRMC	HW-477	5VDC, 3~5mA, 20000 effective life cycles	1	3.49

6	DC Step-Down Module	eBoot	MP1584EN DC-DC 3A	4.5~28VDC Input, 0.8~20VDC Output, 3A max load current, 1.5MHz, -45°C~85°C	1	3.3
7	Thermal Sensor	Innovative Sensor Technology	TSIC 306 TO92	2.97~5.5VDC, -50°C~150°C Operating Temp., ±0.3°C precision, Through-Hole	1	8.15
8	AC-DC Converter	FSP Technology Inc.	FSP040-DAAN3	90~264VAC Input, 24VDC Fixed Output, 40W, 1.67A, 0°C~70°C Operating Temp., Barrel Plug, 2.5mm I.D. x 5.5mm O.D. x 9.5mm	1	27.35
9	AC Power Cable (to the AC-DC converter)	*Various	Various	18AWG, 125VAC, 40W, universal power cord (NEMA 5-15P to IEC320C13), Male to Female	1	-
10	AC Power Cable (to the PTC element)	Various	Various	18AWG, Type A AC plug cable	1	-
11	DC Relay (for fan control)	WAYINTOP	Dual High-Power FET Trigger Switch Driver Module	34mm X 17mm X 1mm, 5~36V Output, 3.3~20V Trigger Level, 15A, 400W, 20KHz	1	2.99
12	Solid State Relay (SSR)	FOTEK	SSR-25DA	63mm X 49mm X 24mm, 24~380VAC Load Voltage, 3~32VDC Trigger Level, 25mA control current, 25A load current	1	25.95
13	Solderable Breadboard	Gikfun	GK1009C	45.72mm X 33.02mm X 1.6mm, 2.54mm hole spacing	1	2.80
14	USB-C Cable	SparkFun Electronics	CAB-15455	146.1mm length, USB 3.0, 5Gbps, 24 AWG, 2 Screw Locks, Data Transfer and charge, Panel Mount	1	15.70
15	Fuse	Conext Link	ATC25-25	19.8mm X 18.6mm, 25A max	1	0.50

				current, Through-hole mount, zinc plated		
16	Fuse Holder	Littelfuse	FHAC0002XP	30A max current, 12AWG cable, in-line fuse holder	1	7.99
17	DC Connector Barrel Power Jack	GOSONO	07112 Barrel Connector	38VDC max voltage, 3A, Barrel Plug, 2.5mm I.D. x 5.5mm O.D.	1	1.20
18	Rocker Switch	Twidec	CA-KCD3-101	15.5mm X 8.4mm X 1.8mm, 125VAC, 15A, 1-way circuit	1	3.20
19	Magnets	Various	Various	3mm X 1mm magnets	18	-
20	M3 Cap Screw (Divider panel)	Various	Various	M3 x 5mm	4	-
21	M3 Cap Screw (Back panel)	Various	Various	M3 x 10mm (with nuts)	5	-
22	M4 Cap Screw	Various	Various	M4 x 35mm (with nuts)	2	-
23	Heat Shrink Tube	Various	Various	4~10mm inner diameter, 125°C max operating temp.	-	-
24	Internal Wire (120VAC line)	Various	Various	12AWG	-	-
25	Internal Wire (24VDC line)	Various	Various	20AWG	-	-
26	Internal Wire (5VDC line)	Various	Various	24AWG	-	-
27	Wire Nut	MotoMaster	B3601	22-14AWG, closed-end connectors, Crimp Mount Style	2	1.2
28	*Main Enclosure	Various	Various	PA6-CF (carbon fiber-reinforced PA6 (Nylon 6))	-	101.99/kg
***TOTAL PRICE (Unit Production Cost)**						**235.75**

Various: means any type, as long as conformance with the "Technical Spec.".
Tech. Spec.: Only important key specifications related to the component's functionality (or directly affect design's performance) are listed.
Total Price: All prices are before tax. The price calculation excludes low-cost consumables such as wires and screws. The price refers to unit production cost. If the product has to be mass-produced and distributed, the cost can be lower.
Main Enclosure: The cost for the enclosure is estimated based on the actual weight of the materials (0.461 kg) used during the 3D printing process.

Appendix M - Assembly Procedure

For manufacturers or subsequent self-assembly, please follow the steps below:

1. Print the enclosure using PA6-CF as specified in Appendices M4 and M5.
2. Install the fan in the compartment (Figure M1).

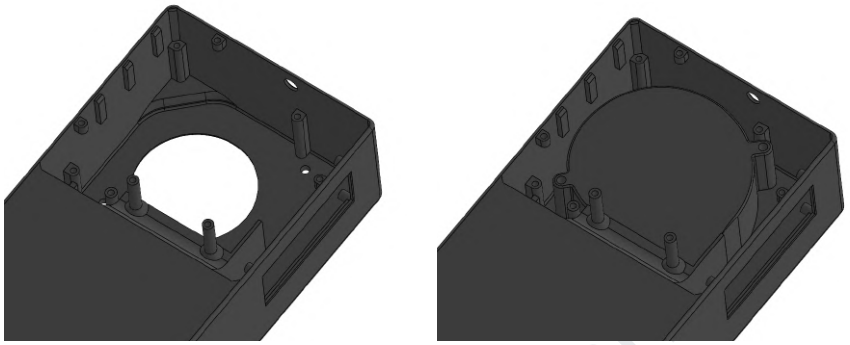

Figure M1. Assembly step 2

3. Mount the divider panel and secure it to the base with four M3×5 mm screws. Additionally, fasten the fan and the divider panel together using two M4×35 mm screws (Figure M2).

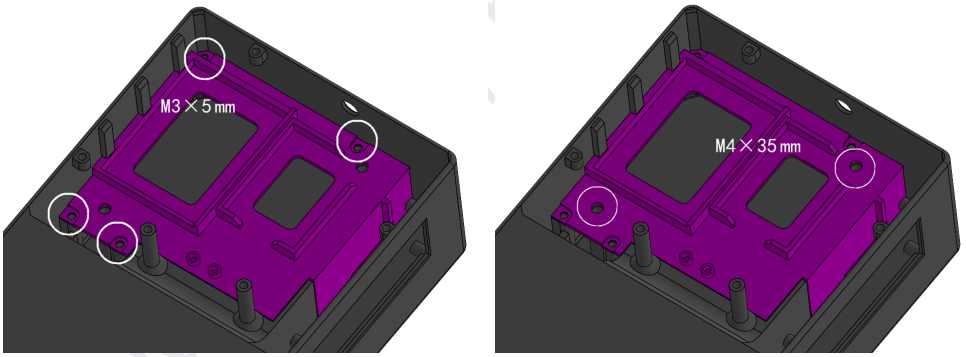

Figure M2. Assembly step 3

4. Install the PTC heater into the PTC compartment. Connect the wiring to the fuse and rocker switch. Route the cables through the routing channel into the electronics compartment (Figure M3).

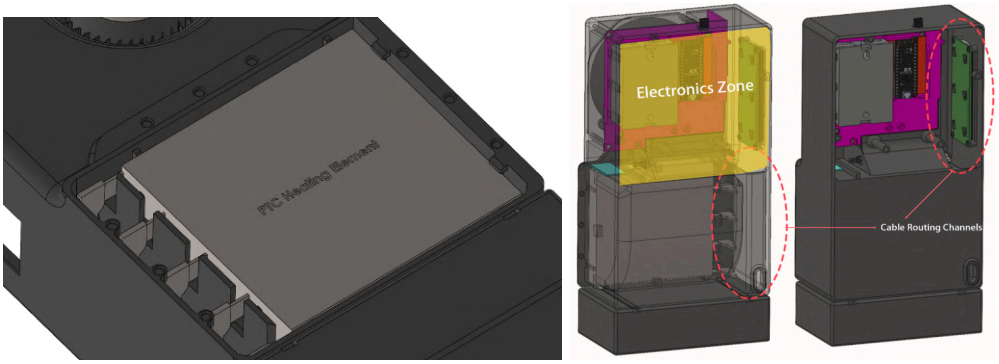

Figure M3. Assembly step 4

5. Connect all electronic components according to the circuit diagram, ensuring each component is placed in its specified location.

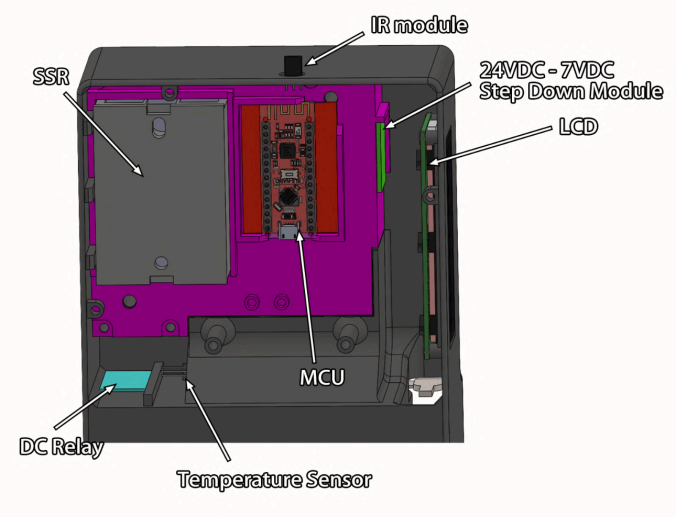

Figure M4. Assembly step 5

6. On the back panel, mount the switch, Type-C port, and barrel jack.

7. Secure the back panel using five M4×35 mm screws (Figure M5).

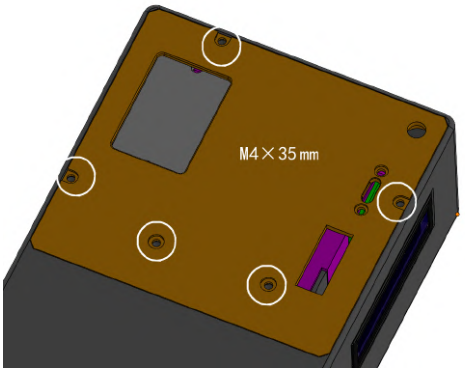

Figure M5. Assembly step 7

8. Connect a computer to the data acquisition port using a Type-C cable. Use the Arduino IDE to upload the code from Appendix J to the MCU. Once completed, the device should be operational.

Appendix N - IR Remote Material Presets

Anisoprint A3 composer can support various filaments, listed below. Recommended Chamber Temperature acquired from 3D printer vendor recommendations and 3D printer forums. These are typically empirical values derived from the 3D printing communities. Preset values in control codes are adjustable upon future need.

Table N1. Common Support Filaments

Name	Recommended Chamber Temperature (°C)	Remote Preset (°C)
PLA	50~60℃ [22]	55
ABS	60~70℃ [23]	65
PETG	70~80℃ [24]	65
PA(Nylon)	50~70℃ [22]	60
TPU	40~60℃ [25]	50
PC	60~70℃ [26]	65
ASA	~70℃ [27]	65
Fiber/glass fiber-filled filaments (general)	50~60℃ [22]	55

Appendix O - MATLAB Serial Read and Data Acquisition Code

To download the code, click the link:
https://drive.google.com/file/d/1L2WZkBzYVXCAPLkVMyrf430is0s9ewzF/view?usp=sharing

Please run the code on MATLAB 2024b or a later version. To read the data, please connect the device to the computer using a USB 3.0 Type-C cable via the data acquisition port.

Once connected, please edit the "COM" (variable "port2" in the code) to be the COM connected to the device.

The complete code is as follows:

```
clc;
clear;
close all;
%% Connect to Arduino Nano
port2 = "COM8";
baudRate2 = 9600;
try
   s2 = serialport(port2, baudRate2);
   configureTerminator(s2, "CR/LF");
   s2.Timeout = 10;
   disp("Successfully connected to Arduino Nano");
catch ME
   disp("Error connecting to Arduino Nano. Using simulated data instead.");
```

```
    s2 = [];
end
%% initialization
timeArray = datetime('now');
logTime = [];
logDesignSensor = [];
logTargetTemp = [];
logHeaterStatus = [];
%% Figure 1: Design Sensor Data
figure(4); clf;
hold on;
hDesignPlot = plot(timeArray, NaN, 'r-o','LineWidth',1.5,'DisplayName','Design Sensor');
xlabel('Time');
ylabel('Design Sensor Reading');
title('Design Sensor Over Time');
legend('Location','best');
ax4 = gca;
ax4.XAxis.TickLabelFormat = 'HH:mm:ss';
grid on;
%% Figure 2: Heater Status vs. Time
figure(5); clf;
hold on;
hHeaterPlot = plot(timeArray, NaN, 'm-o','LineWidth',1.5,'DisplayName','Heater Status');
xlabel('Time');
ylabel('Heater Status');
title('Heater Status vs. Time');
legend('Location','best');
ax5 = gca;
ax5.XAxis.TickLabelFormat = 'HH:mm:ss';
grid on;
%% Figure 3: Target Temperature vs. Time
figure(6); clf;
hold on;
hTargetPlot = plot(timeArray, NaN, 'b-o','LineWidth',1.5,'DisplayName','Target Temp');
xlabel('Time');
ylabel('Target Temperature');
title('Target Temperature Over Time');
legend('Location','best');
ax6 = gca;
ax6.XAxis.TickLabelFormat = 'HH:mm:ss';
grid on;
disp('Starting...');
while true
    % Read from serial port
    if ~isempty(s2)
        line2 = readline(s2);
        if isempty(line2)
            designSensorVal = NaN;
            targetTemp = NaN;
            heaterStatus = NaN;
        else
            line2 = strtrim(line2);
            tokens2 = split(line2, ',');
            if length(tokens2) < 3
                designSensorVal = NaN;
                targetTemp = NaN;
                heaterStatus = NaN;
            else
                designSensorVal = str2double(tokens2(1));
                targetTemp = str2double(tokens2(2));    % 读取 targetTemp
                heaterStatus = str2double(tokens2(3));
            end
        end
    else
        designSensorVal = 100 + randn*3;
        targetTemp = 120 + randn*3;  % 模拟 targetTemp 数据
        heaterStatus = randi([0,1]);
    end
    tNow = datetime('now');
    timeArray = [timeArray; tNow];
    tMin = tNow - minutes(20);
    % Update Figure 1: Design Sensor
    xOld4 = get(hDesignPlot,'XData');
    yOld4 = get(hDesignPlot,'YData');
    set(hDesignPlot,'XData',[xOld4, tNow],'YData',[yOld4, designSensorVal]);
    xlim(ax4,[tMin,tNow]);
    % Update Figure 2: Heater Status
    xOld5 = get(hHeaterPlot,'XData');
    yOld5 = get(hHeaterPlot,'YData');
    set(hHeaterPlot,'XData',[xOld5, tNow],'YData',[yOld5, heaterStatus]);
    xlim(ax5,[tMin,tNow]);
    % Update Figure 3: Target Temperature
    xOld6 = get(hTargetPlot,'XData');
    yOld6 = get(hTargetPlot,'YData');
    set(hTargetPlot,'XData',[xOld6, tNow],'YData',[yOld6, targetTemp]);
    xlim(ax6,[tMin,tNow]);
    drawnow;
    logTime = [logTime; tNow];
    logDesignSensor = [logDesignSensor; designSensorVal];
```

```
    logTargetTemp = [logTargetTemp; targetTemp];  % 记录 targetTemp 数据
    logHeaterStatus = [logHeaterStatus; heaterStatus];
    T = table(logTime, logDesignSensor, logTargetTemp, logHeaterStatus, ...
              'VariableNames', {'Time','DesignSensor','TargetTemp','HeaterStatus'});
    desktopPath = fullfile(getenv('USERPROFILE'), 'Desktop');
    filename = fullfile(desktopPath, 'Temperature.xlsx');
    try
        writetable(T, filename);
    catch writeME
        disp('Failed to save the data');
    end
    disp(['Time: ' datestr(tNow, 'HH:MM:SS') ', DesignSensor: ' num2str(designSensorVal,'%.2f') ...
          ', TargetTemp: ' num2str(targetTemp,'%.2f') ', HeaterStatus: ' num2str(heaterStatus)]);

    pause(0.02);
end
```

Appendix P - Engineering Drawings for the Testing Chamber

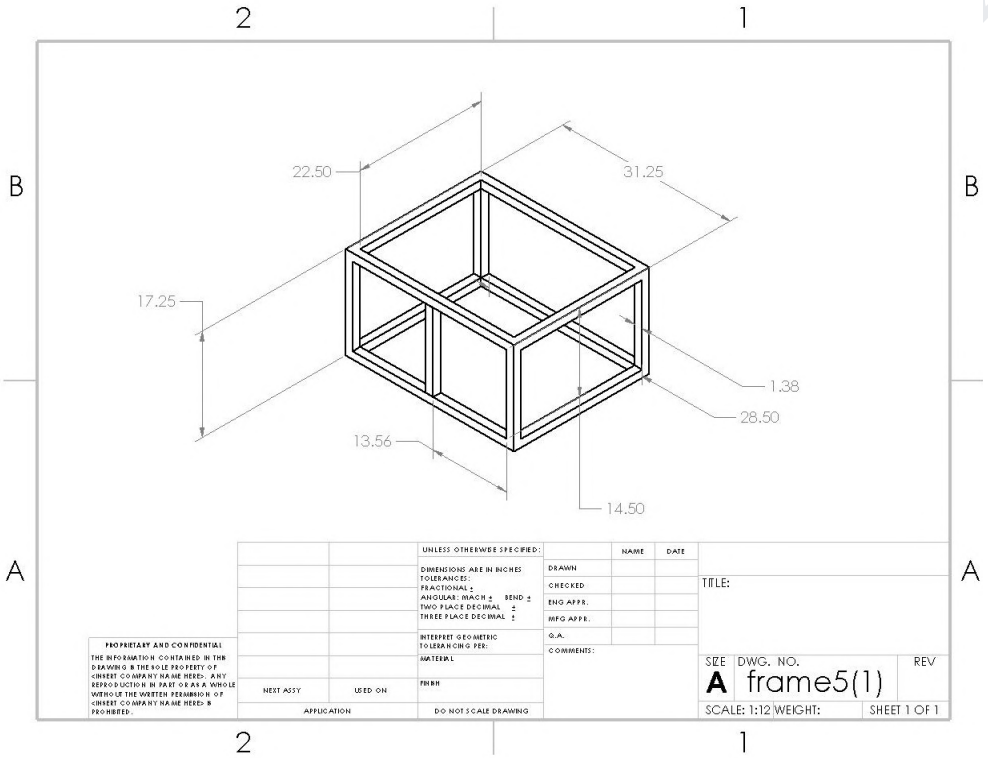

Appendix Q - Anisoprint Support Team Email

One of the team members directly contact the Anisoprint support team to gain advice on the building of the testing chamber. The email is listed below:

Hello
Bangan Wang

The chamber temperature settings are currently embedded within the firmware and cannot be modified. This design ensures consistent performance and adherence to safety standards. However, during the experimental phase, if you need to disable the cooling system, you can disconnect the fan wires from the mainboard. This will stop the cooling process and may help you achieve the desired thermal conditions for your specific application.
The walls of the chamber are constructed using standard acrylic panels without any special treatment. Acrylic was chosen for its durability, transparency, and thermal insulation properties, which are suitable for maintaining a stable printing environment.

Should you require further assistance or have additional questions, please do not hesitate to contact us.

Best regards
Claus
support@anisoprint.com

Appendix R - Sensor Tree Engineering Drawing

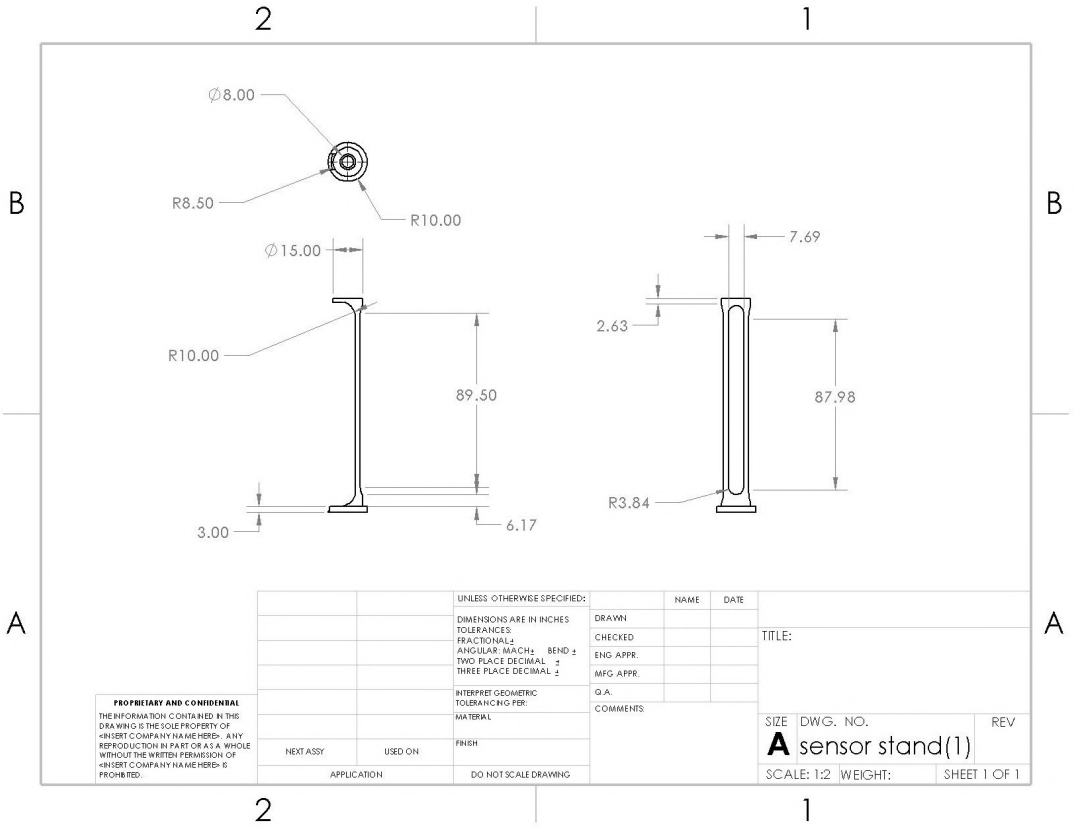

Appendix S - Experiment Data Acquisition Program (MATLAB)

To download the code, please click the link below:
https://drive.google.com/file/d/1hpi4K3QMQN9xmJkbMZAyW33Fvi9yPcb0/view?usp=drive_link

The complete code is shown below:

```
clc;
clear;
close all;
%% Geometry parameter
chamberWidth = 14.25;
chamberDepth = 11.25;
chamberHeight = 17.25;
zLevels = [4.33, 8.66, 12.99];
polePositions2D = [...
    0, chamberDepth;
    chamberWidth, chamberDepth;
    0, 0;
    chamberWidth, 0;
    chamberWidth/2, chamberDepth/2
];
numPoles = 5;
numLevels = 3;
numSensors = numPoles * numLevels;  % 5 x 3 = 15
sensorX = zeros(numSensors, 1);
sensorY = zeros(numSensors, 1);
sensorZ = zeros(numSensors, 1);
index = 1;
```

```
for p = 1:numPoles
   for l = 1:numLevels
       sensorX(index) = polePositions2D(p, 1);
       sensorY(index) = polePositions2D(p, 2);
       sensorZ(index) = zLevels(l);
       index = index + 1;
   end
end
%% Connect to Arduino Mega (15 sensors)
port = "COM3";
baudRate = 9600;
try
   s = serialport(port, baudRate);
   configureTerminator(s, "CR/LF");
   s.Timeout = 10;
   disp("Successfully connected to Arduino Mega.");
catch ME
   disp("Error connecting to Arduino Mega. Using simulated data instead.");
   s = [];
end
%%
timeArray = datetime('now');
globalAvgArray = nan;
globalStdArray = nan;
logTime = [];
logSensors = [];
logGlobalAvg = [];
logGlobalStd = [];
%%
sensorVarNames = cell(1, numSensors);
for i = 1:numSensors
   sensorVarNames{i} = sprintf('Sensor%d', i);
end
%%
figure(1);
hScatter = scatter3(sensorX, sensorY, sensorZ, 100, zeros(numSensors,1), 'filled');
hold on;
xlabel('Width (inches)');
ylabel('Depth (inches)');
zlabel('Height (inches)');
title('3D Sensor Temperature Distribution');
axis([-10 chamberWidth+10 -10 chamberDepth+10 -1 chamberHeight+1]);
grid on;
view(45,30);
axis vis3d;
daspect([1 1 1]);
colorbar;
v1 = [-7.125, -5.625, 0];
v2 = [chamberWidth+7.125, -5.625, 0];
v3 = [chamberWidth+7.125, chamberDepth+5.625, 0];
v4 = [-7.125, chamberDepth+5.625, 0];
v5 = [-7.125, -5.625, chamberHeight];
v6 = [chamberWidth+7.125, -5.625, chamberHeight];
v7 = [chamberWidth+7.125, chamberDepth+5.625, chamberHeight];
v8 = [-7.125, chamberDepth+5.625, chamberHeight];
plot3([v1(1) v2(1)], [v1(2) v2(2)], [v1(3) v2(3)], 'k-', 'LineWidth',2);
plot3([v2(1) v3(1)], [v2(2) v3(2)], [v2(3) v3(3)], 'k-', 'LineWidth',2);
plot3([v3(1) v4(1)], [v3(2) v4(2)], [v3(3) v4(3)], 'k-', 'LineWidth',2);
plot3([v4(1) v1(1)], [v4(2) v1(2)], [v4(3) v1(3)], 'k-', 'LineWidth',2);
plot3([v5(1) v6(1)], [v5(2) v6(2)], [v5(3) v6(3)], 'k-', 'LineWidth',2);
plot3([v6(1) v7(1)], [v6(2) v7(2)], [v6(3) v7(3)], 'k-', 'LineWidth',2);
plot3([v7(1) v8(1)], [v7(2) v8(2)], [v7(3) v8(3)], 'k-', 'LineWidth',2);
plot3([v8(1) v5(1)], [v8(2) v5(2)], [v8(3) v5(3)], 'k-', 'LineWidth',2);
plot3([v1(1) v5(1)], [v1(2) v5(2)], [v1(3) v5(3)], 'k-', 'LineWidth',2);
plot3([v2(1) v6(1)], [v2(2) v6(2)], [v2(3) v6(3)], 'k-', 'LineWidth',2);
plot3([v3(1) v7(1)], [v3(2) v7(2)], [v3(3) v7(3)], 'k-', 'LineWidth',2);
plot3([v4(1) v8(1)], [v4(2) v8(2)], [v4(3) v8(3)], 'k-', 'LineWidth',2);
figure(2);
hAvgPlot = plot(timeArray, globalAvgArray, '-o', 'LineWidth', 1.5);
hold on;
hStdPlot = plot(timeArray, globalStdArray, '-s', 'LineWidth', 1.5);
xlabel('Time');
ylabel('Temperature (°C)');
legend('Global Avg', 'Global Std', 'Location', 'best');
title('Global Temperature Statistics');
ax2 = gca;
ax2.XAxis.TickLabelFormat = 'HH:mm:ss';
grid off;
%% For each sensor
figure(3);
hold on;
hSensorPlots = gobjects(numSensors,1);
for i = 1:numSensors
   hSensorPlots(i) = plot(timeArray, NaN, ...
       'LineWidth', 1.5, ...
       'DisplayName', sprintf('Sensor %d',i));
end
xlabel('Time');
ylabel('Temperature (°C)');
```

```
title('Individual Sensor Temperatures Over Time');
legend('Location','best');
ax3 = gca;
ax3.XAxis.TickLabelFormat = 'HH:mm:ss';
grid on;
%% Main loop
while true
   %% 1) Data reading
   if ~isempty(s)
       line = readline(s);
       if isempty(line)
           sensorTemp = zeros(numSensors, 1);
       else
           line = strtrim(line);
           tokens = split(line, ',');
           if length(tokens) < numSensors
               sensorTemp = zeros(numSensors, 1);
           else
               sensorTemp = zeros(numSensors, 1);
               for i = 1:numSensors
                   sensorTemp(i) = str2double(tokens{i});
               end
           end
       end
   else
       sensorTemp = 25 + 1*randn(numSensors, 1);
   end
   validIdx = sensorTemp <= 100;
   if sum(validIdx) > 0
       globalAvg = mean(sensorTemp(validIdx));
       globalStd = std(sensorTemp(validIdx));
   else
       globalAvg = NaN;
       globalStd = NaN;
   end
   %% 3) Update Figure
   tNow = datetime('now');
   timeArray = [timeArray; tNow];
   globalAvgArray = [globalAvgArray; globalAvg];
   globalStdArray = [globalStdArray; globalStd];
   set(hAvgPlot, 'XData', timeArray, 'YData', globalAvgArray);
   set(hStdPlot, 'XData', timeArray, 'YData', globalStdArray);
   tMin = tNow - minutes(20);
   xlim(ax2, [tMin, tNow]);
   set(hScatter, 'CData', sensorTemp);
   for i = 1:numSensors
       xOld = get(hSensorPlots(i), 'XData');
       yOld = get(hSensorPlots(i), 'YData');
       set(hSensorPlots(i), 'XData', [xOld, tNow], 'YData', [yOld, sensorTemp(i)]);
   end
   drawnow;
   %% 4) Record Data
   logTime = [logTime; tNow];
   logSensors = [logSensors; sensorTemp'];
   logGlobalAvg = [logGlobalAvg; globalAvg];
   logGlobalStd = [logGlobalStd; globalStd];
   %% 5) Save the data to Excel
   T = table(logTime, logSensors(:,1), logSensors(:,2), logSensors(:,3), ...
             logSensors(:,4), logSensors(:,5), logSensors(:,6), logSensors(:,7), ...
             logSensors(:,8), logSensors(:,9), logSensors(:,10), ...
             logSensors(:,11), logSensors(:,12), logSensors(:,13), ...
             logSensors(:,14), logSensors(:,15), ...
             logGlobalAvg, logGlobalStd, ...
             'VariableNames', [{'Time'}, sensorVarNames, {'GlobalAvg','GlobalStd'}]);
   desktopPath = fullfile(getenv('USERPROFILE'), 'Desktop');
   filename = fullfile(desktopPath, 'TempCorrelation.xlsx');
   try
       writetable(T, filename);
   catch writeME
       disp('Failed to save the data');
   end
   %% 6 Output
   disp(['Time: ' datestr(tNow, 'HH:MM:SS') ', Global Avg: ' num2str(globalAvg, '%.2f') ...
         '°C, Global Std: ' num2str(globalStd, '%.2f') '°C']);

   pause(0.2);
end
```


Appendix T - Layout Study of the Centrifugal Fan and PTC Heater

Objective: *Investigate the effects of general layouts (of heater and fan) on chamber temperature uniformity and speed of temperature rise.*

The team came up with two different layout configurations during the conceptual design phase:

1. The intake fan is installed at the bottom of the enclosure. The air is drawn into the design, heated by the PTC heater, and expelled from the top.

2. The intake fan draws air from the top, heated by the PTC heater and subsequently expelled from the bottom.

On Mounting Bracket A, the team installed a 300W DC PTC heater alongside an 11 CFM fan. Two configurations were deployed at the same position in the chamber and two experiments (Figure T1).

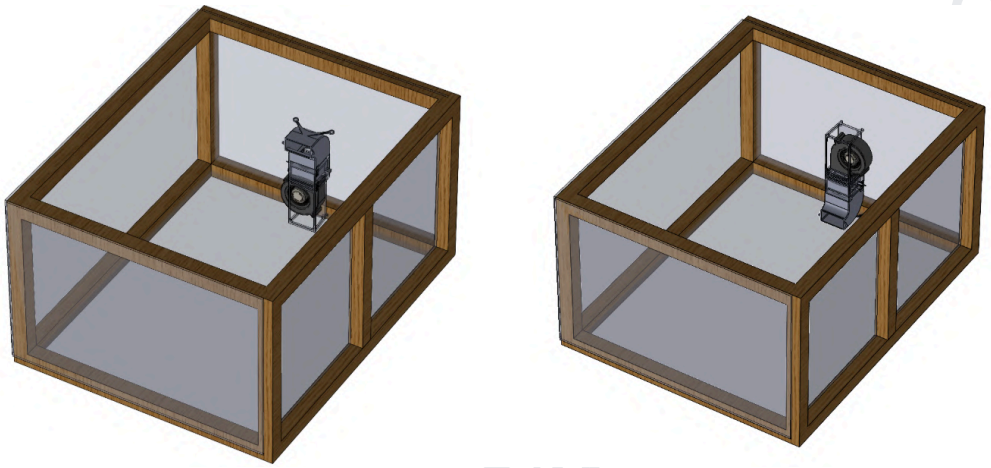

Figure T1. Two configurations (left: Config.1; right: Config.2)

Evaluation Metric: For each configuration, the chamber was heated from an ambient temperature of 25°C to 45°C. The standard deviation of the sensor matrix readings at 45°C was compared. The speed of the chamber temperature rising was also compared.

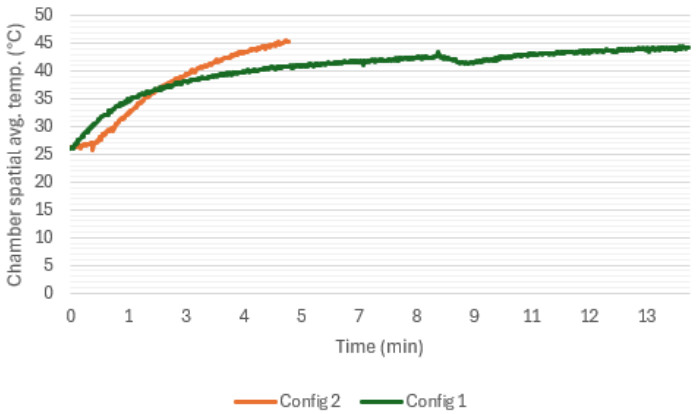

Figure T2. Chamber average temperature profile

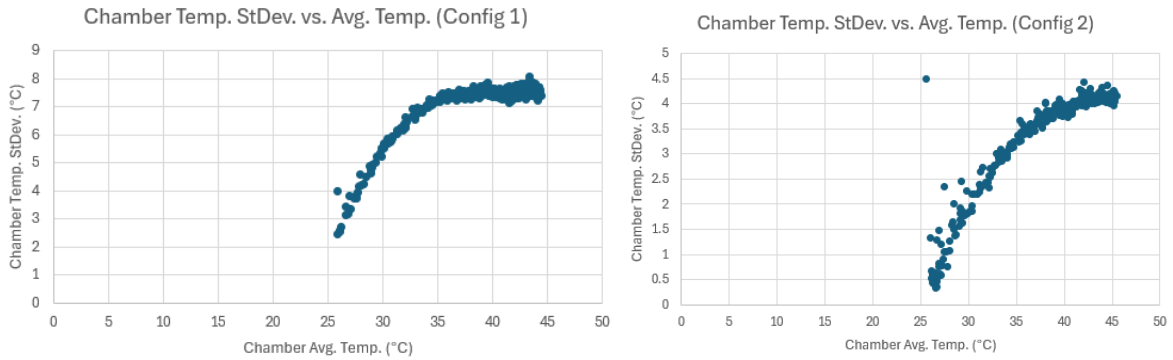

Figure T3. Temp. standard deviation vs. Average chamber temp. (for each configuration)

Table T1 - Chamber temperature standard deviation @ 45°C

Config.1	Config.2
7.456480275	4.02649771

Results: **Configuration 2 had a significantly lower standard deviation at the standard deviation**. Figure T3 shows that at the same chamber temperature, configuration 2 has a much smaller standard deviation across the entire sensor matrix. Additionally, Figure T2 result shows that configuration 2 also has a faster speed of temperature rising (~5min to reach 45°C). In both aspects (temperature uniformity and heat-up speed), configuration 2 is much better.

One possible reason is the heated air from the bottom takes advantage of natural convection; as warm air rises, it mixes with cooler air, promoting more effective circulation. Thus, two mounting brackets (A and B) that will be used throughout the experiments will adopt this layout.

Appendix U - Mounting Bracket A (for low-power PTC heaters) Engineering Drawings

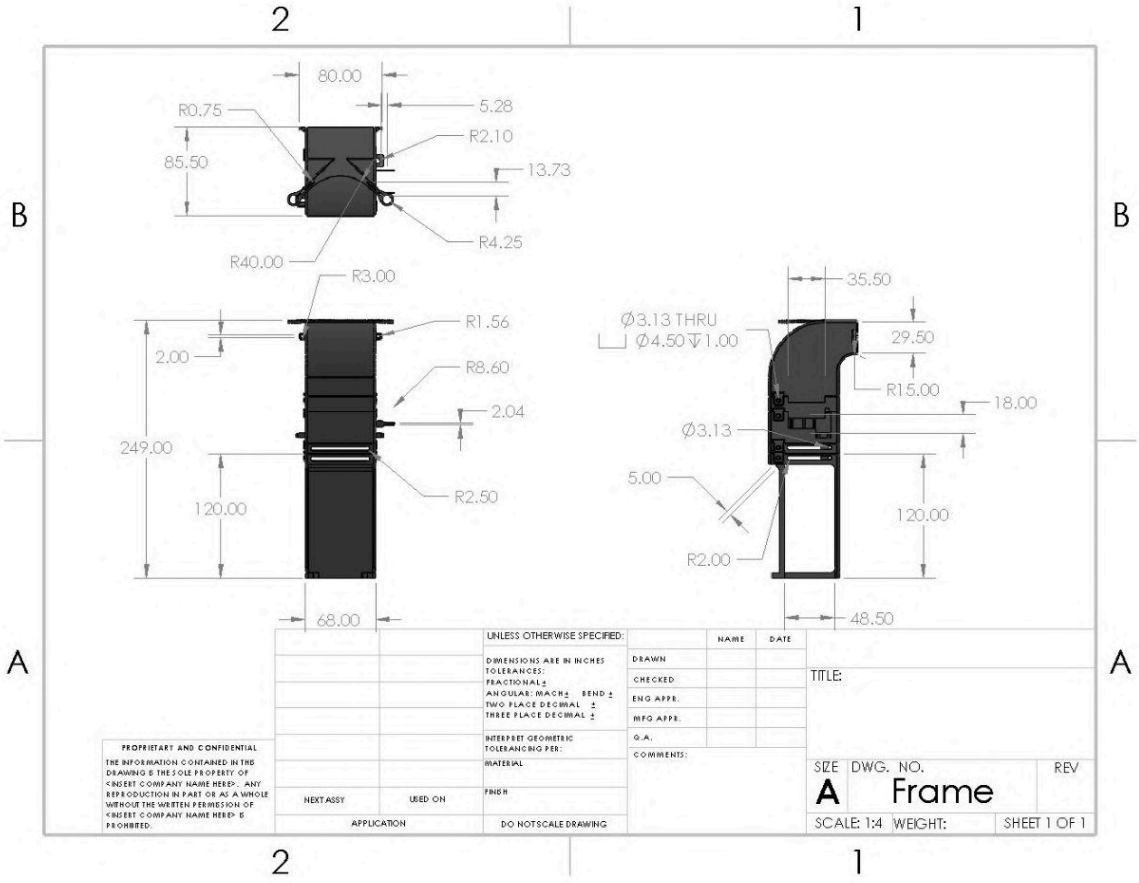

Appendix V - Mounting Bracket B (for high-power PTC heaters) Engineering Drawings

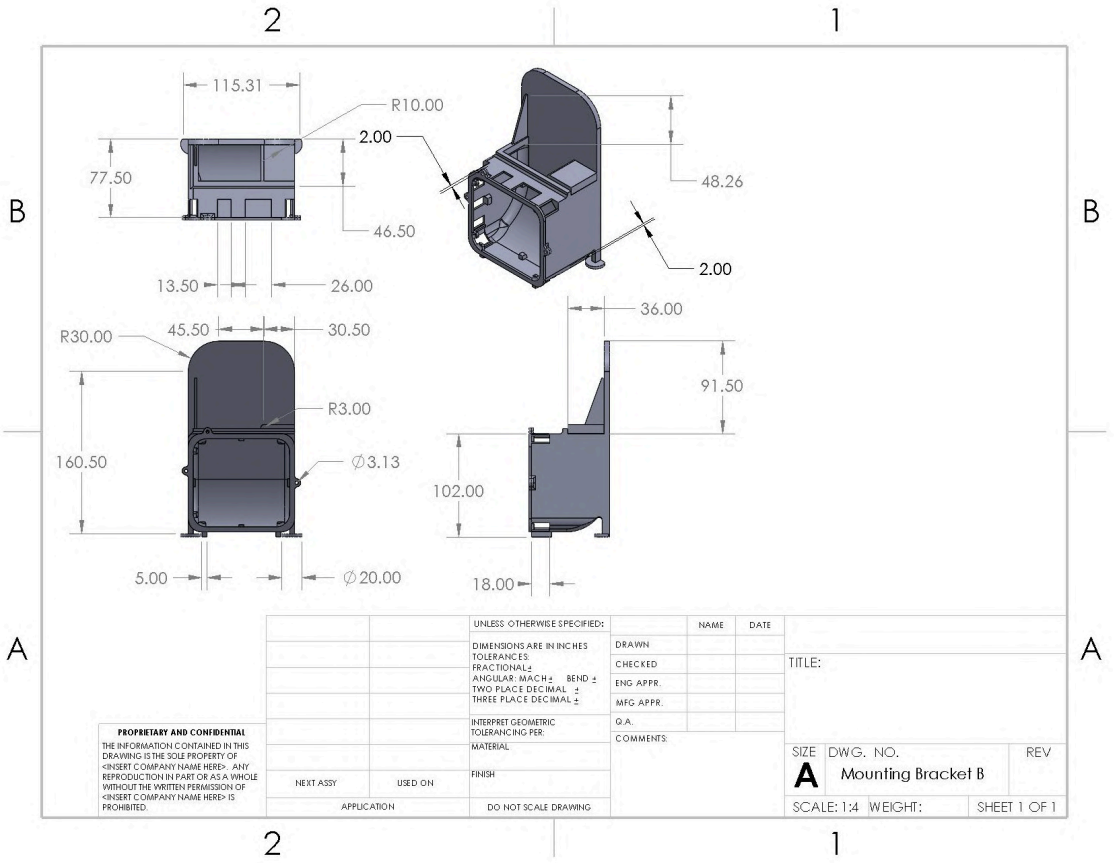

Appendix W - High Current Risk for High-power DC PTC Heater

For a 300W heater operating at 24V, the current can be calculated using the formula I = P / V, which gives I ≈ 300W / 24V ≈ 12.5A. A higher power will lead to a higher current. If the PTC heater goes to 500W (24 VDC), the current can be greater than 20A.

Circuits designed for high currents require thicker, more expensive cables and connectors to safely handle the load, not only increasing the product cost but also making the design bulky. Moreover, the process of finding a single DC power source that can support such a high current is another big challenge. Thus, the team chose to use an AC PTC heater which can directly draw power from the wall outlet.

Appendix X - PTC Heater Working Mechanism and Relationship to CFM

PTC heaters operate based on a positive temperature coefficient effect, meaning that as the temperature increases, the internal impedance also increases, allowing the heater to self-regulate. However, in practical applications, if heat dissipation is insufficient, the surface temperature of the PTC heater may exceed its ideal operating range, leading to localized overheating. The increase in resistance under constant voltage results in a drop in power output (since $P = V^2/R$), which adversely affects the heating performance (Figure X1).

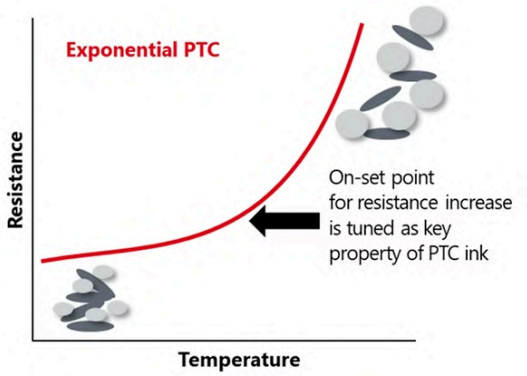

Figure X1. Self-regulated PTC element [28]

Adequate airflow not only helps to uniformly mix the air inside the chamber and improve heat exchange efficiency but also effectively removes excess heat. This keeps the PTC heater within its optimal operating temperature range and ensures that its resistance remains at the intended level, thereby allowing it to deliver maximum heating power.

In the design, even though the team procured a heater rated at 1500W, the actual measured output power was only about 800W. Due to design constraints related to the enclosure's volume, the team was unable to use a higher airflow fan to reduce the heater's surface temperature to achieve full-rated power. Fortunately, the actual power output of 800W meets the design requirements, and when paired with a 47.3 CFM fan, the overall performance remains excellent.

Appendix Y - Full Factorial DOE Setup

Theoretically, a full factorial experiment would involve 45 configurations (5×3×3), but due to geometric constraints, not all control factor levels can be combined. For example, when CF A is 70° and CF B is -8°, the resulting geometry is invalid and cannot form a louver deflector.

Table Y1 - Full factorial DOE (36 experiments in total) setup and result

Config. ID	CF A (θ)	CF B (Δθ)	CF C (*L*)	Standard Deviation @ 60°C
1	0	0	10.0	5.946113817
2	10	0	10.0	2.760555346
3	10	8	10.0	6.430388196
4	10	-5	10.0	3.997905127
5	30	0	10.0	2.235556179
6	30	8	10.0	2.884559552
7	30	-5	10.0	4.845990783
8	50	0	10.0	6.242516053
9	50	8	10.0	3.623303281
10	50	-5	10.0	4.751387567
11	70	0	10.0	4.347813682

12	70	8	10.0	6.841278563
13	0	0	18.6	5.640091954
14	10	0	18.6	3.670095089
15	10	8	18.6	7.850753928
16	10	-5	18.6	3.803827356
17	30	0	18.6	2.587175692
18	30	8	18.6	4.848290462
19	30	-5	18.6	4.19766383
20	50	0	18.6	7.053020485
21	50	8	18.6	4.12468731
22	50	-5	18.6	4.560096278
23	70	0	18.6	3.766480791
24	70	8	18.6	5.621429479
25	0	0	27.2	5.303274162
26	10	0	27.2	3.704944022
27	10	8	27.2	8.164263467
28	10	-5	27.2	4.254029123
29	30	0	27.2	3.12278207
30	30	8	27.2	5.590510774
31	30	-5	27.2	5.525290139
32	50	0	27.2	6.431442851
33	50	8	27.2	4.545435084
34	50	-5	27.2	4.709186636
35	70	0	27.2	4.26254912
36	70	8	27.2	4.854736641

For each configuration, the change of chamber temperature standard deviation over time is plotted (36 curves in total). ("*BA*" stands for Deflector Base Angle; "*Inc*" stands for Angle Increment).

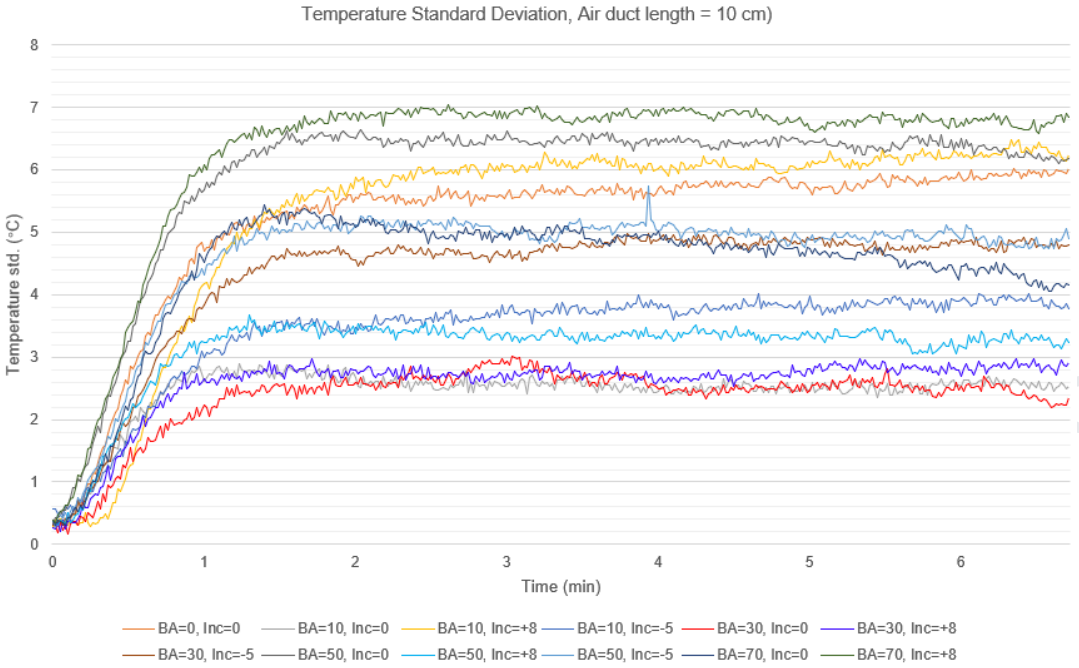
Temperature Standard Deviation, Air duct length = 10 cm)
Temperature std. (°C)
Time (min)
BA=0, Inc=0
BA=10, Inc=0
BA=10, Inc=+8
BA=10, Inc=-5
BA=30, Inc=0
BA=30, Inc=+8
BA=30, Inc=-5
BA=50, Inc=0
BA=50, Inc=+8
BA=50, Inc=-5
BA=70, Inc=0
BA=70, Inc=+8

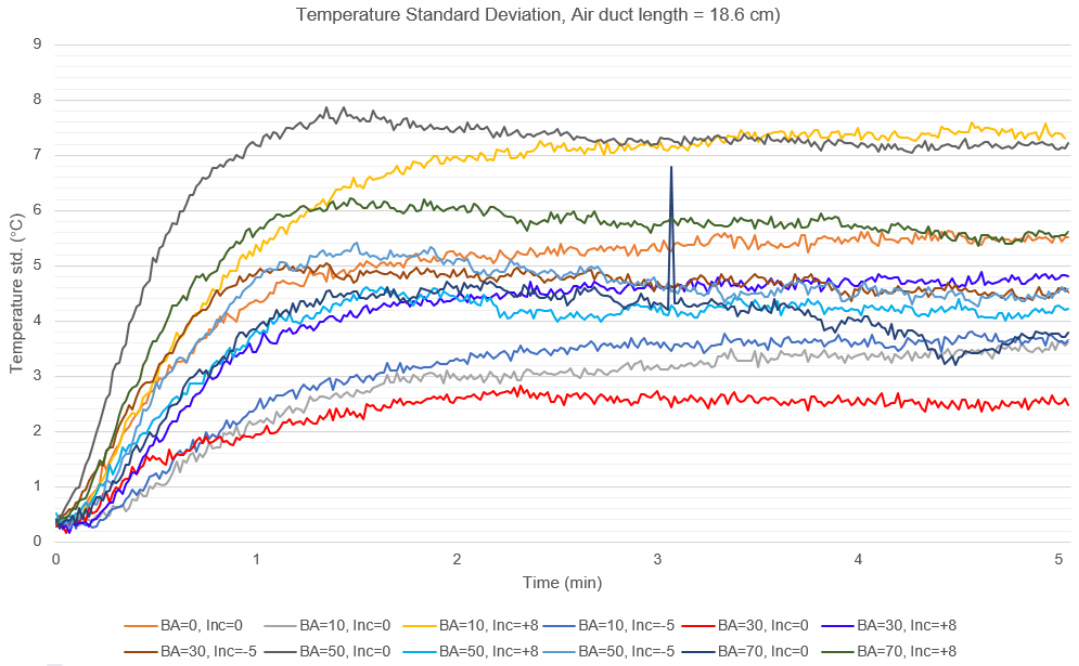
Temperature Standard Deviation, Air duct length = 18.6 cm)
Temperature std. (°C)
Time (min)
BA=0, Inc=0
BA=10, Inc=0
BA=10, Inc=+8
BA=10, Inc=-5
BA=30, Inc=0
BA=30, Inc=+8
BA=30, Inc=-5
BA=50, Inc=0
BA=50, Inc=+8
BA=50, Inc=-5
BA=70, Inc=0
BA=70, Inc=+8

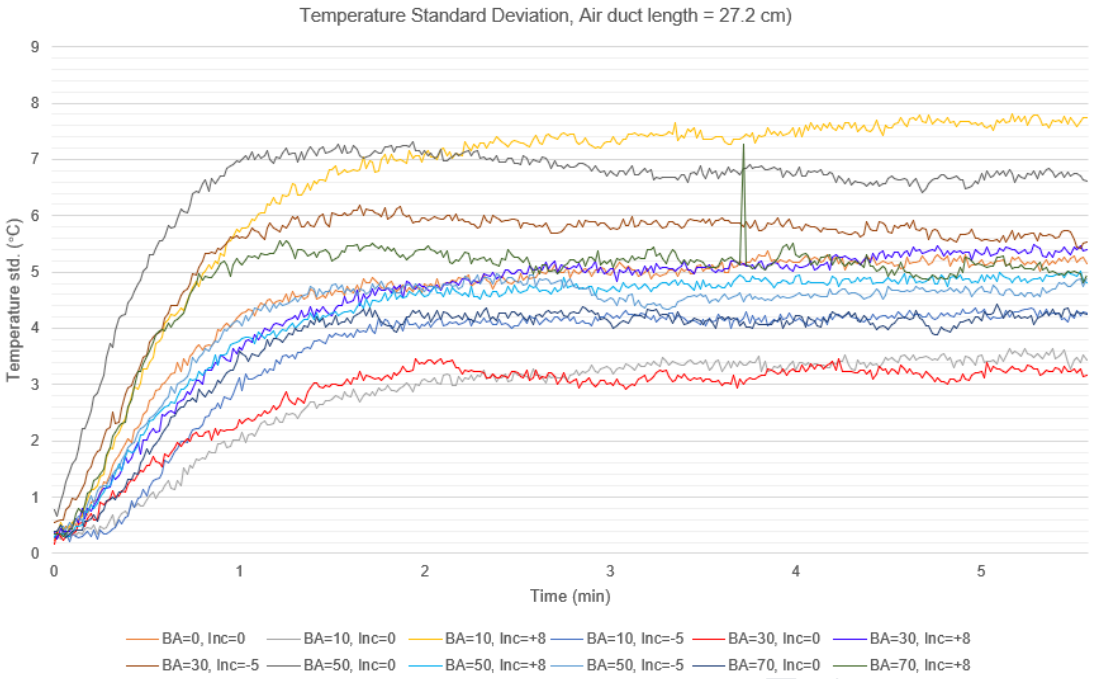

Appendix Z - RSM Modeling Accuracy Report (Experiment ID 3)

The model used to predict the chamber temperature standard deviation is:

$$\text{Chamber Temp. StDev.} = 3.800 - 0.060A + 0.103B + 0.067C + 0.001A^2 + 0.023B^2 - 4\times10^{-5}C^2 - 0.005\,AB - 0.001\,AC + 0.004\,BC$$

SUMMARY OUTPUT						
Regression Statistics						
Multiple R	0.594175142					
R Square	0.353044099					
Adjusted R Square	0.129097825					
Standard Error	1.336579422					
Observations	36					
ANOVA						
	df	SS	MS	F	Significance F	
Regression	9	25.3464515	2.816272	1.576468	0.174543447	
Residule	26	46.4475583	1.786445			
Total	35	71.7940098				
	Coefficients	Standard Error	t Stat	P-value	Lower 95%	Upper 95%
Intercept	**3.800865074**	2.243968887	1.693814	0.102249	-0.811679032	8.41340918
X Variable 1	**-0.060121509**	0.047143331	-1.27529	0.213484	-0.157026015	0.036782997
X Variable 2	**0.103056793**	0.152454187	0.675985	0.505019	-0.210317275	0.416430862
X Variable 3	**0.067367857**	0.244417661	0.275626	0.785014	-0.435039841	0.569775554
X Variable 4	**0.001267974**	0.000548429	2.31201	0.028958	0.000140661	0.002395287
X Variable 5	**0.023071986**	0.01255272	1.838007	0.077514	-0.0027305	0.048874472
X Variable 6	**-4.02318E-05**	0.006389294	-0.0063	0.995024	-0.013173614	0.01309315
X Variable 7	**-0.005477545**	0.002329815	-2.35106	0.026579	-0.010266548	-0.000688541
X Variable 8	**-0.001298195**	0.001408298	-0.92182	0.365099	-0.004192994	0.001596603
X Variable 9	**0.003830799**	0.006376278	0.600789	0.553182	-0.009275829	0.016937427

Figure E14. RSM model accuracy report

Appendix AA - GRG Extrapolate Searching Range

The team employed the Generalized Reduced Gradient (GRG) method to extrapolate the regression optimization model obtained from Experiment ID 3. Instead of being limited to predetermined discrete levels, this approach allows for the identification of the optimal combination of continuous parameters. The parameter search ranges are defined as follows:

- CF A: 0° to 70°
  (exceeding 70° would pose geometric limitations, making it difficult to 3D print).
- CF B: -15° to 15°.
- CF C: 10 cm to 30 cm
  (within chamber geometric limits; values beyond this range would exceed the printer's size constraints).

Appendix AB - Preliminary Correlation Experiment Data

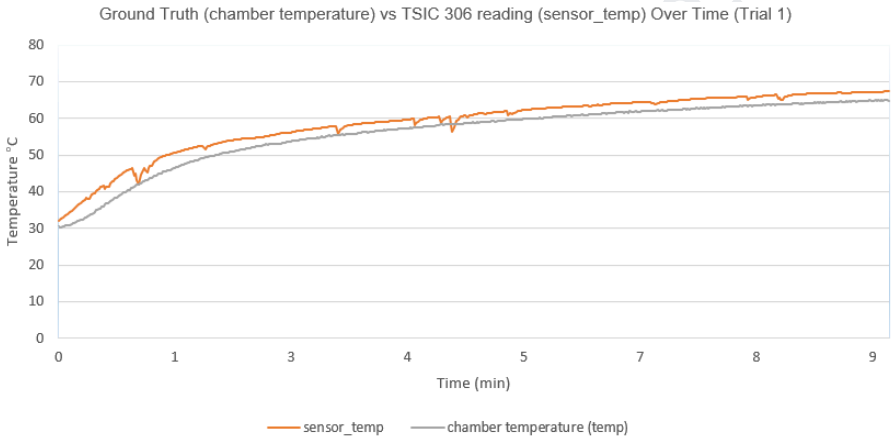

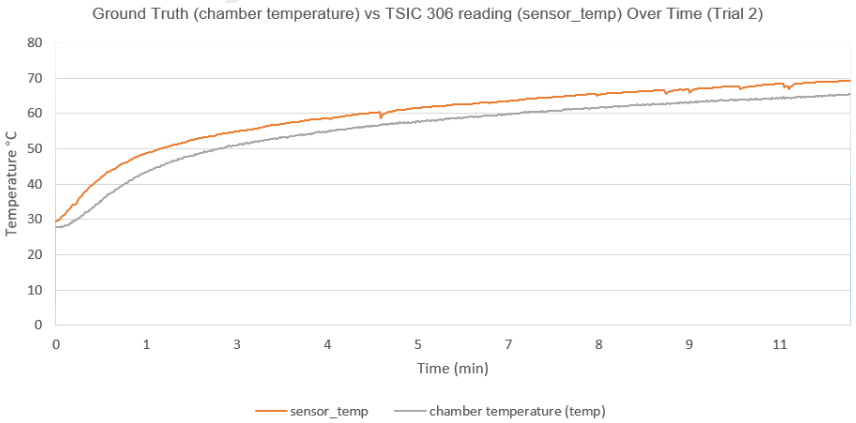

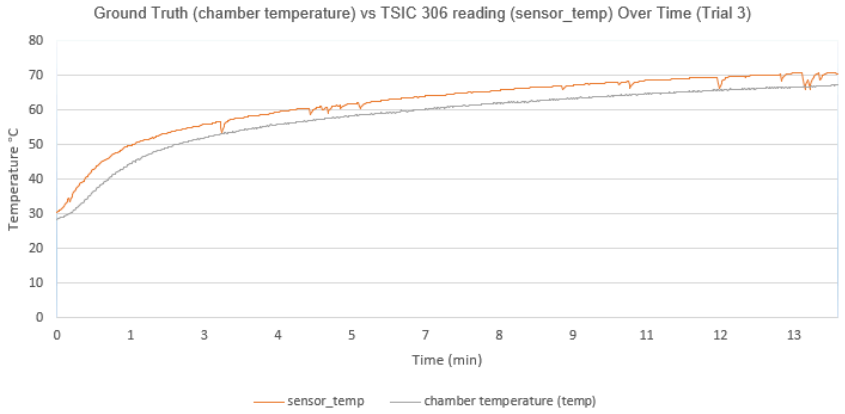

Figure AB1. Ground truth chamber (spatial average) temperature, TSIC 306 reading vs. time (for three trials)

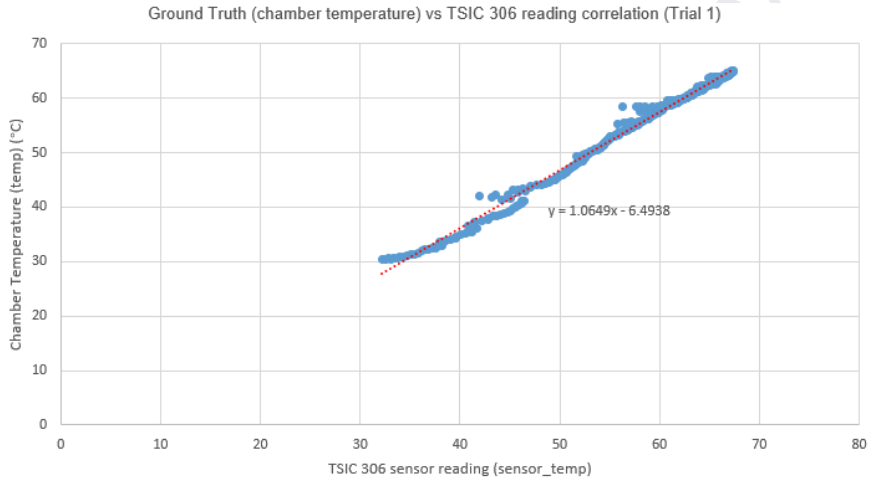

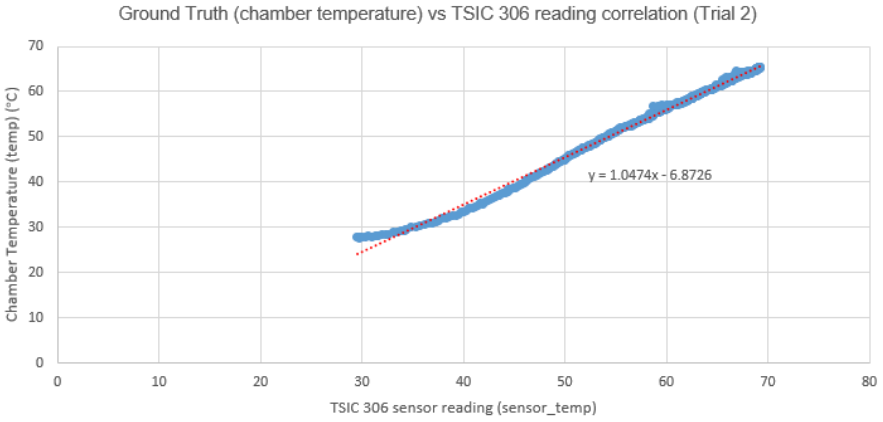

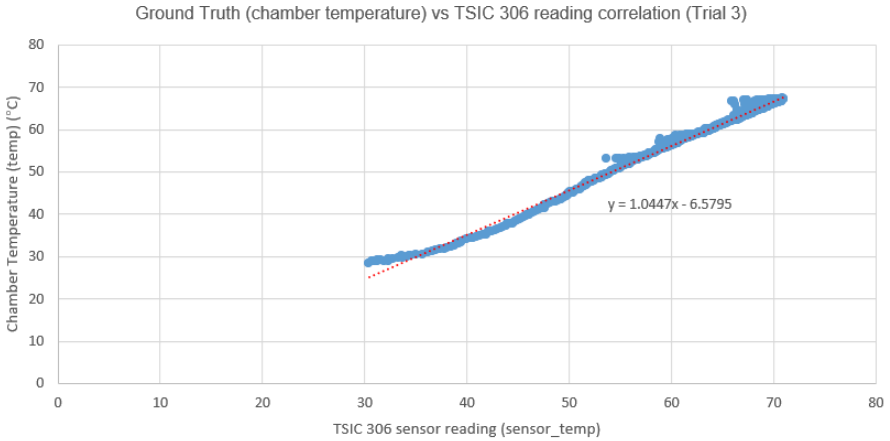

Figure AB2. Correlation between the ground truth chamber temperature and TSIC 306 reading (for three trials)

Appendix AC - Complete Test Result for ($base\_threshold = 1; k = 1$)

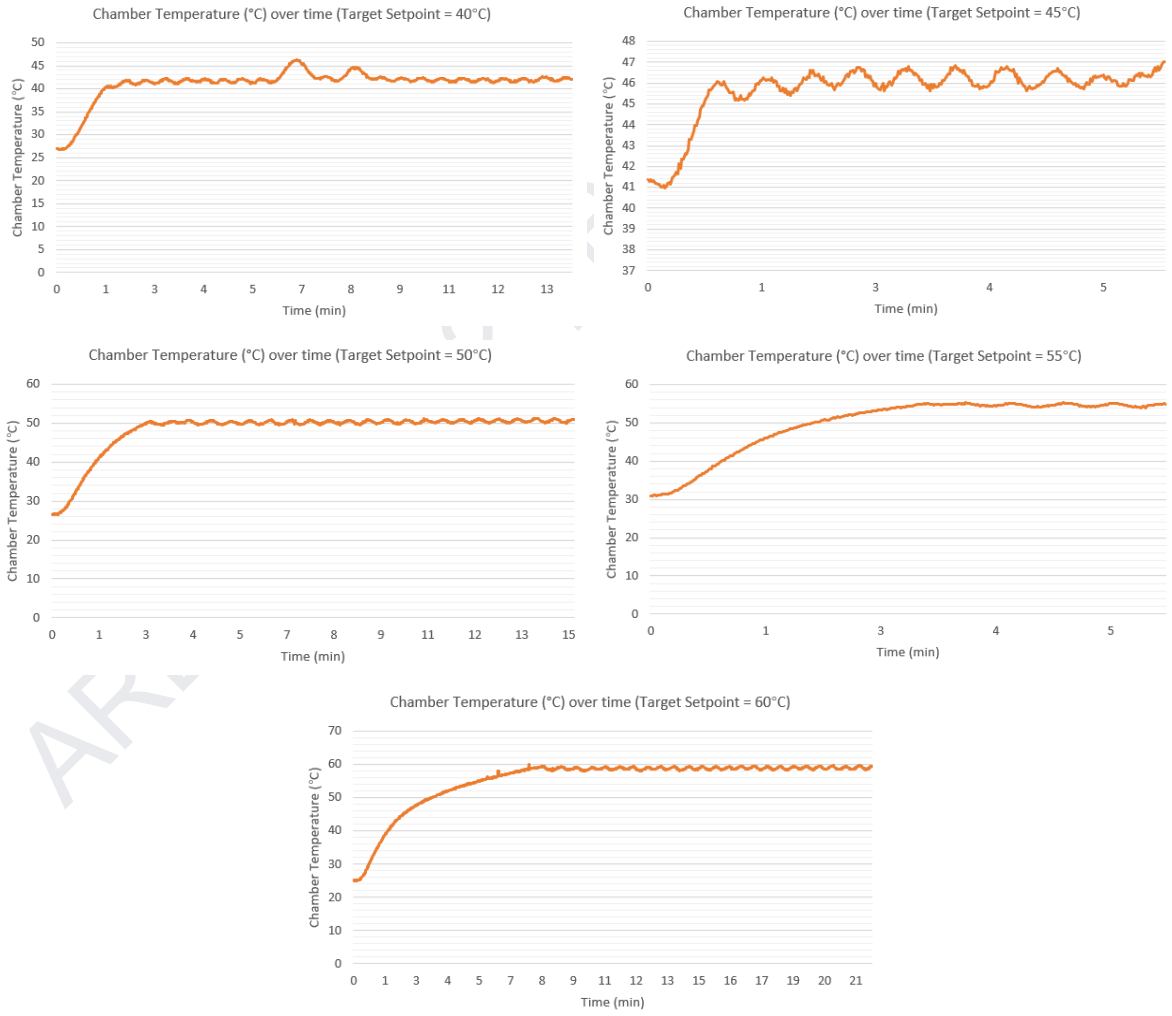

Figure AC1. Chamber spatial average temperature (setpoint = 40, 45, 50, 55, 60°C) ($base\_threshold = 1; k = 1$)

The temporal average is computed over the steady-state period. Specifically, this average is calculated from the moment the chamber temperature first reaches the target value until the end of the test; If a steady-state error is presented, the team defined the system as having reached the steady state when the temperature changes by less than 0.5°C per second. Once this condition is met, the average temperature measured during that interval is taken as the steady-state temperature.

Appendix AD - Complete Test Result for Dynamic Base Threshold Mechanism (Verification Run)

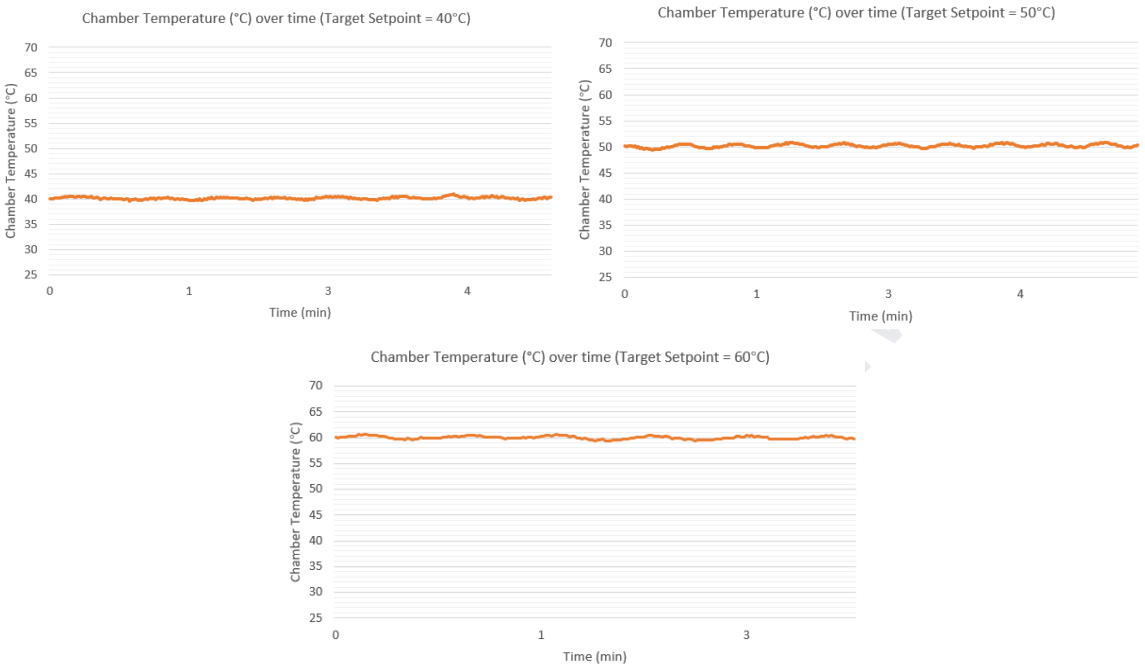

Figure AD1. Chamber spatial average temperature (@ steady state) after implementing dynamic $base\_threshold$

Appendix AE - Reason to tune the k at target setpoint = 50°C

In the Appendix AD verification run, the oscillation at 50°C was the largest, with an amplitude of 0.6623°C. Tuning the k under the worst-case conditions ensures that the controller is robust enough to handle the maximum oscillations the system might experience. Therefore, the k was tuned at target setpoint = 50°C.

Table AE1 - Oscillation in Appendix E22 verification run

Target Setpoint ($Target\ Temp$) (°C)	**Oscillation Amplitude (°C)**
40	0.5882
50	0.6623
60	0.5819

Appendix AF - Complete Test Result for k tuning

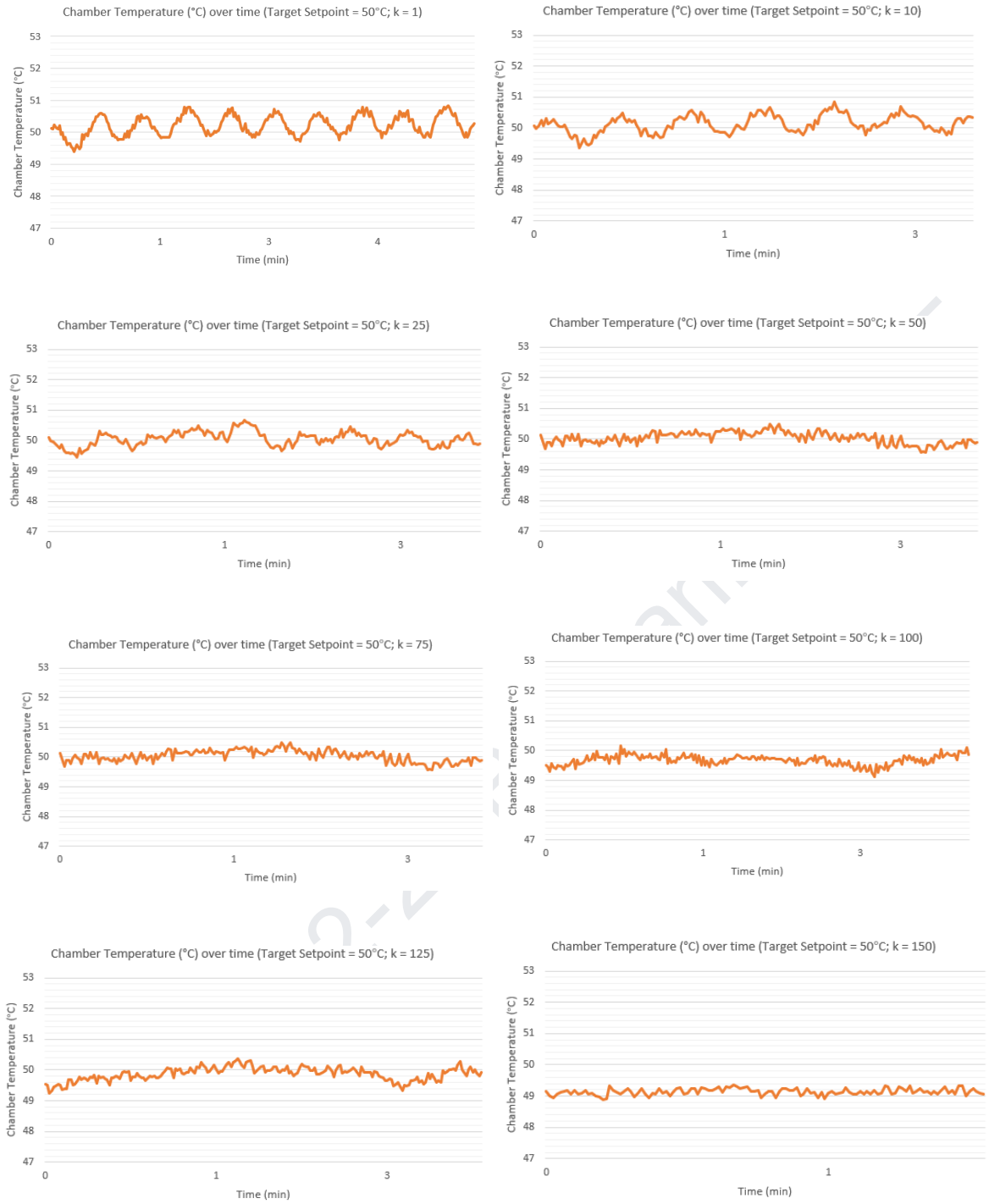

Figure AF1. Chamber spatial average temperature (@ steady state) for $k \in \{1,\ 10,\ 25,\ 50,\ 75,\ 100,\ 125,\ 150\}$

Appendix AG - Long-Term Temperature Control Performance Evaluation

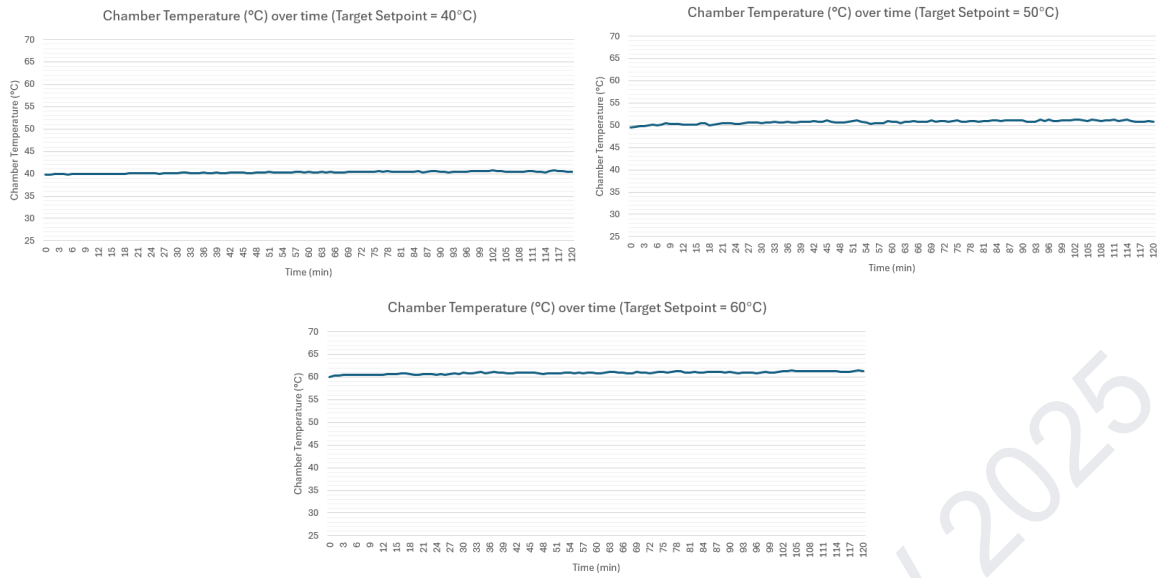

Figure AG1. Chamber spatial average temperature @ steady state (setpoint = 40, 50, 60°C)

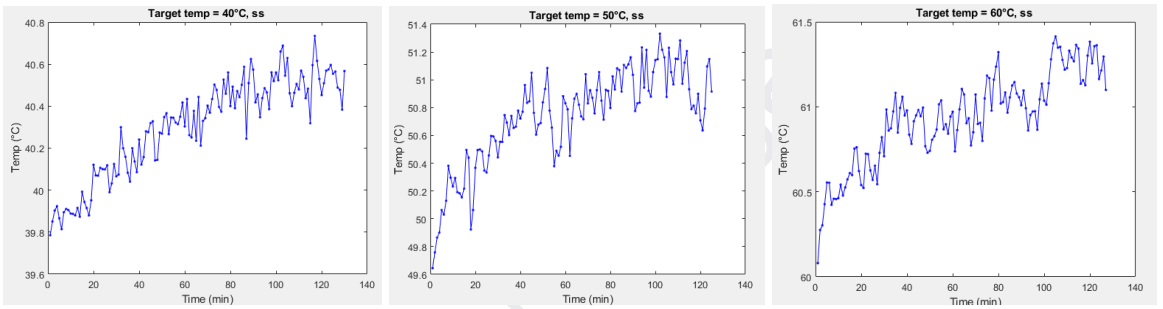

Figure AG2. Temperature Drifting @ Target Setpoint = 40, 50, 60°C

Appendix AH - Complete Data for Final Verification

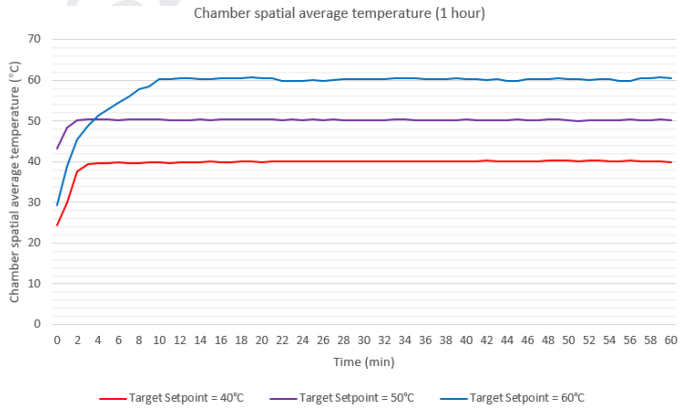

Figure AH1. Chamber spatial average temperature profile (setpoint = 40, 50, 60°C)

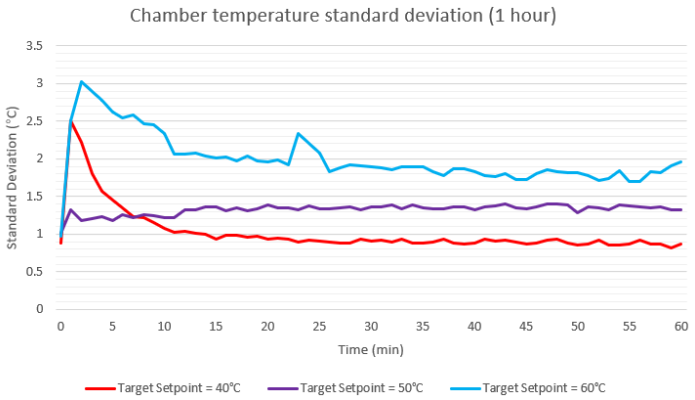

Figure AH2. Chamber standard deviation (setpoint = 40, 50, 60°C)

Appendix AI - Insulation and Safety - conformance to IEC 60335-1

AI.1 - Thermal Insulation and Safety:

Thermal standard adherence:

Product safety performance was evaluated against **IEC 60335-1**, specifically, safe thermal isolation between heated elements (PTC heater) and electronics. **Clearance and spacing** (2-4mm air gaps or insulated layers) to reduce heat transfer to the enclosure and electronics.

The enclosure is manufactured from **PA6-CF** (carbon fiber-reinforced Nylon), specifically chosen for its high heat deflection temperature (**186°C**), excellent resistance to high temperatures generated by the PTC heater, and to prevent deformation or melting under prolonged high temperatures. Material choice was supported by empirical experiments under worst-case operating conditions to ensure long-term structural integrity and safety (Appendix E). Air gap (**2 – 4 mm**) is maintained around the **PTC heater mounting slot** (Figure AI1) To further prevent the component's direct contact with heated air.

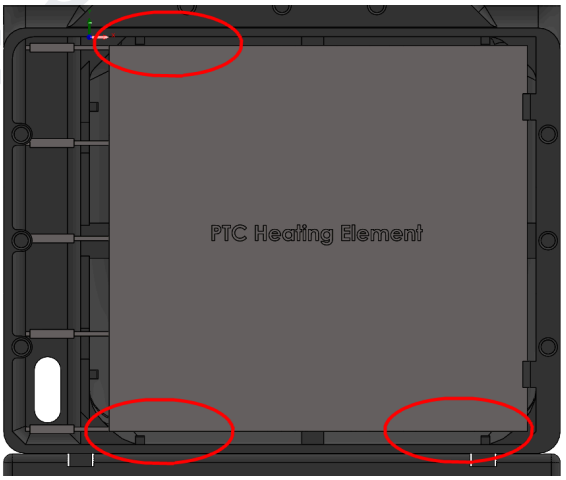

Figure AI1. Mounting clearance (2 – 4 mm) for PTC slot

The **electronic components** are located at the top of the enclosure, thus physically separated from the heater's high-temperature zone: ensuring effective isolation from direct heat sources. (detailed discussion Appendix H), safely below the recommended long-term operating limit of **85°C** for electronic components.

AI.2 - Electrical Insulation and Safety:

All electrical components are enclosed within the PA6-CF housing, which prevents exposure to external elements or indeliberate human contact with energized parts. All electrical elements within the design are insulated and fully enclosed, enhancing safety and stability.

The grade of wires used for either system was selected based on the amplitude of the current that needs to be handled. Specifically, **12 AWG wires** are adopted for high-power circuits (max current: 6.70 A), whereas **20 AWG and 24 AWG wires** are for lower-power and control circuits (AWG specification table in Appendix AJ).

A specified **25A fuse** and SSR relay are incorporated in the high-voltage circuit for overcurrent and short-circuit protection. High-voltage, low-voltage, and signal wires are separated and routed with adequate spacing to prevent electromagnetic interference (EMI), Clearly defined **cable routing channels** are provided within the enclosure to organize wiring neatly, preventing cable crossing or tangling. They keep wires away from moving parts or hot areas, reducing the risk of abrasion or melting.

All connections, except deliberate power connection interfaces, are permanently soldered. **Heat shrink tube** is applied for insulation in component connections where applicable.

AI.3 - Fail-safe mechanism for fire hazard avoidance:

Although not explicitly mentioned in IEC 60335-1, a Fail-safe mechanism is integrated within the control system, the product will not operate beyond a safe temperature limit of 75℃. The system Normally operates below 65℃, it however incorporates a trigger for a forced shutdown when the integrated sensor detects a 75℃ reading.

Appendix AJ - AWG (American Wire Gauge) System Datasheet[29]

AWG	Diameter [inches]	Diameter [mm]	Area [mm^2]	Resistance [Ohms / 1000 ft]	Resistance [Ohms / km]	Max Current [Amperes]	Max Frequency for 100% skin depth
0000 (4/0)	0.46	11.684	107	0.049	0.16072	302	125 Hz
000 (3/0)	0.4096	10.40384	85	0.0618	0.202704	239	160 Hz
00 (2/0)	0.3648	9.26592	67.4	0.0779	0.255512	190	200 Hz
0 (1/0)	0.3249	8.25246	53.5	0.0983	0.322424	150	250 Hz
1	0.2893	7.34822	42.4	0.1239	0.406392	119	325 Hz
2	0.2576	6.54304	33.6	0.1563	0.512664	94	410 Hz
3	0.2294	5.82676	26.7	0.197	0.64616	75	500 Hz
4	0.2043	5.18922	21.2	0.2485	0.81508	60	650 Hz
5	0.1819	4.62026	16.8	0.3133	1.027624	47	810 Hz
6	0.162	4.1148	13.3	0.3951	1.295928	37	1100 Hz
7	0.1443	3.66522	10.5	0.4982	1.634096	30	1300 Hz
8	0.1285	3.2639	8.37	0.6282	2.060496	24	1650 Hz
9	0.1144	2.90576	6.63	0.7921	2.598088	19	2050 Hz
10	0.1019	2.58826	5.26	0.9989	3.276392	15	2600 Hz
11	0.0907	2.30378	4.17	1.26	4.1328	12	3200 Hz
12	0.0808	2.05232	3.31	1.588	5.20864	9.3	4150 Hz
13	0.072	1.8288	2.62	2.003	6.56984	7.4	5300 Hz
14	0.0641	1.62814	2.08	2.525	8.282	5.9	6700 Hz
15	0.0571	1.45034	1.65	3.184	10.44352	4.7	8250 Hz
16	0.0508	1.29032	1.31	4.016	13.17248	3.7	11 k Hz
17	0.0453	1.15062	1.04	5.064	16.60992	2.9	13 k Hz
18	0.0403	1.02362	0.823	6.385	20.9428	2.3	17 kHz
19	0.0359	0.91186	0.653	8.051	26.40728	1.8	21 kHz
20	0.032	0.8128	0.518	10.15	33.292	1.5	27 kHz
21	0.0285	0.7239	0.41	12.8	41.984	1.2	33 kHz
22	0.0254	0.64516	0.326	16.14	52.9392	0.92	42 kHz
23	0.0226	0.57404	0.258	20.36	66.7808	0.729	53 kHz
24	0.0201	0.51054	0.205	25.67	84.1976	0.577	68 kHz
25	0.0179	0.45466	0.162	32.37	106.1736	0.457	85 kHz
26	0.0159	0.40386	0.129	40.81	133.8568	0.361	107 kHz
27	0.0142	0.36068	0.102	51.47	168.8216	0.288	130 kHz

Appendix AK - Complete Assessment on Voltage, Current, and Power Constraints. – Conformance to IEC 60364-1

Products procured are validated to closely adhere to IEC 60364 standards in requirements of power ratings as offered in major cities in North American Buildings. As per the previous investigation on the Mechanical Engineering building (MC) power delivery setup discussed in the Project Requirement, the lab conforms with the specifications described in this standard and IEC 60364 is therefore applicable in this case. IEC 60364-1 discusses standard nominal voltages of AC typically 120VAC or 230VAC(not applicable in MC laboratories,) and DC: at 12V, 24V, and 48V, with a total power requirement at 2000W per wall power distribution plug with ±10% tolerance. **All electronics (in the design) power requirements are listed** and verified valid upon part procurement for acceptance. The design is verified to be operational within MC building laboratories according to the IEC 60364 standard.

High power circuit: 120VAC, 60Hz:

PTC Element:

- Power: Rated 1500W, tested Peak around 800W (Appendix K)
- Maximum Current: 12A

Solid State Relay (FOTEK SSR-25DA - SSR Unit):
- Load Voltage up to 380VAC
- Max Load Current: 25A
- Trigger Level: 3~32VDC
- Control Current: 25mA

Fuse (protect short-circuit and overcurrent):
- Rated Current: 25A

Power Switch:
- Rated 125 VAC, 15A

Wire:
- 12 AWG, Maximum 9A.

Low Power Circuit: 24VDC

Voltage Source (FSP040-DAAN3 - AC-DC Modular Adapter)
- Input: 90~264 VAC
- Output: 24 VDC
- Maximum Power: 40W
- Maximum Current: 1.67A

Voltage Step-down regulation (MP1584EN)
- Input: 2.5 ~ 28VDC
- Output: 0.8 ~ 20 VDC (5V for MCU implementation)
- Maximum Current: 3A

MCU (Arduino Nano) and peripherals:
- Input: 5V

LCD Display 16x2 Character (powered by MCU Regulator)
- Input: 5V

Infrared Remote Control (HW477) (powered by MCU Regulator)
- Input: 5V, Current: 3~5mA

Integrated Temperature Sensor (TSIC 306 TO92: -50~150℃, Acc ±0.3℃) (powered by MCU Regulator)
- Input: 2.97 ~ 5.5VDC

Centrifugal Fan Blower:
- Input Voltage (12 ~ 26.4 VDC)
- Maximum Power 19.9W

Wire Specifications: (Low-Level Circuit)

- Wire Gauge for 24V lines: 20 AWG
- Wire Gauge for 5V lines: 24 AWG

To prevent electromagnetic interference, the power and control circuits are wired separately (Figure AK1) with adequate spacing.

Figure AK1. Cable wiring

Appendix AL - Fastening Design Specifications – Conformance to VDI 2230

The design utilizes screws + nuts for fastening major components (Fan Blower, Back Panel, LCD Display, Divider Panel) and Snap-fit Clip and Slots for light-weight components (Rocker Switch, Solid State Relay, PTC Heating Element.)

Specifically for bolt and screw fasteners, the design utilizes ISO 4762 socket head cap screws Sizes: M3 × 10 mm, M3 × 5 mm, M4 × 35 mm, where applicable (detail in Appendix M).

Fastener joint design performed regarding **VDI 2230** – *Systematic calculation of high-duty bolted joints*. The overall weight of the design is 0.97 kg, and none of these fasteners load above 5 kg, transverse or shear. No formal preload calculation is required suggested by the standard.

Appendix AM - Electrical assembly - conformance to IEC 61010-1

The detailed assembly process during production is specified in **Appendix M**. This assembly process was conducted by the team to closely adhere to **IEC 61010-1** for installation in applicable requirements. Specifically, all components procured are certified under such regulation or equivalent. Electric assembly is done with **clearly labeled writing and color-coding**, **during power down**, and uses of **insulated barriers between electrical components and conductive materials**.

For soldering and insulation on applicable wire-device connection with heat shrink tubing, insulation work was conducted closely in adherence with **IPC/WHMA-A-620**: *wires are **stripped, cut, and handled without damage to insulation or conductors***.

Appendix AN - Additive Manufacturing (3D printing) - conformance to ISO/ASTM 52910

ASTM 52910 offers general guidelines for 3D printed products for commercial usage. This guideline is not specific to a specific printer a printing material in concern. Here, the team adhere to this standard as best practice suggestions.

Geometry and Topology Optimization were extensively applied to Leverage lightweight techniques (topology optimization) during the design of product enclosure. The team constructed a monolithic design: The entire enclosure was printed as 2 major parts to maximize product strength. Applicable printing parameters (Appendix AP) and Drying procedures (Appendix AQ) are performed as per industry best practices to maximize printing quality. Visual inspection of the printed enclosure was performed as per steps in ASTM 52910 yielding no visible crack and significant warpage.

ISO/ATSM 52910 requires a specific documentation method for the printing process, selection of materials, layer resolutions, and post-processing (drying) methods. Adherence was done with the best effort: Records of enclosure iterations, key parameters, materials, and process settings were documented during the printing process to ensure traceability and repeatability.

Appendix AO - Hazard Evaluation – Risk assessment adhering to ISO 12100

ISO 12100 Offers a general framework for risk assessment as well as laying upon a general approach to identifying risks systematically by traversing through stages of the design: Installation, Use/ operation, Maintenance, and Decommissioning, considering Mechanical, Electrical, Thermal, Noise, Radiation, EMI and Ergonomics. The below provides the identified major risks and their detailed discussion/consideration. Resolutions to these risks were not conducted strictly as per ISO12100 due to the time and complexity constraint of a capstone design, each risk was mitigated in a case-by-case manner.

PTC element assessed for overheating and melt-down (discussed in Appendix E);
Investigation of the vendor spec sheet and power constraints (discussed in Appendix AK);
enclosure material assessed for potential deformation and melt-down (discussed in Appendix E)
assessed supplier spec sheet with PTC maximum temperature performance (discussed in Appendix E)
Insulation assessed for Electric shock (discussed in Appendix AI)
Control system potential failure (no safety factor applicable) (Appendix J, fail-safe mechanism incorporated)

ISO 12100 as a Type-A standard offers no detailed Safety Factor for specific products, the team resolved for a Safety Factor back in IEC 61010-1, which specifies a list of testing requirement safety factors for Thermal, Electrical, and Mechanical experiments (solid mechanics is not applicable due to non-major loading.) A maximum SF of 2.0 was adopted in the design process. All assessments return an acceptable safety margin.

Appendix AP - Fabrication Settings (3D printer setting)

To properly print the material, a hardened steel nozzle should be installed on the printer to avoid abrasion.

Table AP1 - Printing Setting

Description	Setting
Build Plate & Bed Temperature	Smooth PEI Plate (100 – 120 °C); Textured PEI Plate (100 – 120 °C)
Printing Speed	< 100 mm/s
Part Cooling Fan	0 – 40%
Annealing	90 – 130°C, 6 – 12 hours

For details, please visit:
https://bambulab.com/en/filament/pa6-cf

Appendix AQ - Material Drying Process (pre-printing)

The entire enclosure was 3D printed using PA6-CF. Before printing, the filament should be dried to prevent poor layer adhesion and brittleness caused by the material high moisture absorption rate. The filament should be dried in the blast drying oven at 80°C, 8 – 12 hours.

For details, please visit:
https://bambulab.com/en/filament/pa6-cf

Appendix AR - Energy Input During 3D Printing Process.

To print the entire design enclosure, the Bambulab P1S 3D printer requires approximately 24 hours. With an average power consumption of around 140 W, as measured by the power meter, the total energy consumption amounts to roughly 3.35 kWh.

Appendix AS - Energy Input During 3D Printing Process.

Assuming that in practical application the device is used for printing 3 times per week, with each session lasting 10 hours, the temperature control unit operates for 30 consecutive hours weekly. At 840 W (Appendix K), the weekly energy consumption is approximately 25.2 kWh.